Electronic Supplementary Material (ESI) for RSC Advances.

Supporting information

Sulphonated Graphene Oxide Catalyzed Continuous Flow Pyrazolo Pyrimidinones, Sildenafil and other PDE-5 Inhibitors Synthesis

Vinay Kumar Sthalam,[a, b] Bhushan Mahajan,[a, b] Purushotham Reddy Karra,[a] Ajay K. Singh,[a,b]*, Srihari Pabbaraja,[a, b]*

[a]Department of Organic Synthesis and Process Chemistry, CSIR-Indian Institute of Chemical Technology, Hyderabad-500007, India.

[b]Academy of Scientific and Innovative Research (AcSIR), CSIR-Human Resource Development Centre (CSIR-HRDC) Campus, Ghaziabad-201002, Uttar Pradesh

E-mail: ajaysingh015@gmail.com; srihari@iict.res.in

Table of Contents

1. General

1.1. Materials: Most of the reagents and chemicals are bought from Spectrochem, Avra and Sigma-Aldrich and were used as such without any further purification. Graphite powder (300-µm flake size), was obtained from alfa. Deionized water (18.2 mS conductivity) was used in all experiments. All work-up and purification procedures were carried out with reagent-grade solvents. Analytical thin-layer chromatography (TLC) was performed using analytical chromatography silica gel 60 F254 precoated plates (0.25 mm). The developed chromatogram was analysed by UV lamp (254 nm). PTFE (id = 500 µm) tubing, *T*-junction and back pressure controller (BPR) was purchased from Upchurch IDEX HEALTH & SCIENCE. HPLC pump used was purchased from KNAUER. SS318 capillary bought from the spectrum market, Mumbai, India. Heating reactor was bought from the Amar Equipment, Mumbai. Syringe pump was bought from the Harward, USA.

1.2. Analysis:

High-resolution mass spectra (HRMS) were obtained from a JMS-T100TD instrument (DART) and Thermo Fisher Scientific Exactive (APCI). Nuclear magnetic resonance (NMR) spectra were recorded on a Bruker 600, 500, 400 or 300 MHz in $CDCl_3$ or DMSO-d_6 solvent. Chemical shifts for ^1H NMR are expressed in parts per million (ppm) relative to tetramethylsilane (δ 0.00 ppm). Chemical shifts for ^{13}C NMR are expressed in ppm relative to $CDCl_3$ (δ 77.0 ppm). Data are reported as follows: chemical shift, multiplicity (s = singlet, d = doublet, dd = doublet of doublets, t = triplet, q = quartet, quin = quintet, sext = sextet, m = multiplet), coupling constant (Hz), and integration.

Gas Chromatography-Mass Spectrometry (GC-MS): GC-MS analysis was conducted on Shimadzu technology GCMS-QP2010 instrument equipped with a HP-5 column (30 m × 0.25 mm, Hewlett-Packard) and inbuilt MS 5975C VL MSD system with triple axis detector.

Liquid Chromatography-Mass Spectrometry (LC-MS):LC-MS analysis was conducted on Shimadzu technology LCMS-8040 instrument.

High Pressure Liquid Chromatography: HPLC analysis was conducted on Shimadzu technology LAB solutions.

Attenuated total reflectance (ATR): IR analysis was recorded on an ECO-ATR, ALPHA BRUKER.

2. Synthesis and characterization of heterogeneous catalyst

2.1. Synthesis of graphene oxide (GO): GO was obtained by the oxidation of graphite powder using modified Hummer methods.[1-4] The graphite powder (2.0 g) taken in concentrated H_2SO_4 (100 mL), was stirred on ice bath for 1 h and then to this was added slowly $KMnO_4$ (8.0 g). The reaction mixture was further stirred for 2 h, then ice bath was removed and stirring was continued for 24 h. The reaction mixture was kept on ice bath and 200 mL deionized water was slowly added to dilute the reaction mixture, then hydrogen peroxide solution (30%) (12 mL) was added drop wise till the solution color changed to orange/gold. The orange color solution was centrifuged at 800 rpm (10 minute) to isolate unexploited graphene oxide (GO), then the supernatant solution was transferred to other centrifuging tube and centrifuged at 4000 rpm for 30 minutes to get golden color solid. The solid material was washed thoroughly by repeated centrifugation with deionized water (till the *pH* of solution becomes 6.6). Finally, the solid material was dried under reduced pressure to obtain 3.67 g of GO as orange gold color solid.

2.2. Synthesis of sulphonated graphene oxide (SGO)

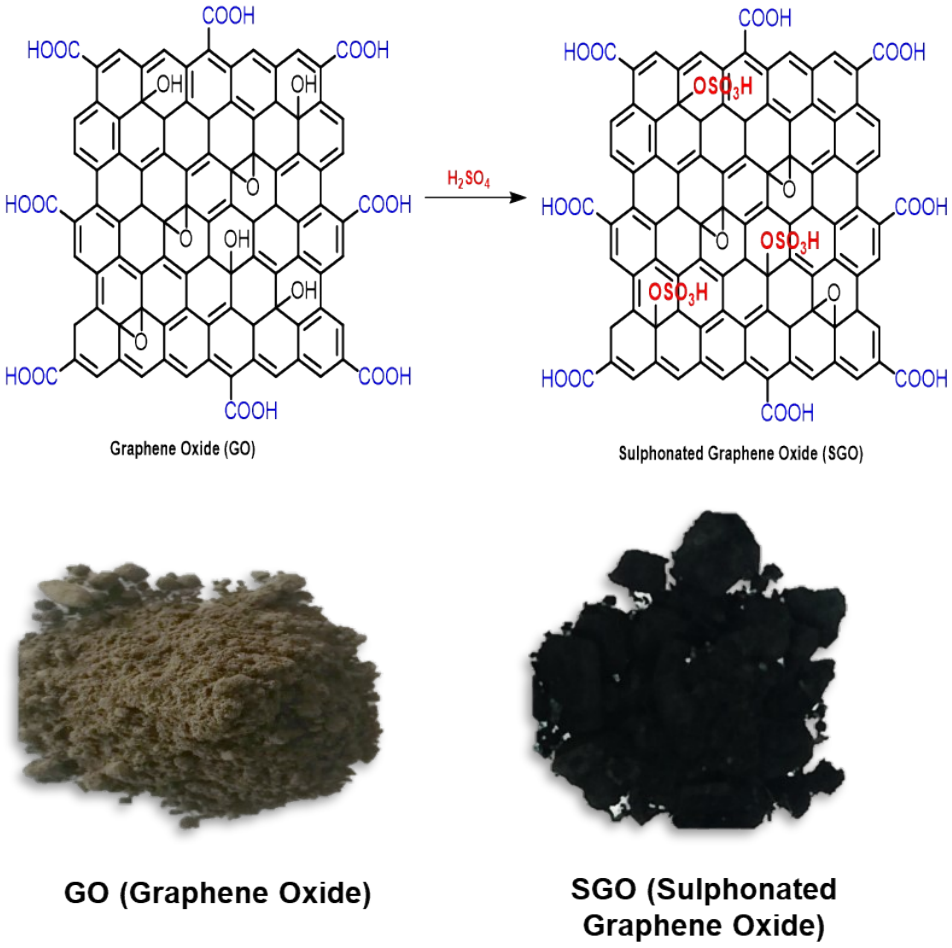

Figure S1. Scheme and snapshot of the synthesized GO & SGO catalyst.

Sulfonated graphene oxide (SGO) was prepared by following the reported protocol.[5] Accordingly, GO (2.0 g) dispersed in chloroform (50 mL) was sonicated for 1h. After sonication, to the dispersed GO suspension, chlorosulfonic acid (0.5 g, 1.5 mL) was added carefully. The solution was then immediately stirred and refluxed for 4 h at 70 °C. The resulting suspension was cooled, and then filtered (centrifuged) out and washed with excess ethanol to remove organic impurities on the surface and water until the pH of the filtrate became neutral. The sample was then dried at 120 °C for 12 h in a vacuum oven to provide 1.4 g of sulphonated graphene oxide.

2.3. Characterization of GO and SGO

Scanning electron microscopic analysis of synthesized SGO-catalyst: Field emission scanning electron microscopy (FESEM) was performed on a Carl Zeiss SIGMA HD field-emission scanning electron microscope.

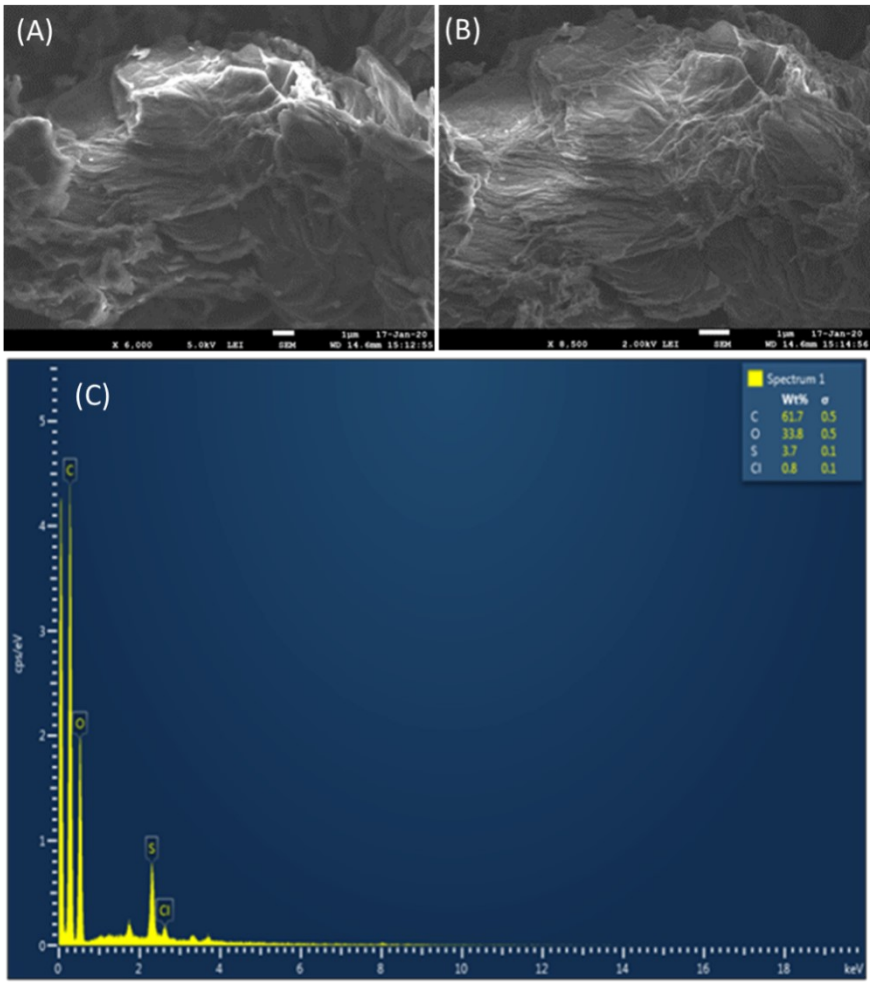

Figure S2. Scanning electron microscopy (SEM) view of the highly efficient catalyst SGO; (A & B) low- and high-resolution SEM image; (C) EDX spectra.

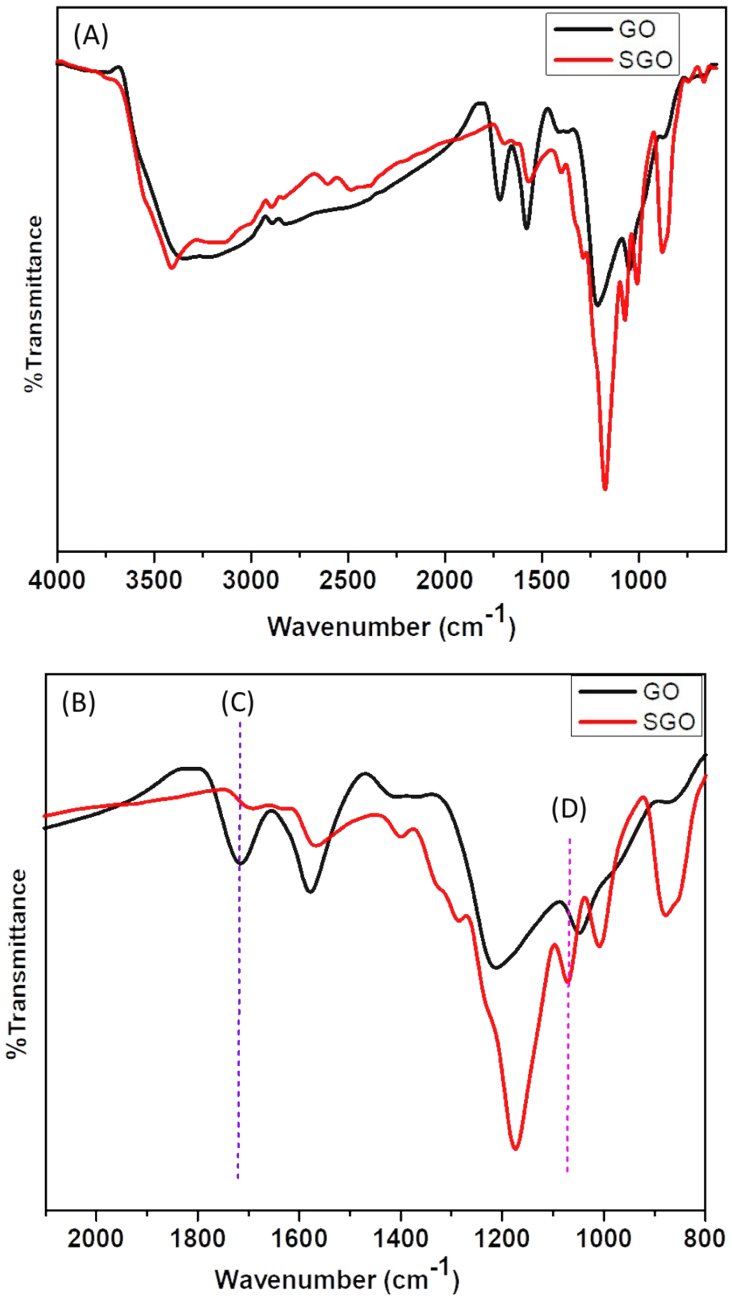

IR data of GO and SGO: ATR-IR spectroscopy was used to characterize the surface feature of the particles. The spectra were acquired using a Perkin Elmer ATR-IR spectrometer. A small drop of test sample was placed on smart gate surface over wave numbers ranging from 650 to 4000 cm^{-1}. The IR spectra of these two samples exhibit similar characteristic peaks as shown in Fig. S3.) Compared with GO, SGO exhibits an additional band at 1090 cm^{-1}, which is associated with a S=O bond, indicating the successful grafting of SO_3H groups onto graphene oxide.[6] The reduced peak at 1720 cm^{-1} for SGO is assigned to a C=O bond, attributed to the reduced carbonyl functionality on the samples due to heating while the sulphonation reaction or during the drying process.[6]

Figure S3. Comparative ATR spectra of synthesized catalyst; (A) synthesized composites (GO & SGO) (B) Determination of the particular spectral region; and (C) dotted highlight region representing an reduced band at 1720 cm^{-1}, which is associated with a C=O bond;(D) dotted highlight region representing an additional band at 1090 cm^{-1}, which is associated with a S=O bond.

X-ray photo-electron spectroscopy (XPS) of highly efficient integrated SGO Catalyst: Fig. S4 shows the X-ray photoelectron spectrum (XPS) of SGO, which gives signals mainly associated with C1s, O1s, and S2p, confirming the presence of a sulphur element in SGO. The high resolution C1s XPS spectrum (Fig. S4A) shows peaks at 284.5, 286.0, 288.4, and 289.3eV. which are attributed to the non-oxygenated ring carbon, the carbon in the C–O bond, the carbonyl carbon, and the carboxylate carbon, respectively. Obviously, the peak at 284.7 eV is dominant, suggesting that most of the oxygen-containing functional groups have been successfully removed in SGO.[6] The high resolution O1s XPS spectrum (Fig. S4B)[7] shows peaks at 529.9, 530.5 and 531.1 eV, which are attributed to C(O) OH, C=O, and C- O.(Fig. S4C) shows the S2p spectrum of SGO, The SGO displays a peak at 167.61 eV associated with an S–O bond Fig. S4B.[5]

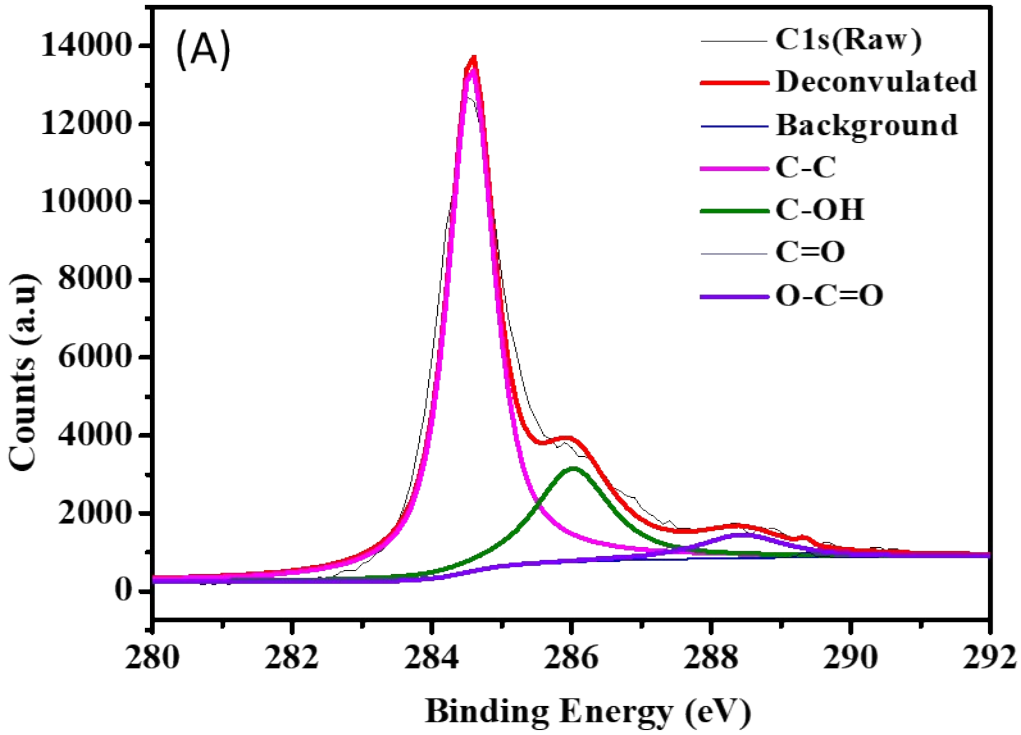

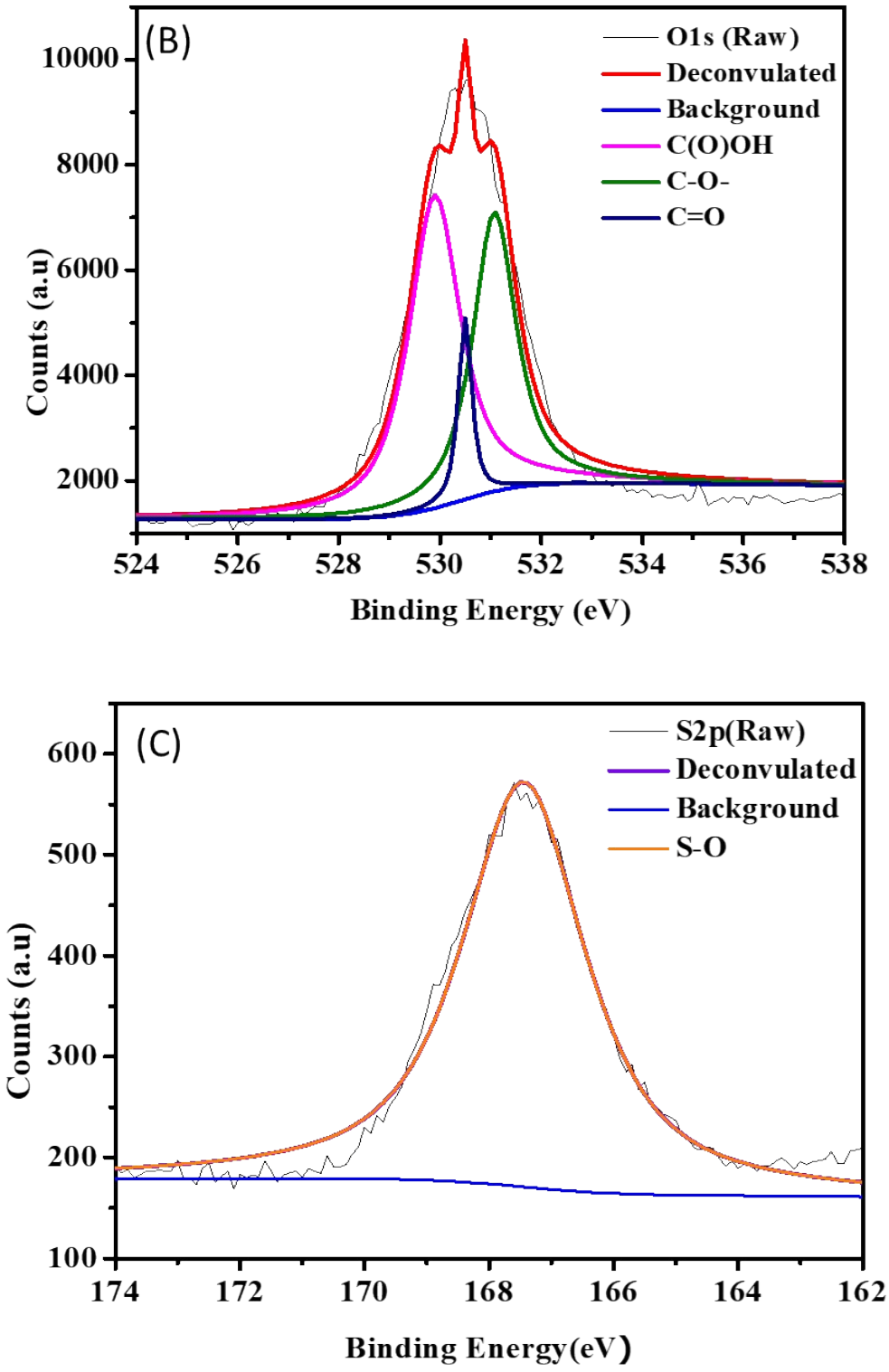

Figure S4. XPS data of the synthesized the catalyst SGO; (A) C1s spectra; (B)O1s spectra; (C)S2p spectra.

Raman spectra of GO & SGO:

Fig. S5 shows the Raman spectra of GO and SGO. GO shows peaks at 1594 and 1363 cm^{-1},[6] which are attributed to the G band (the vibration of sp^2carbon atoms in a graphitic 2D hexagonal lattice) and the D band (the vibrations of sp^3carbon atoms of defects and disorder), respectively SGO exhibit similar Raman spectra to GO, but their intensity ratios of D to G bands are a little different (Fig. S5A & S5B). In our study, the I_D/I_G ratio of the SGO (Fig. S5B) is higher than that of GO (Fig. S5A) as a result of the chemical modification of the GO surface with SO_3H groups, in accordance with previously reported literature.[8-9] The ratio between the intensity of D band (ID) to G band (IG) increased from 0.99 for GO to 1.03 for SGO.

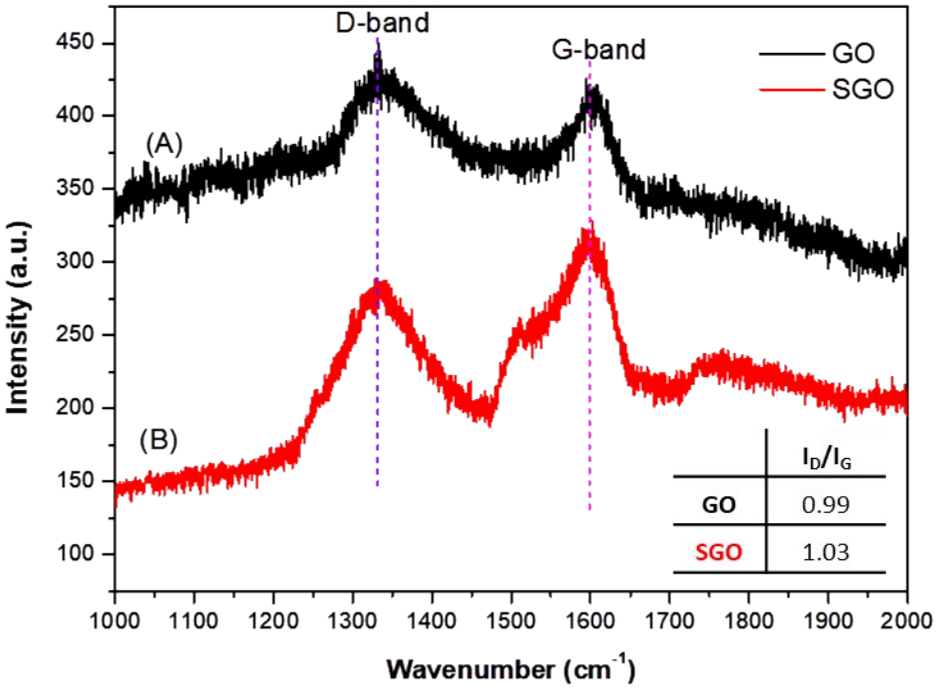

Figure S5. Raman spectra of (A) GO and (B) SGO.

X-ray diffraction patterns (XRD) spectra of GO & SGO:

XRD Spectra: Powder X-ray diffraction patterns (XRD) of the GO and SGO were recorded on a Bruker AXS diffractometer (D8 advance) at a generator voltage of 40 kV and current 30 mA using Cu-Kα radiation (λ = 1.5406 Å). Fig. S6 shows the XRD patterns of graphene oxide (GO) and Sulphonated graphene oxide (SGO). GO shows a peak at 10.2° according to the reported protocol and the peak at 24.1° associated with sulphonated graphene oxide (SGO) after sulfonation (Fig. S6B), which is indicating the partial removal of oxygen functionalities between the graphitic layers.[10,6]

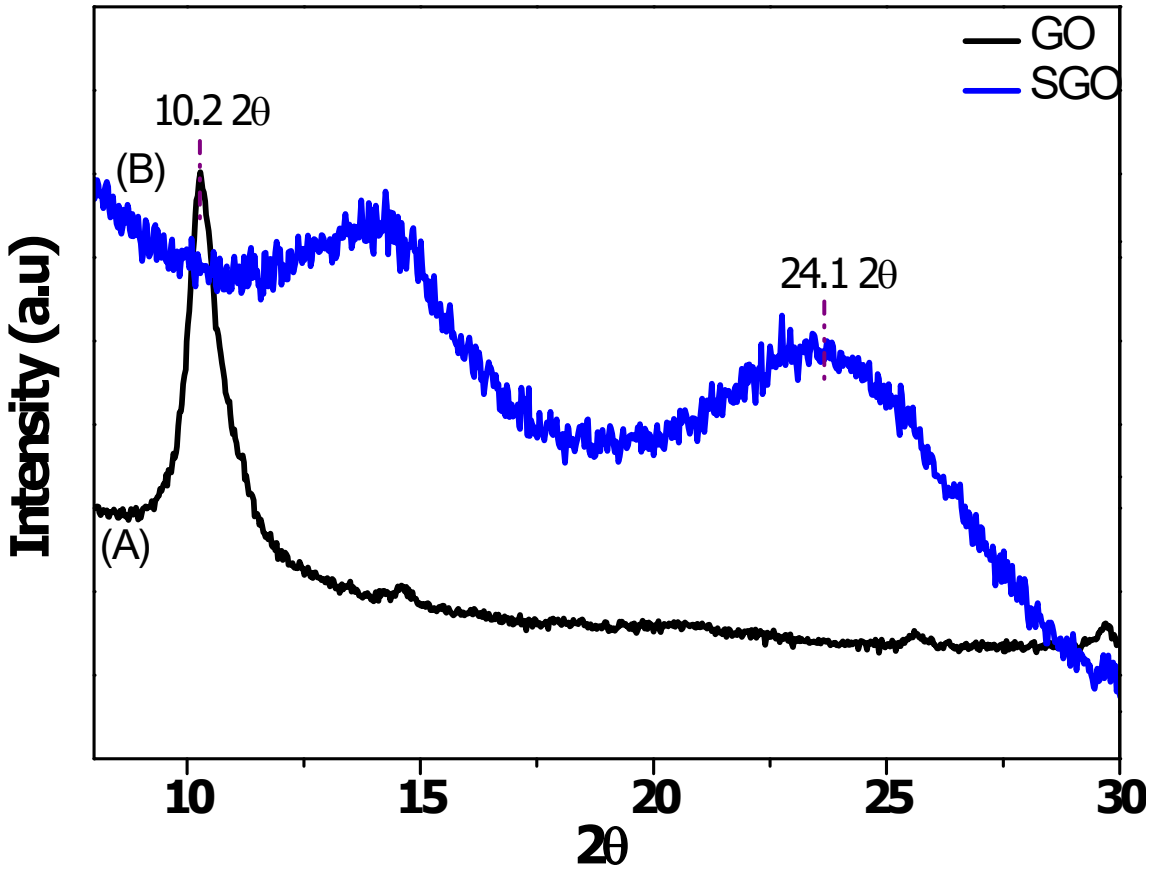

Figure S6. X-Ray diffractometry analysis of the synthesized (A) GO and (B) SGO

3. Continuous-flow tandem catalysis reaction for the synthesis of synthesis of pyrazolo pyrimidinone (4a):

3.1. Synthesis of starting materials 2-ethoxybenzaldehyde (2a):

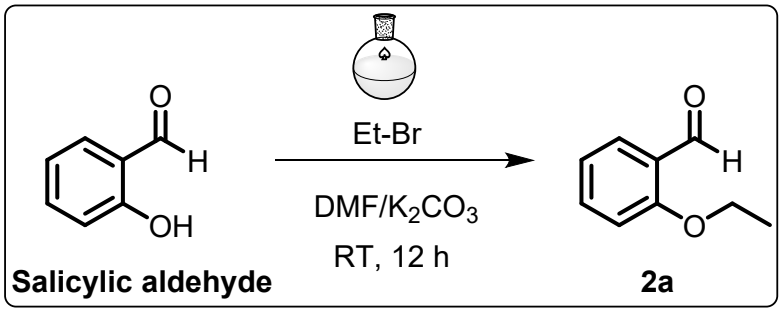

Scheme S1. General synthetic scheme 2-ethoxybenzaldehyde (**2a**).

Previously reported method has been applied for the synthesis of 2-ethoxybenzaldehyde.[11] To a solution of *o*-hydroxy benzaldehyde (30.0 g, 0.25 mol, 1.0 equiv.) in dry DMF (300 mL), anhydrous K_2CO_3 (69.0 g, 0.5 mol, 2.0 equiv.) was added and stirred for 15 min. To this reaction mixture ethyl bromide (44.5 mL, 0.6 mol, 1.2 equiv.) was added and stirred at ambient temperature for overnight (17 h). After completion of the reaction, water (200 mL) was added to the reaction mixture and extracted with EtOAc (500 mL × 2). The organic layer was washed with water (500 mL) and brine solution (500 mL). The organic phase was dried over anhydrous sodium sulfate, filtered and concentrated. The residue was purified by flash column chromatography hexane/ethyl acetate; 95:05) to provide as a light yellow oily 2-ethoxy benzaldehyde (**2a,** 31 g) in 85% yield.

3.2 Optimization protocols for the cyclization of 2a and 3 for the synthesis of pyrazolo pyrimidinone (4a): To optimize the condensation and cyclization reaction, we have choosen the stock solution of compound **2a** (5.0 g, 33.3 mmol, 1.0 equiv.) and **3** (6.68 g, 36.6 mmol, 1.1 equiv.) in $CHCl_3$(1250 mL), that were taken in a bottle and connected with a HPLC pump as a model flow reaction. The stock solution was passed through the SS-316 catalyst filled metal cartridge (id = 7 mm, length 100 mm, vol = 4 mL) with varied residance time, temperature, and pressure etc. for the reaction to occur (table S1). Various acidic functionalized heterogeneous catalyst (Amberlyst, GO, SGO) were tested for the reaction (Table 1, entries 1-3). After stabilizing the solution flow rate, reaction mixture was then out-flowed wherein the product mixture was collected and evaporated under reduced pressure to remove excess chloroform. The resulting mixture was washed with water (250 mL) and brine solution (250 mL) and extracted through regular protocols. The organic phase was dried over anhydrous sodium sulfate, filtered and concentrated. The residue was purified by flash column chromatography hexane/ethyl acetate; 60:40) to provide a solid of pyrazolo pyrimidinone (**4**).

Table S1: Optimization of compound **4a** synthesis in continuous flow process.

Entry	Flow rate ($\mu Lmin^{-1}$)	Catalyst	Pressure (bar)	Temperature (^oC)	Time (min)	Yield (%)
1	500	SGO	17	120	8	70
2	100	SGO	17	120	40	87
3	250	SGO	5	120	16	NA
4	250	SGO	10	120	16	33
5	**250**	**SGO**	**17**	**120**	**16**	**87**
6	250	SGO	17	60	16	NA
7	250	SGO	17	80	16	5
8	250	SGO	17	100	16	53
9	250	SGO	17	140	16	80
10	250	SGO	32	120	16	84
11	Batch	SGO	No	reflux	1440	78

Reaction condition: Feed solution molar ratio [**2a**: **3**: $CHCl_3$ (1: 1.1: 236); 0.053 *M* in $CHCl_3$]; catalyst (1 g) filled SS-cartridge (id = 7 mm, length 100 mm, vol = 4 mL); temperature 120 ^oC; under 17 bar pressure; Yields are based on the isolated yields; NA = yields are less than 2%.

Table S2. Comparative pyrazolo pyrimidinones synthesis performance of batch and continuous flow process.

Entry	Process	Time (h)	Yield (%)	Ref.
1	Batch	38	51	[12]
2	Batch	0.25	60	[13]
3	Batch	9	90	[14]
4	Batch	8	81	[15]
5	Batch	2.5	72	[16]
6	Batch	6	76	[17]
7	**Flow (our study)**	**0.26**	**85**	**This study**

3.3. Substrate scope of 4(a-g) of continuous flow cascade condensation and cyclization reaction:

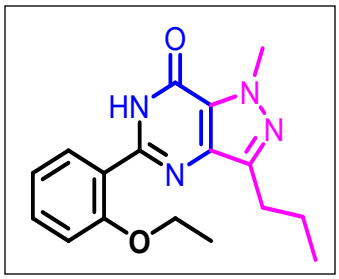

5-(2-Ethoxyphenyl)-1-methyl-3-propyl-1,6-dihydro-7H-pyrazolo[4,3-d] pyrimidin-7-one (4a): A solution of compound **2a** (0.1 g, 0.66 mmol, 1.0 equiv.) and **3** (0.136 g, 0.366 mmol, 1.1 equiv.) in $CHCl_3$ (25 mL), were taken in a bottle and connected with a HPLC pump. A single SS-316 catalyst cartridge reactor (vol. =4 mL) was assembled and joined to the other components of the continuous flow system. The stock solution was infused with a flow rate of 0.25 mL min^{-1}, in accordance with the residance time and passed through an acidic functionalized heterogeneous catalyst [SGO filled SS-cartridge (id = 7 mm, length 100 mm, vol = 4 mL)]; for the reaction to occur. A residence time of 16 min, temperature 120 °C; under 17 bar pressure was found to be enough for the cyclization of the compound **2a** to form the compound **4a** (Table S1). Under the stabilized state, the outflowed product was collected in round bottom flask and evaporated under reduced pressure to remove excess chloroform. The resulting mixture was diluted with chloroform (50 mL × 2), washed with water (25 mL) and brine solution (25 mL). The organic phase was dried over anhydrous sodium sulfate, filtered and concentrated. The residue was purified by flash column chromatography hexane/ethyl acetate; 60:40) to provide an off-white solid (176 mg, 85%). m.p. = 122-124 ºC; The spectra data matched with values reported in the literature.[18]

^{1}H NMR (400 MHz, $CDCl_3$) δ 11.12 (s, 1H), 8.47 (dd, *J* = 7.9, 1.8 Hz, 1H), 7.45 (ddd, *J* = 8.9, 7.4, 1.8 Hz, 1H), 7.17 – 7.12 (m, 1H), 7.04 (d, *J* = 8.3 Hz, 1H), 4.33 – 4.28 (m, 2H), 4.27 (s, 3H), 2.96 – 2.91 (m, 2H), 1.88 (dd, *J* = 15.0, 7.5 Hz, 2H), 1.60 (t, *J* = 7.0 Hz, 3H), 1.03 (t, *J* = 7.4 Hz, 3H).

^{13}C NMR (126 MHz, $CDCl_3$) δ 156.50, 153.97, 148.41, 146.66, 138.75, 132.41, 131.09, 124.49, 121.88, 120.24, 112.95, 65.32, 38.20, 27.85, 22.42, 14.75, 14.11.

MS (ESI): *m/z* found: 313.10$[M+H]^+$.

HRMS (ESI): *m/z* calcd for $C_{17}H_{21}N_4O_2$ $[M]^+$: 313.1665, found: 313.1661.

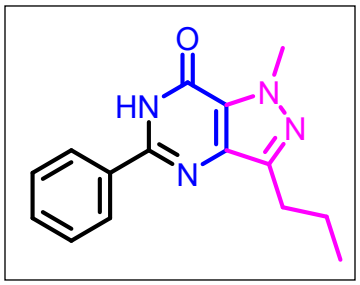

1-Methyl-5-phenyl-3-propyl-1,6-dihydro-7H-pyrazolo[4,3-d] pyrimidin-7-one(4b): Compound**4b** was prepared according to representative procedure given in above for example **4a,** starting from benzaldehyde (0.66 mmol). The crude material was purified by silica gel column chromatography (hexane/ethyl acetate; 70:30) to provide a white solid (141 mg, 80%) m.p. = 221-223 ºC; The spectra data matched with values reported in the literature.[18]

^{1}H NMR (400 MHz, $CDCl_3$) δ 11.30 (s, 1H), 8.18 – 8.11 (m, 2H), 7.53 (dd, *J* = 5.1, 1.8 Hz, 3H), 4.29 (s, 3H), 2.99 – 2.91 (m, 2H), 1.88 (dd, *J* = 15.1, 7.5 Hz, 2H), 1.03 (t, *J* = 7.4 Hz, 3H).

^{13}C NMR (101 MHz, $CDCl_3$) δ 155.71, 149.51, 146.95, 139.33, 132.91, 131.09, 128.96, 127.12, 124.40, 38.22, 27.77, 22.42, 14.08.

MS (ESI): *m/z* found: 269.05$[M+H]^+$.

HRMS (ESI): *m/z* calcd for $C_{15}H_{17}N_4O$ $[M]^+$: 269.1402, found: 269.1396.

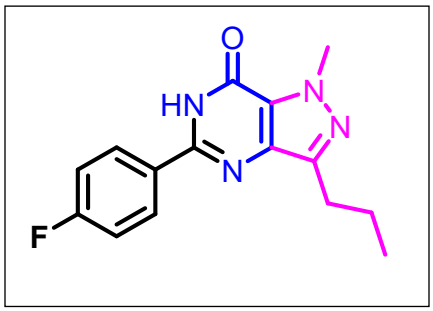

5-(4-Fluorophenyl)-1-methyl-3-propyl-1,6-dihydro-7H-pyrazolo[4,3-d] pyrimidin-7-one(4c): Compound**4c** was prepared according to representative procedure in above example **4a,** starting from 4-fluoro benzaldehyde (0.66 mmol). The crude material was purified by silica gel column

chromatography (hexane/ethyl acetate; 70:30) to provide **4c** as an off-white solid (155 mg, 82%) m.p. = 206-208ºC; The spectra data matched with values reported in the literature.[18,19]

^{1}H NMR (400 MHz, $CDCl_3$) δ 11.26 (s, 1H), 8.15 (d, *J* = 4.5 Hz, 2H), 7.21 (t, *J* = 8.5 Hz, 2H), 4.29 (s, 3H), 2.96 – 2.91 (m, 2H), 1.87 (dd, *J* = 15.1, 7.5 Hz, 2H), 1.03 (t, *J* = 7.4 Hz, 3H).

^{13}C NMR (101 MHz, $CDCl_3$) δ 164.60 (d, *J* = 252.50 Hz), 155.73, 148.56, 146.91, 139.25, 129.35(d, *J* = 9.10 Hz), 116.03 (d, *J* = 22.22 Hz), 38.22, 27.76, 22.40, 14.07.

^{19}F NMR (471 MHz, $CDCl_3$) δ -108.85 (s).

MS (ESI): *m/z* found: 287.05$[M+H]^+$.

HRMS (ESI): *m/z* calcd for $C_{15}H_{16}N_4OF$ $[M+H]^+$: 287.1308, found: 287.1306.

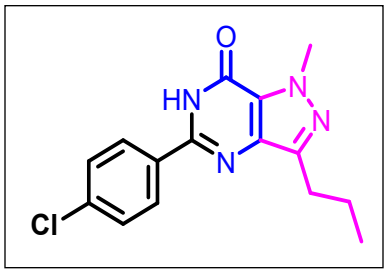

5-(4-Chlorophenyl)-1-methyl-3-propyl-1,6-dihydro-7H-pyrazolo[4,3-d]pyrimidin-7-one(4d): Compound **4d** was prepared according to representative procedure in above example **4a**,starting from 4-chloro benzaldehyde (0.66 mmol). The crude material was purified by silica gel column chromatography (hexane/ethyl acetate; 70:30) to provide a fluffy white solid (167 mg, 84%); m.p. = 239-241 ºC; The spectra data matched with values reported in the literature.[18, 20, 21]

^{1}H NMR (400 MHz, $CDCl_3$) δ 11.28 (s, 1H), 8.11 (d, *J* = 8.7 Hz, 2H), 7.49 (d, *J* = 8.7 Hz, 2H), 4.29 (s, 3H), 2.95 – 2.91 (m, 2H), 1.87 (dd, *J* = 15.1, 7.5 Hz, 2H), 1.03 (t, *J* = 7.3 Hz, 3H).

^{13}C NMR (101 MHz, $CDCl_3$) δ 155.75, 148.40, 147.01, 139.23, 137.36, 131.35, 129.14, 128.49, 124.32, 38.25, 29.75, 27.76, 22.39, 14.07.

MS (ESI): *m/z* found: 303.00$[M+H]^+$.

HRMS (ESI): *m/z* calcd for $C_{15}H_{16}N_4OCl$ $[M+H]^+$: 303.1013, found: 303.0998.

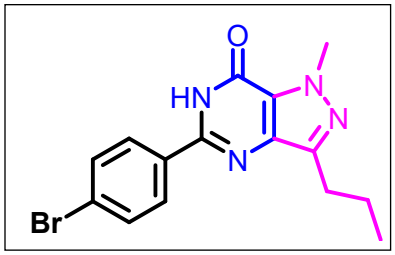

5-(4-Bromophenyl)-1-methyl-3-propyl-1,6-dihydro-7H-pyrazolo[4,3-d] pyrimidin-7-one (4e): Compound **4e** was prepared according to representative procedure in above example **4a,** starting from 4-bromo benzaldehyde (0.66 mmol). The crude material was purified by silica gel column chromatography (hexane/ethyl acetate; 70:30) to provide **4e** as a white solid (183 mg, 80%); m.p. = 246-248ºC; The spectra data matched with values reported in the literature.[20]

^{1}H NMR (400 MHz, $CDCl_3$) δ 10.94 (s, 1H), 8.01 (d, *J* = 5.0 Hz, 2H), 7.66 (d, *J* = 5.9 Hz, 2H), 4.29 (s, 3H), 2.93 (t, *J* = 7.5 Hz, 2H), 1.87 (dd, *J* = 14.7, 7.3 Hz, 2H), 1.03 (t, *J* = 7.3 Hz, 3H).

^{13}C NMR (101 MHz, $CDCl_3$) δ 155.53, 148.37, 147.04, 139.16, 132.20, 131.79, 128.64, 125.79, 124.82, 124.41, 38.34, 27.76, 22.39, 14.07.

MS (ESI): found: *m/z* 348.95(M^++2).

HRMS (ESI): *m/z* calcd for $C_{15}H_{16}N_4OBr$ $[M+H]^+$: 347.0507, found: 347.0504.

5-(2-Methoxyphenyl)-1-methyl-3-propyl-1,6-dihydro-7H-pyrazolo[4,3-d]pyrimidin-7-one(4f): Compound **4f** was prepared according to representative procedure in above example **4a,**starting from 2-methoxy benzaldehyde (0.66 mmol). The crude material was purified by silica gel column chromatography (hexane/ethyl acetate; 70:30) to provide a white solid (163 mg, 83%) m.p. = 139-141 ºC; The spectra data matched with values reported in the literature. [22, 23]

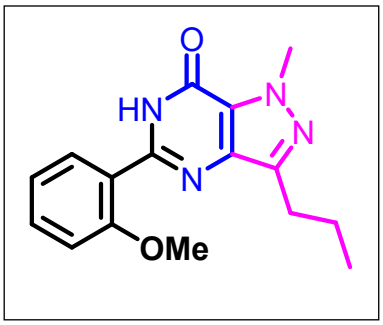

^{1}H NMR (500 MHz, $CDCl_3$) δ 10.88 (s, 1H), 8.46 (dd, *J* = 7.9, 1.8 Hz, 1H), 7.48 (ddd, *J* = 8.4, 7.4, 1.8 Hz, 1H), 7.17 – 7.14 (m, 1H), 7.06 (d, *J* = 7.9 Hz, 1H), 4.27 (s, 3H), 4.05 (s, 3H), 2.95 – 2.91 (m, 2H), 1.87 (dd, *J* = 15.1, 7.5 Hz, 2H), 1.03 (t, *J* = 7.4 Hz, 3H).

^{13}C NMR (101 MHz, $CDCl_3$) δ 157.08, 154.01, 148.28, 146.67, 138.72, 132.49, 131.20, 124.46, 121.94, 120.23, 111.85, 56.21, 38.25, 27.84, 22.42, 14.10.

MS (ESI): *m/z* found: 299.05$[M+H]^+$.

HRMS (ESI): *m/z* calcd for $C_{16}H_{19}N_4O_2$ $[M+H]^+$: 299.1508, found: 299.1505.

1-Methyl-3-propyl-5-(2,3,4-trimethoxyphenyl)-1,6-dihydro-7H-pyrazolo[4,3-d]pyrimidin-7-one(4g): Compound **4g** was prepared according to representative procedure in above example **4a**, starting from 2,3,4-trimethoxy benzaldehyde (0.66 mmol). The crude material was purified by silica gel column chromatography (hexane/ethyl acetate; 70:30) to provide a white solid (191mg, 81%) m.p. = 175-177ºC.

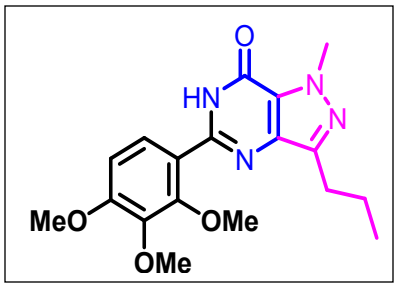

^{1}H NMR (500 MHz, $CDCl_3$) δ 10.97 (s, 1H), 8.14 (d, *J* = 8.9 Hz, 1H), 6.85 (d, *J* = 9.2 Hz, 1H), 4.27 (s, 3H), 4.02 (s, 3H), 3.94 (s, 3H), 3.92 (s, 3H), 2.93 – 2.90 (m, 2H), 1.87 (dd, *J* = 15.1, 7.6 Hz, 2H), 1.03 (t, *J* = 7.3 Hz, 3H).

^{13}C NMR (101 MHz, $CDCl_3$) δ 156.19, 154.12, 152.15, 147.99, 146.50, 142.10, 138.75, 128.19, 125.59, 117.64, 108.44, 61.99, 61.13, 56.20, 38.24, 27.84, 22.41, 14.12.

MS (ESI): *m/z* found: 359.10$[M+H]^+$.

HRMS (ESI): *m/z* calcd for $C_{18}H_{23}N_4O_4$ $[M+H]^+$: 359.1719, found: 359.1713.

3.4. Mechanistic study:

To gain insight into the reaction pathway for the SGO, we have performed a control experiment with electron withdrawing substituent 4-bromo benzaldehyde as model substrate. Under the optimized reaction condition and in a short residence time of 4 min. imine intermediate was obtained (Figure S7, Figure S45-47). The imine intermediate (Schiff adduct B, Figure S7) was further converted into corresponding cyclized product via the intramolecular addition of amide amine onto imine followed by oxidation to get the pyrazolo pyrimidinone. To check the oxidative pathway (involvement of aerial oxidation), when an experiment was performed under an argon atmosphere with the Schiff Adduct B, the yield of the reaction product was found to be 65%, and the product formation might be attributed to the dissolved oxygen in the solvent.

Control experiment: A solution of compound 4-bromo benzaldehyde (0.1 g, 0.54 mmol, 1.0 equiv.) and **3** (0.108 g, 0.59 mmol, 1.1 equiv.) in $CHCl_3$ (25 mL), were taken in a bottle and connected with a HPLC pump. A single SS-316 catalyst cartridge reactor (vol. =4 mL) was assembled and joined to the other components of the continuous flow system. The stock solution was infused with a flow rate of 1 mL min^{-1}, in accordance with the short residance time and passed through an acidic functionalized heterogeneous catalyst [SGO filled SS-cartridge (id = 7 mm, length 100 mm, vol = 4 mL)]; for the reaction to occur. To the obtained Imine intermediate, we have conducted the control experiment under the short residence time of 4 min, temperature 120 ^{o}C; with 17 bar pressure and the outflowed product was collected in round bottom flask and evaporated under reduced pressure to remove excess chloroform. The resulting mixture was diluted with chloroform (50 mL × 2), washed with water (25 mL) and brine solution (25 mL). The organic phase was dried over anhydrous sodium sulfate, filtered and the crude reaction mixture was analyzed by LC-MS (Figure **S47**). Further the crude mixture was purified by flash

column chromatography and hexane/ethyl acetate; 70:30) to provide a light-yellow solid of imine intermediate (66 mg, 35%) m.p. = 154-156 ºC.

.

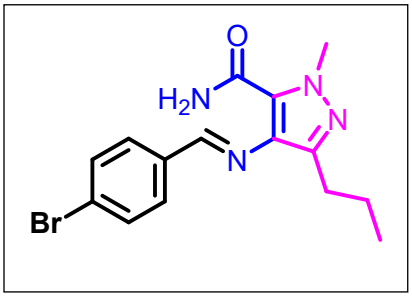

^{1}H NMR (400 MHz, $CDCl_3$) δ 8.49 (s, 1H), 8.43 (s, 1H), 7.69 – 7.59 (m, 4H), 6.04 (s, 1H), 4.20 (s, 3H), 2.74 – 2.69 (m, 2H), 1.74 (dt, *J* = 14.7, 7.4 Hz, 2H), 1.01 (t, *J* = 7.4 Hz, 3H).

^{13}C NMR (101 MHz, $CDCl_3$) δ 161.66, 158.23, 141.10, 134.86, 132.32, 131.22, 129.55, 128.66, 126.32, 40.21, 29.62, 21.86, 14.12.

MS (ESI): *m/z* found: 349.06$[M+H]^+$.

HRMS (ESI): *m/z* calcd for $C_{15}H_{18}BrN_4O$ $[M+H]^+$: 348.0586, found: 348.0599.

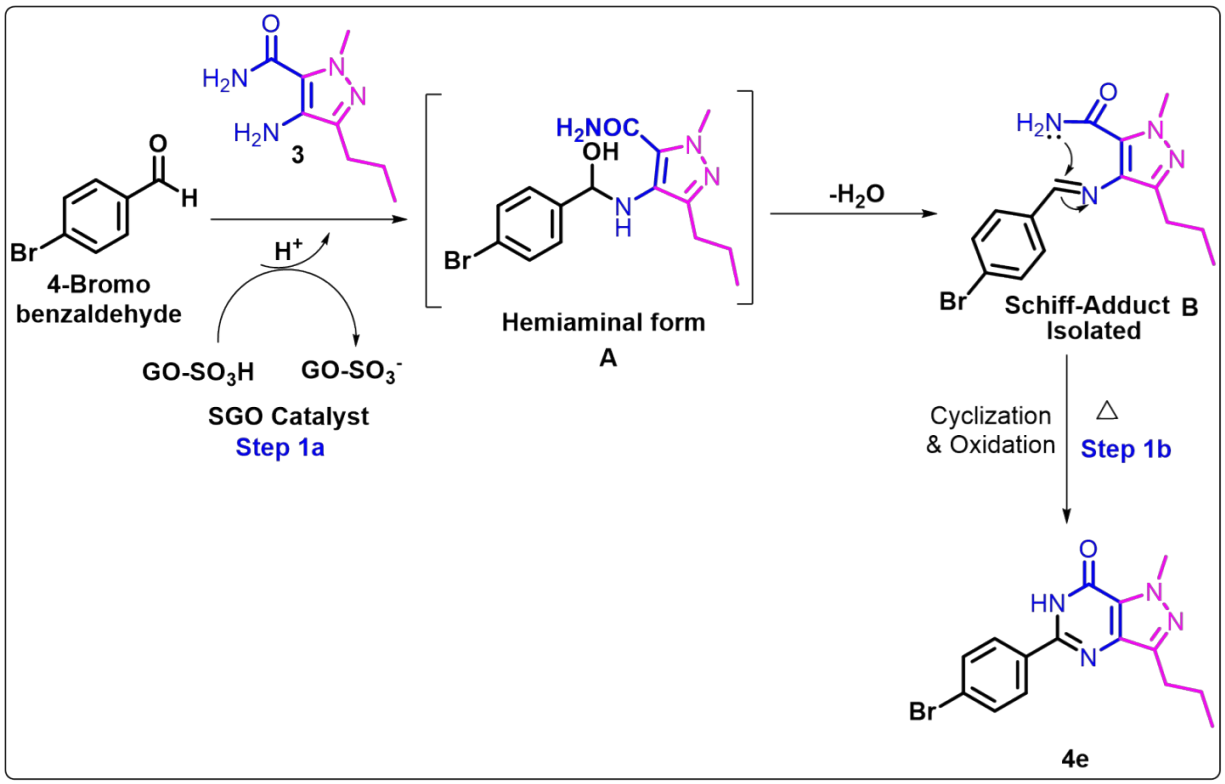

Figure S7. Possible mechanism of Step-1 a two-step protocol (condensation and cyclization) for the formation of pyrazolo pyrimidinones using SGO.

4. Continuous flow sulphonation and extraction and separation:

4.1. Individual protocol for sulphonation and extraction, separation: A single PTFE reactor coil (vol. = 5 mL) was assembled and joined to the other components of the continuous flow system to ensure efficient mixing. The feed solution was prepared in a volumetric flask under anhydrous condition before injected into the capillary microreactor with a *T*-mixer using two separate pumps. The feed solution of **4a** (0.1 g, 0.32 mmol, 1.0 equiv.) in $CHCl_3$ (0.032 *M*) and a solution of HSO_3Cl **(5)** (0.32 mmol, 1.0 equiv.) in $CHCl_3$ (0.032 *M*) were introduced separately with the help of pump. The syringe pump was set to infuse at 0.25 mL min^{-1}. The solution passing through the integrated continuous flow system was collected for a 2 min equilibration period, before a sample was collected. After completion, the collected reaction mixture was evaporated under reduced pressure to remove excess chloroform. The resulting mixture was diluted with chloroform (25 mL × 2), washed with water (10 mL) and brine solution (10 mL). The organic phase was dried over anhydrous sodium sulfate, filtered and concentrated.

Table S3: Optimization of the sulphonation reaction.

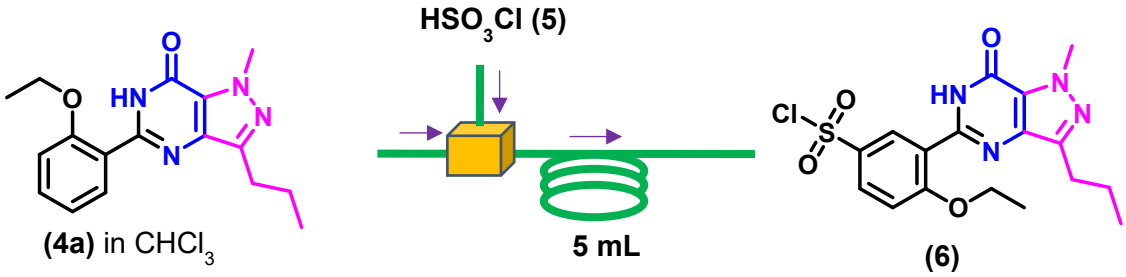

Entry	Flow rate (µL/min)		Residence time (Min.)	Yield (%)
	4a	HSO_3Cl (5)		
1	2500	2500	1	50
2	1250	1250	2	65
3	500	500	5	80
4	**250**	**250**	**10**	**88**
5	100	100	25	88

Reaction condition: stock solution of **4a** (0.032 M in $CHCl_3$); stock solution of **5** (0.032 M in $CHCl_3$); PTFE tubing (id: 1 mm and length 6.4 meter); room temperature 25±5 °C; yields are based on the isolated yields.

4.2. Micro-patterned micro separator: During the reaction process, we had to use a strong acid $ClSO_3H$ for chloro sulphonation step, further to remove the excess amount of the chlorosulfonic acid and to minimize the post-down stream purification process and reduce tedious work up steps, we further appended continuous aqueous quenching, droplet based extraction which becomes unfavorable for the polyimide film based micro channel that is used generally for separation.[24-26] Keeping this drawback in mind, we have fabricated a micro separator with a stainless steel body Figure 2, part 1 (60 mm length × 60 mm width × 10 mm thickness). The second Teflon (60 mm length × 60 mm width × 2 mm thickness) layer was made with a laser cutter, to (Figure S7, parts 2 and 3) protect the stainless steel from the corrosive acid/base. The third layer consists of a laser-grooved Teflon film (60 mm × 60 mm × 1 mm thickness) zig zag groove with rectangular shape (2 mm × 80.0 mm). To align the film patterns, the four corners of each two Teflon film were drilled to make a hole (1 mm diameter). Thereafter, a polypropylene coated polytetrafluoroethylene (PTFE) membrane (Whatmann, 0.45 μm pore, 47 mm dia.) was sandwiched between two Teflon sheets with identical dimensions to fit the groove channels and coupled to each other by inserting metal pins through the holes at the film corners. Finally, the metal holder was tightly screwed to pack all the layers of the device, to ensure no leaks.

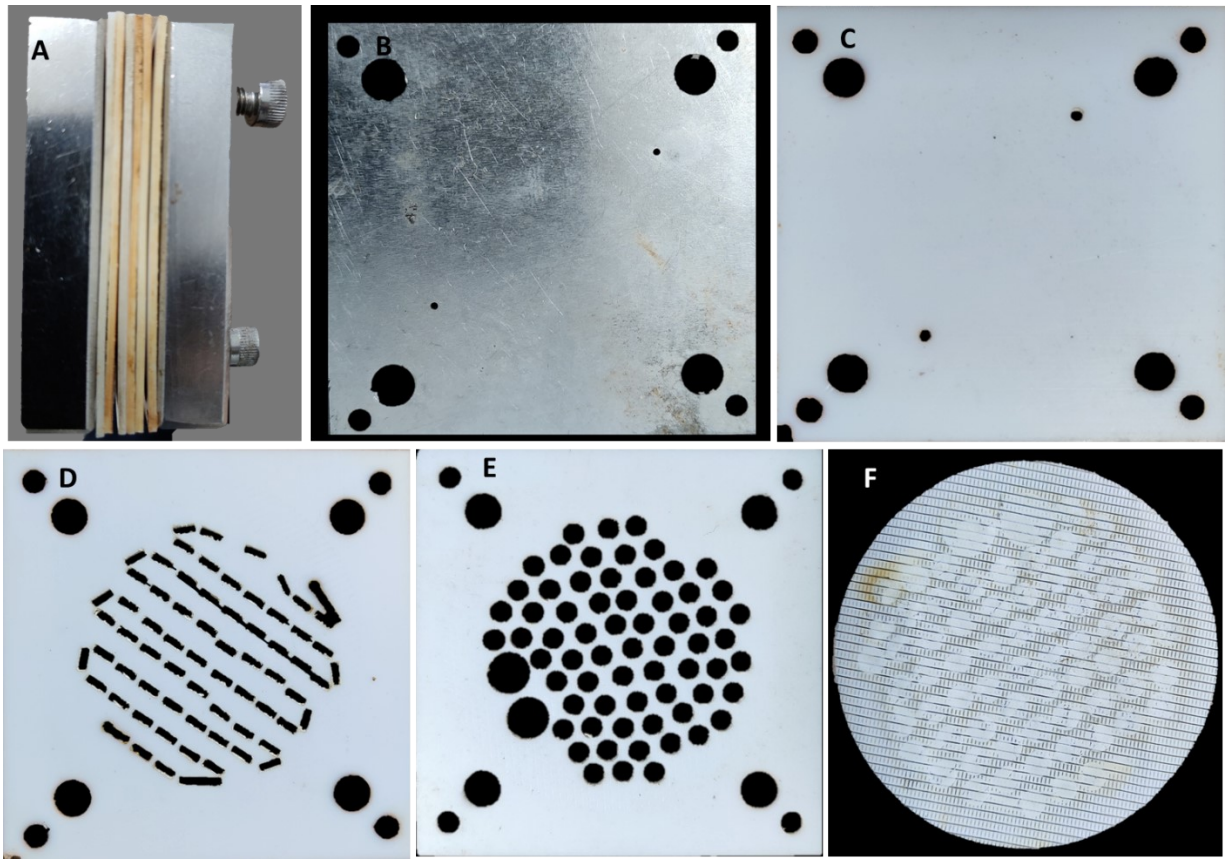

Figure S8. Illustration of a fluoropolymer PTFE membrane micro separation joined between two PTFE films with a laser cut channel; (a) images and components of micro separator; (b) model of micro separator.

Table S4: Optimization for the down-stream process.

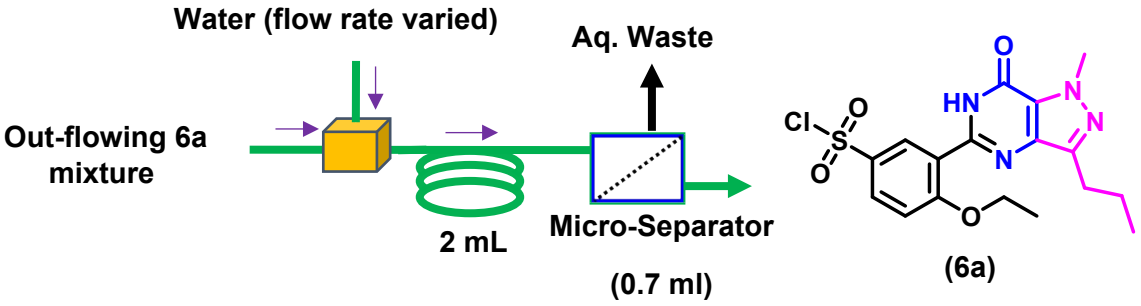

Entry	Flow rate (μL/ min)		Extraction & separation time (min.)	Yield (%)
	Out-flowing 6a mixture	Water		
1	500	3000	0.7	85
2	500	2000	0.9	86
3	**500**	**1500**	**1.08**	**88**

Yields reported are based on LC-MS analysis.

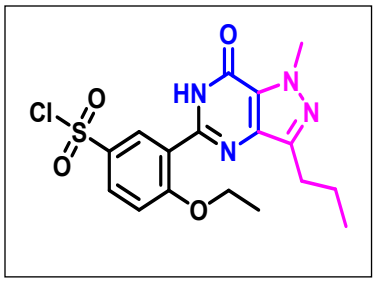

4.3. Synthesis of 4-Ethoxy-3-(1-methyl-7-oxo-3-propyl-6,7-dihydro-1H-pyrazolo[4,3-d] pyrimidin-5-yl) benzene sulfonyl chloride (6) under continuous flow manner. The freshly prepared solution of **4a** (0.3 g, 0.96 mmol, 1.0 equiv.) in $CHCl_3$ (0.032 *M*) and a solution of HSO_3Cl in $CHCl_3$ (0.032 *M*) were introduced PTFE reactor coil (vol. = 5 mL) with a T-mixer using two separate pumps. The flow rate (250 µL/min.) of the **4a** solution was kept at same the rate of HSO_3Cl, in accordance with the stoichiometry of reagent and substrates to occur the sulphonation reaction during 8.9 min of retention time and room temperature with ambiant pressure. Next, the out-flowed reaction mixture was quenched with water with 1.5 mL/min. flow rateand then aquoeous-organic droplet were smoothly passed through perfluoroalkoxy (PFA) tubing (id = 1000 µm, l = 2.5 m, vol. = 2 mL) for the extraction to occur. A retention time of 1.0 min. was found to be enough for the extraction of the compound **6**. Further the aqueous and $CHCl_3$ continuous flow droplet was separated through our previously reported micro-separator(detailed design is shown in Figure S8).[27] The crude material was dried under the reduced pressure and further purified by silica gel column chromatography (hexane/ethyl acetate; 60:40) to provide **6a** as an off-white solid (315 mg, 80%) m.p. =177- 179 ºC. The spectra data matched with values reported in the literature.[28]

^{1}H NMR (300 MHz, $CDCl_3$) δ 10.75 (s, 1H), 9.11 (d, *J* = 2.6 Hz, 1H), 8.11 (dd, *J* = 9.0, 2.6 Hz, 1H), 7.23 (d, *J* = 9.0 Hz, 1H), 4.48 – 4.40 (m, 2H), 4.28 (s, 3H), 2.96 (t, *J* = 7.6 Hz, 2H), 1.87 (dd, *J* = 15.0, 7.5 Hz, 2H), 1.67 (s, 3H), 1.05 (t, *J* = 7.4 Hz, 3H).

^{13}C NMR (101 MHz, $CDCl_3$) δ 160.84, 153.53, 147.28, 145.64, 138.21, 137.60, 131.04, 130.94, 124.53, 121.81, 113.56, 66.65, 38.31, 27.65, 22.38, 14.50, 14.04.

MS (ESI): *m/z* found: 411.15(M^+).

5. Continuous flow amination:

5.1. Individual continuous flow amination reaction: The freshly prepared solution of **6a** (1000 mg, 2.42 mmol, 1.0 equiv.) in $CHCl_3$ (100 mL) and *N*-methyl piperazine**7a** (268 mg, 2.66 mmol, 1.10 equiv.) in $CHCl_3$(100 mL) were introduced into the capillary microreactor with a T-mixer using two separate pumps. Both the solutions passing through the continuous flow system were jointly collected after a 2 min equilibration period. To check the reaction performance, we have varied flow rate (retention time), and different tubular reactor, or plate reactor (details in below) to enhance the mixing the capacity (Table S5). A retention time of 5 min. under room temperature and no pressure was found to be enough for the amination reaction (Table S5, entry 6). We have observed that, when the flow rate was increased there was drop in the yield of the product formation. (Table S5, entry 7). Under the stabilized state, the outflowed product was collected in round bottom flask and evaporated under reduced pressure to remove excess chloroform. The resulting mixture was diluted with chloroform (100 mL × 2), washed with water (50 mL) and brine solution (50 mL). The organic phase was dried over anhydrous sodium sulfate, filtered and concentrated.

5.2. Micro-patterned flow reactor:

Micro flow reactor outer body was fabricated with a stainless-steel body Figure S7, part 1 (220 mm length × 220 mm width × 10 mm thickness). The second Teflon (220 mm length × 220 mm width × 1 mm thickness) layer was made with a laser cutter, to (Figure S8, parts 2 and 3) protect the stainless steel from the corrosive piperazine. The third and fourth layer consists of a laser-grooved teflon film (220 mm × 220 mm × 1 mm thickness) zigzag groove with rectangular shape (vol. 10 ml). To align the film patterns, the four corners of each two Teflon film were drilled to make a hole (1 mm diameter). Thereafter, a repeat of two teflon sheets with identical dimensions

to fit the groove channels and coupled to each other by inserting metal pins through the holes at the film corners. Finally, the metal holder was tightly screwed to pack all the layers of the device, to ensure no leaks.

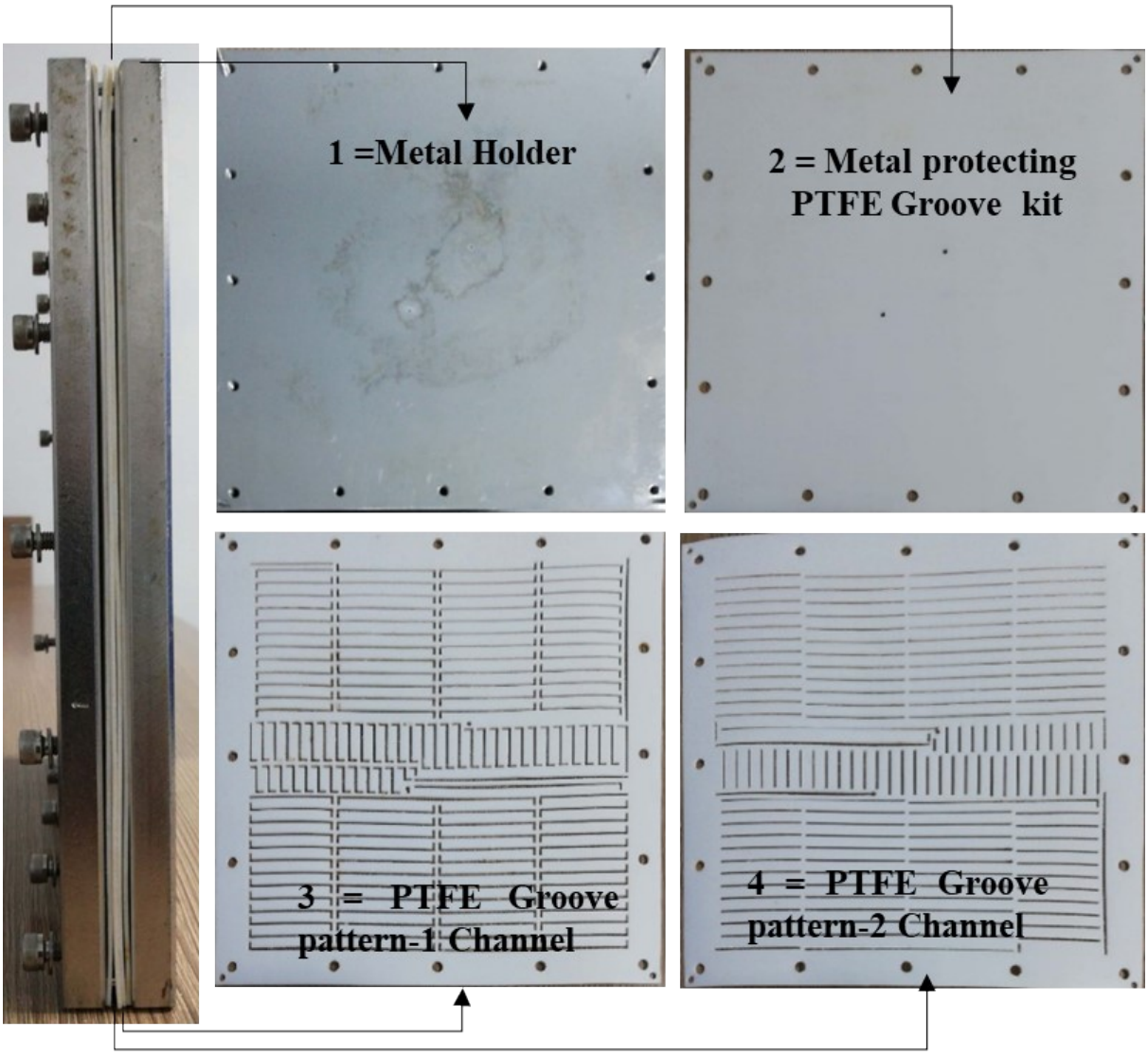

Figure S9. Illustration of a fluoropolymer PTFE micro flow reactor joined between two PTFE films with a laser cut channel; (A) model of micro flow reactor; (B) images and components of micro flow reactor (10 mL).

Table S5. Optimization of amination of sulphonyl chloride compound **6** in continuous flow process.

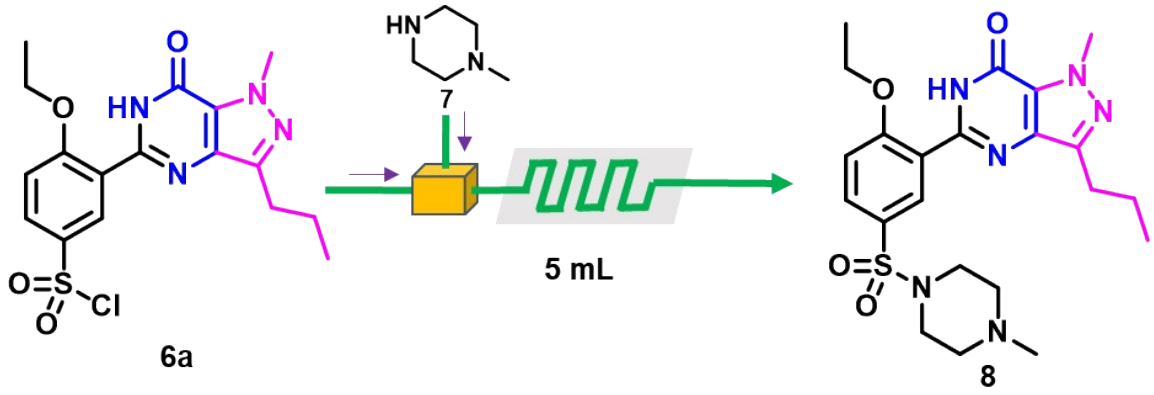

Entry	Flow rate (μL min^{-1})		Residence time	Yield (%)
	6a	**7**	**(min.)**	**Yield**
1	200	200	12.5	92
2	250	250	10	91
3	500	500	5	90
4	750	750	3.33	88
5	1000	1000	2.5	87
6*	**1000**	**1000**	**5**	**94**
7*	2000	2000	2.5	90

Reaction condition: stock solution of **6a** (0.021 *M* in $CHCl_3$); stock solution of **7** (0.021 *M* in $CHCl_3$); PTFE tubing (id: 1 mm and length 6.4 meter); room temperature 25±5 °C; Yields are based on the isolated yields; *represent the high throughput micro-patterned reactor volume 10 mL.

5.3. Optimized reaction condition for the manufacturing of 8a in individual continuous flow approach.

The stock solution of compound **6a** (1.0 g, 2.42 mmol, 1.0 equiv.) and *N*-methyl piperazine **7** (0.268 g, 2.66 mmol, 1.10 equiv.) in chloroform (200 mL), were prepared in a volumetric flask. Both the solutions injected into rectangular PTFE plate reactor (width = 1 mm, height = 1 mm; length = 5-meter, volume = 5 mL × 2) reactor through a pump with flow rate with 1 mL/min. (retention time 5 min.) at room temperature and ambient pressure. The out-flowed reaction was dried under the reduced pressure and finally 94% yield of sildenafil **8a** (Table S5, entry 6) was obtained.

5.4: Integrated continuous flow process system for the cascade condensation, cyclization, sulphonation and amination reaction for the synthesis of 5-(2-ethoxy-5-((4-methylpiperazin-1-yl)sulfonyl)phenyl)-1-methyl-3-propyl-1,6-dihydro-7H-pyrazolo[4,3-d]pyrimidin-7-one (8a):

After the successful completion of the individual reaction optimization in continuous flow manner, we have interconnected all the pre-optimized reactor sets (Figure 3). A stock solution of molar ratios **2a**: **3**: $CHCl_3$ (1: 1.1: 236), was taken in bottle and connected with a HPLC pump. A single SS-316catalyst cartridge reactor (vol. = 4 mL) was assembled and joined to the other components of the continuous flow system. The stock solution is infused with a flow rate of 0.25 mL min^{-1}, in accordance with the retention time passed through an acidic functionalized heterogeneous catalyst [SGO filled SS-cartridge (id = 7 mm, length 100 mm, vol = 4 mL)]; for the reaction to occur. The outflowed product mixture**4a** was directly connected with additional T-junction (T_2) and a solution of HSO_3Cl in $CHCl_3$ (0.032 *M*) were introduced PTFE reactor coil (vol. = 5 mL). The flow rate (250 μL/min.) of the **4a** solution was kept at same the rate of HSO_3Cl, in accordance with previous optimized individual reaction. Next, the out-flowed sulphonated product mixture was quenched at T_3-junction with water (flow rate 1.5 mL/min.) and then aqueous-organic droplet were smoothly passed through perfluoro alkoxy (PFA) tubing (id = 1000 μm, l = 2.5 m, vol. = 2 mL) for the extraction to occur. Further the aqueous and $CHCl_3$ continuous flow droplet was separated through our previously reported micro-separator and organic layer was re-circulated with additional pump. The stock solution of *N*-methyl piperazine **7a** (0.021 *M* in $CHCl_3$,) was directly connected with out-flowed product mixture **6a** at T_4-junction and infusing with the flow rate 1 mL/min into rectangular PTFE plate reactor (width = 1 mm, height = 1 mm; length = 5-meter, volume = 10) reactor. Under the established reaction

conditions, the reaction mixture was then evaporated under reduced pressure. The resulting mixture was diluted with chloroform, washed with water and brine solution. The organic phase was dried over anhydrous sodium sulfate, filtered and concentrated. The crude material was purified by silica gel column chromatography (DCM/MeOH; 95:05) to provide Sildenafil **8a** as a white solid in 65% overall yield obtained in 32.3 min. of retention time; m.p. = 186-188 ºC; The spectra data matched with values reported in the literature.[18,28]

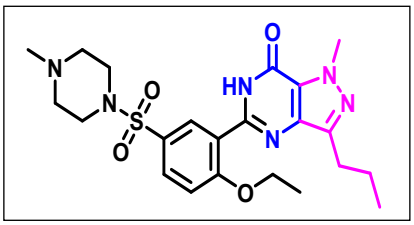

^{1}H NMR (500 MHz, $CDCl_3$) δ 10.87 (s, 1H), 8.78 (d, *J* = 2.2 Hz, 1H), 7.83 (dd, *J* = 8.7, 2.4 Hz, 1H), 7.15 (d, *J* = 8.8 Hz, 1H), 4.36 (q, *J* = 7.0 Hz, 2H), 4.27 (s, 3H), 3.16 (s, 4H), 2.94 – 2.91 (m, 2H), 2.59 (s, 4H), 2.34 (s, 3H), 1.86 (dd, *J* = 15.0, 7.5 Hz, 2H), 1.63 (t, *J* = 7.0 Hz, 3H), 1.02 (t, *J* = 7.4 Hz, 3H).

^{13}C NMR (126 MHz, $CDCl_3$) δ 159.42, 153.70, 146.99, 146.48, 138.38, 131.66, 131.16, 128.79, 124.54, 121.32, 113.09, 66.08, 53.95, 45.66, 45.50, 38.26, 27.76, 22.31, 14.57, 14.07.

MS (ESI): *m/z* found: 475.10$[M+H]^+$.

HRMS (ESI): *m/z* calcd for $C_{22}H_{31}N_6O_4S$ $[M+H]^+$: 475.2127, found: 475.2123.

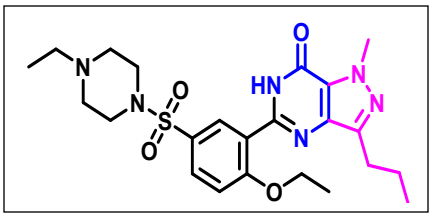

5-(2-Ethoxy-5-((4-ethylpiperazin-1-yl)sulfonyl)phenyl)-1-methyl-3-propyl-1,6-dihydro-7H-pyrazolo[4,3-d]pyrimidin-7-one(8b): Compound **8b** was prepared according to representative procedure given in **5.2** using **6a**(100 mg) and *N*-ethyl piperazine **(7b)**. The crude material was purified by silica gel column chromatography (DCM/MeOH; 95:05) to provide **8b** as a light creamy solid (75 mg, 63%) m.p. = 208-210 ºC; The spectra data matched with values reported in the literature.[28-30]

^{1}H NMR (400 MHz, $CDCl_3$) δ 10.82 (s, 1H), 8.82 (d, *J* = 2.4 Hz, 1H), 7.84 (dd, *J* = 8.7, 2.4 Hz, 1H), 7.15 (d, *J* = 8.8 Hz, 1H), 4.37 (d, *J* = 7.0 Hz, 2H), 4.28 (s, 3H), 3.11 (s, 4H), 2.95 – 2.91 (m, 2H), 2.57 – 2.52 (m, 4H), 2.41 (q, *J* = 7.2 Hz, 2H), 1.86 (d, *J* = 7.5 Hz, 2H), 1.64 (d, *J* = 7.0 Hz, 3H), 1.05 – 1.00 (m, 6H).

^{13}C NMR (101 MHz, $CDCl_3$) δ 159.31, 153.67, 147.03, 146.42, 138.41, 131.76, 131.27, 128.84, 124.52, 121.11, 113.05, 66.13, 51.93, 51.83, 46.11, 38.26, 27.78, 22.30, 14.57, 14.07, 11.94.

MS (ESI): *m/z* found: 489.10$[M+H]^+$.

HRMS (ESI): *m/z* calcd for $C_{23}H_{33}N_6O_4S$ $[M+H]^+$: 489.2284, found: 489.2278.

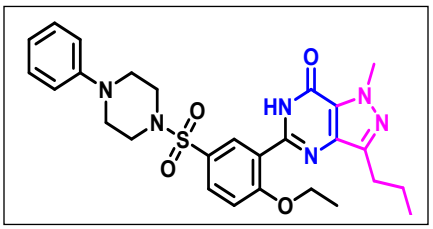

5-(2-Ethoxy-5-((4-phenylpiperazin-1-yl)sulfonyl)phenyl)-1-methyl-3-propyl-1,6-dihydro-7H-pyrazolo[4,3-d]pyrimidin-7-one(8c): Compound **8c** was prepared according to the representative procedure given in **5.2** using **6a** (100 mg) and *N*-phenyl piperazine **(7c)**. The crude material was purified by silica gel column chromatography (DCM/MeOH; 95:05) to provide **8c** as a white solid (78 mg, 60%); m.p. = 203–205 °C; The spectra data matched with values reported in the literature.[19]

^{1}H NMR (400 MHz, $CDCl_3$) δ 10.82 (s, 1H), 8.87 (d, *J* = 2.4 Hz, 1H), 7.88 (dd, *J* = 8.8, 2.4 Hz, 1H), 7.26 – 7.22 (m, 2H), 7.17 (d, *J* = 8.8 Hz, 1H), 6.88 (dd, *J* = 13.4, 7.5 Hz, 3H), 4.39 (q, *J* = 7.0 Hz, 2H), 4.28 (s, 3H), 3.25 (d, *J* = 2.7 Hz, 8H), 2.94 (t, *J* = 7.5 Hz, 2H), 1.87 (dd, *J* = 14.9, 7.4 Hz, 2H), 1.65 (t, *J* = 7.0 Hz, 3H), 1.03 (t, *J* = 7.4 Hz, 3H).

^{13}C NMR (101 MHz, $CDCl_3$) δ 159.42, 153.66, 150.63, 147.04, 146.42, 138.40, 131.73, 131.25, 129.29, 124.53, 121.22, 120.92, 116.94, 113.17, 66.16, 49.23, 46.13, 38.28, 29.73, 27.78, 22.31, 14.58, 14.09.

MS (ESI): *m/z* found: 537.10$[M+H]^+$.

HRMS (ESI): *m/z* calcd for $C_{27}H_{33}N_6O_4S$ $[M+H]^+$: 537.2284, found: 537.2287.

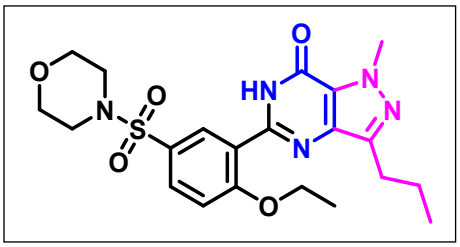

5-(2-Ethoxy-5-(morpholinosulfonyl)phenyl)-1-methyl-3-propyl-1,6-dihydro-7H-pyrazolo[4,3-d]pyrimidin-7-one(8d): Compound**8d** was prepared according to the representative procedure given in **5.2** starting from **6a** (100 mg) and morpholine (**7d**).The crude material was purified by silica gel column chromatography (DCM/MeOH; 95:05) to provide **8d** as an off-white solid (68.5mg, 61%) m.p. = 178-180 ºC; The spectra data matched with values reported in the literature.[28]

^{1}H NMR (500 MHz, $CDCl_3$) δ 10.82 (s, 1H), 8.83 (d, *J* = 2.4 Hz, 1H), 7.84 (dd, *J* = 8.7, 2.4 Hz, 1H), 7.18 (d, *J* = 8.8 Hz, 1H), 4.39 (q, *J* = 7.0 Hz, 2H), 4.28 (s, 3H), 3.78 – 3.75 (m, 4H), 3.09 – 3.06 (m, 4H), 2.95 – 2.91 (m, 2H), 1.86 (dd, *J* = 15.0, 7.5 Hz, 2H), 1.66 (d, *J* = 7.0 Hz, 3H), 1.02 (t, *J* = 7.4 Hz, 3H).

^{13}C NMR (101 MHz, $CDCl_3$) δ 159.48, 153.63, 147.01, 146.40, 138.37, 131.72, 131.19, 128.68, 124.52, 121.25, 113.18, 66.14, 46.04, 38.27, 27.77, 22.29, 14.58, 14.07.

MS (EI): *m/z* found: 462.05$[M+H]^+$.

HRMS (ESI): *m/z* calcd for $C_{21}H_{28}N_5O_5S$ $[M+H]^+$: 462.1811, found: 462.1810.

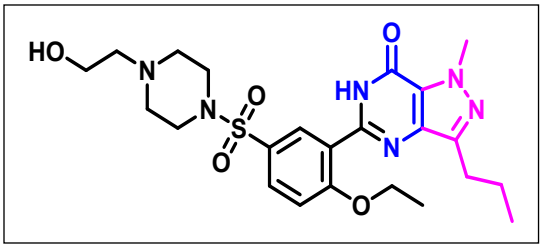

5-(2-Ethoxy-5-((4-(2-hydroxyethyl)piperazin-1-yl)sulfonyl)phenyl)-1-methyl-3-propyl-1,6-dihydro-7H-pyrazolo[4,3-d]pyrimidin-7-one(8e): Compound **8e** was prepared according to the representative procedure given in **5.2** starting from **6a** (100 mg) and 2-(Piperazin-1-yl) ethanol(**7e**). The crude material was purified by silica gel column chromatography (DCM/MeOH; 95:05) to provide **8e** as an off-white solid (78.6 mg, 64%) m.p. = 188-190 ºC; The spectra data matched with values reported in the literature.[28]

^{1}H NMR (400 MHz, $CDCl_3$) δ 10.84 (s, 1H), 8.81 (d, *J* = 1.6 Hz, 1H), 7.85 – 7.81 (m, 1H), 7.17 (d, *J* = 8.7 Hz, 1H), 4.39 (d, *J* = 6.9 Hz, 2H), 4.27 (s, 3H), 3.59 – 3.56 (m, 2H), 3.11 (s, 4H), 2.93 (t, *J* = 7.4 Hz, 2H), 2.62 (s, 4H), 2.57 – 2.54 (m, 2H), 1.85 (dt, *J* = 14.5, 7.3 Hz, 3H), 1.65 (t, *J* = 6.8 Hz, 3H), 1.03 (t, *J* = 7.3 Hz, 3H).

^{13}C NMR (126 MHz, $CDCl_3$) δ 159.41, 153.66, 147.00, 146.46, 138.38, 131.70, 131.17, 128.85, 124.51, 121.19, 113.13, 66.14, 58.98, 57.81, 52.01, 46.15, 38.27, 27.76, 22.29, 14.58, 14.08.

MS (EI): *m/z* found: 505.10$[M+H]^+$.

HRMS (ESI): *m/z* calcd for $C_{23}H_{33}N_6O_5S$ $[M+H]^+$: 505.2233, found: 505.2235.

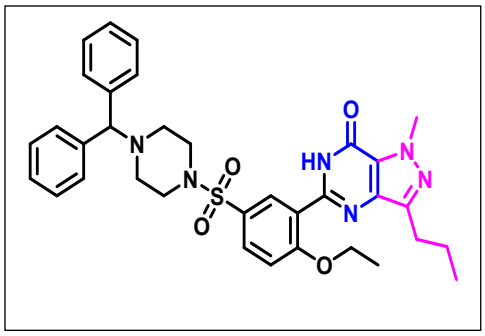

5-(5-((4-Benzhydrylpiperazin-1-yl)sulfonyl)-2-ethoxyphenyl)-1-methyl-3-propyl-1,6-dihydro-7H-pyrazolo[4,3-d]pyrimidin-7-one (8f): Compound **8f** was prepared according to the representative procedure given in **5.2** starting from **6a** (100 mg)and 1-Benzhydrylpiperazine **(7f)**. The crude material was purified by silica gel column chromatography (DCM/MeOH; 95:05) to provide **8f** as an Off-white solid (90 mg, 59%). m.p. = 232-234ºC;

^{1}H NMR (300 MHz, $CDCl_3$) δ 10.86 (s, 1H), 8.81 (d, *J* = 2.1 Hz, 1H), 7.84 (dd, *J* = 8.7, 2.2 Hz, 1H), 7.32 (d, *J* = 7.2 Hz, 4H), 7.18 (ddd, *J* = 14.0, 11.8, 7.1 Hz, 7H), 4.40 (q, *J* = 6.9 Hz, 2H), 4.29 (s, 3H), 4.23 (s, 1H), 3.08 (s, 4H), 2.91 (t, *J* = 7.5 Hz, 2H), 2.49 (s, 4H), 1.83 (dd, *J* = 14.9, 7.4 Hz, 2H), 1.67 (s, 3H), 0.96 (t, *J* = 7.4 Hz, 3H).

^{13}C NMR (126 MHz, $CDCl_3$) δ 159.33, 153.70, 147.06, 146.53, 141.98, 138.43, 131.80, 131.19, 129.17, 128.64, 127.75, 127.24, 124.52, 121.16, 113.08, 75.69, 66.12, 50.98, 46.39, 38.28, 27.76, 22.26, 14.62, 14.02.

MS (EI): *m/z* found: 627.10$[M+H]^+$.

HRMS (ESI): *m/z* calcd for $C_{34}H_{39}N_6O_4S$ $[M+H]^+$: 627.2753, found: 627.2756.

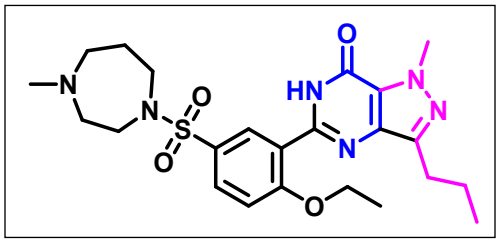

5-(2-Ethoxy-5-((4-methyl-1,4-diazepan-1-yl)sulfonyl)phenyl)-1-methyl-3-propyl-1,6-dihydro-7H-pyrazolo[4,3-d]pyrimidin-7-one(8g): Compound **8g** was prepared following the representative procedure given in **5.2** starting from **6a** (100 mg) and 1-methyl-1,4-diazepane **(7f)**. The crude material was purified by silica gel column chromatography (DCM/MeOH; 95:05) to provide **8g** as an off-white solid (71 mg, 60%); m.p. = 128-130 ºC;

^{1}H NMR (500 MHz, $CDCl_3$) δ 10.88 (s, 1H), 8.83 (d, *J* = 2.4 Hz, 1H), 7.86 (dd, *J* = 8.7, 2.5 Hz, 1H), 7.14 (d, *J* = 8.8 Hz, 1H), 4.38 (t, *J* = 7.0 Hz, 2H), 4.28 (s, 3H), 3.53 – 3.49 (m, 2H), 3.45 (t, *J* = 6.5 Hz, 2H), 2.96 – 2.91 (m, 2H), 2.84 – 2.77 (m, 4H), 2.43 (s, 3H), 2.00 – 1.98 (m, 2H), 1.86 (dt, *J* = 14.8, 7.4 Hz, 2H), 1.64 (t, *J* = 7.0 Hz, 3H), 1.03 (t, *J* = 7.4 Hz, 3H).

^{13}C NMR (101 MHz, $CDCl_3$) δ 159.15, 153.74, 146.94, 146.57, 138.40, 132.22, 130.96, 130.27, 124.49, 121.28, 113.14, 66.04, 58.60, 55.92, 46.86, 46.50, 45.76, 38.25, 27.76, 26.35, 22.31, 14.56, 14.07.

MS (EI): *m/z* found: 489.10$[M+H]^+$.

HRMS (ESI): *m/z* calcd for $C_{23}H_{33}N_6O_4S$ $[M+H]^+$: 489.2284, found: 489.2283.

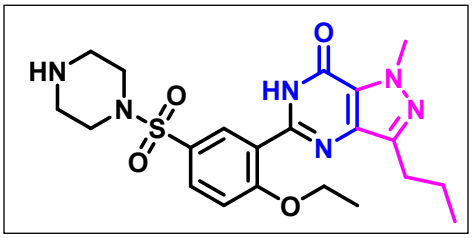

5-(2-Ethoxy-5-(piperazin-1-ylsulfonyl)phenyl)-1-methyl-3-propyl-1,6-dihydro-7H-pyrazolo[4,3-d]pyrimidin-7-one(8h): Compound **8h** was prepared following the representative procedure given in**5.2** starting from **6a** (100 mg)and piperazine **(7h)**.The crude material was purified by silica gel column chromatography (DCM/MeOH; 90:10) to provide **8h** as an Off-white solid (70 mg, 62%) m.p. = 148-150 ºC; The spectra data matched with values reported in the literature.[28,30]

^{1}H NMR (400 MHz, $CDCl_3$) δ 10.83 (s, 1H), 8.82 (d, *J* = 2.4 Hz, 1H), 7.84 (dd, *J* = 8.7, 2.4 Hz, 1H), 7.16 (d, *J* = 8.8 Hz, 1H), 4.38 (d, *J* = 7.0 Hz, 2H), 4.28 (s, 3H), 3.07 – 3.04 (m, 4H), 2.96 – 2.91 (m, 6H), 1.89 – 1.83 (m, 2H), 1.70 (s, 1H), 1.65 (s, 3H), 1.02 (t, *J* = 7.4 Hz, 3H).

^{13}C NMR (101 MHz, $CDCl_3$) δ 159.31, 153.66, 147.03, 146.46, 138.41, 131.71, 131.18, 129.19, 124.53, 121.13, 113.08, 66.13, 46.88, 45.35, 38.28, 27.79, 22.30, 14.59, 14.07.

MS (EI): *m/z* found: 461.10$[M+H]^+$.

HRMS (ESI): *m/z* calcd for $C_{21}H_{29}N_6O_4S$ $[M+H]^+$: 461.1971, found: 461.1966.

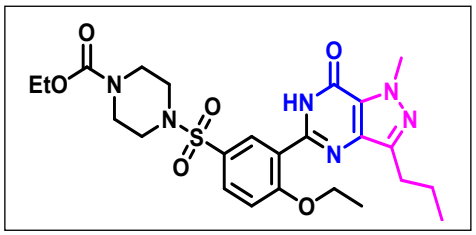

Ethyl 4-((4-ethoxy-3-(1-methyl-7-oxo-3-propyl-6,7-dihydro-1H-pyrazolo[4,3-d]pyrimidin-5-yl) phenyl) sulfonyl)piperazine-1-carboxylate (8i): Compound **8i** was prepared following the representative procedure given in **5.2** from **6a** (100 mg) and ethyl piperazine-1-carboxylate **(7i)**.The crude material was purified by silica gel column chromatography (DCM/MeOH; 95:05) to provide **8i** as an Off-white solid (83 mg, 64%) m.p. = 228-230 ºC; The spectra data matched with values reported in the literature. [31, 32]

^{1}H NMR (400 MHz, $CDCl_3$) δ 10.80 (s, 1H), 8.81 (d, *J* = 2.4 Hz, 1H), 7.83 (dd, *J* = 8.8, 2.4 Hz, 1H), 7.16 (d, *J* = 8.8 Hz, 1H), 4.38 (q, *J* = 7.0 Hz, 2H), 4.28 (s, 3H), 4.08 (q, *J* = 7.1 Hz, 2H), 3.62 – 3.56 (m, 4H), 3.08 – 3.03 (m, 4H), 2.93 (t, *J* = 7.5 Hz, 2H), 1.87 (dd, *J* = 14.9, 7.5 Hz, 2H), 1.66 (d, *J* = 7.0 Hz, 3H), 1.21 (t, *J* = 7.1 Hz, 3H), 1.03 (t, *J* = 7.4 Hz, 3H).

^{13}C NMR (101 MHz, $CDCl_3$) δ 159.48, 155.03, 153.62, 147.04, 146.34, 138.35, 131.62, 131.11, 129.00, 124.53, 121.29, 113.24, 66.20, 61.81, 45.88, 43.12, 38.29, 27.78, 22.30, 14.58, 14.07.

MS (ESI): *m/z* found: 533.05$[M+H]^+$.

HRMS (ESI): *m/z* calcd for $C_{24}H_{33}N_6O_6S$ $[M+H]^+$: 533.2182, found: 533.2186.

6.0 Synthesis of sildenafil in gram-scale: After the successfully completion of the individual and integrated optimization reaction in continuous flow manner, we proceeded further for the integrated flow system towards gram scale synthesis of sildenafil **8a** (supporting video). A stock solution molar ratio of **2a**: **3**: $CHCl_3$ (1: 1.1: 236), was taken in bottle and connected with a HPLC pump. A single SS-316 heterogenous acid cartridge reactor (vol. =4 mL) was assembled and joined to the other components of the continuous flow system. The stock solution is infused with a flow rate of 250 μL min^{-1}, in accordance with the residance time passed through an acidic functionalized heterogeneous acid [SGO filled SS-cartridge (id = 7 mm, length 100 mm, vol = 4 mL)]; for the reaction to occur. The outflowed product mixture **4a** was directly connected with additional *T*-junction (T_2) and a solution of HSO_3Cl in $CHCl_3$ (0.032 *M*) were introduced PTFE reactor coil (vol. = 5 mL). The flow rate (250 μL/min.) of the **4a** solution was kept at same the rate of HSO_3Cl, in accordance with previously optimized procedure. Next, the out-flowed sulphonated product mixture was quenched at T_3-junction with water (flow rate 1.5 mL/min.) and then aqueous-organic droplet were smoothly passed through perfluoro alkoxy (PFA) tubing (id = 1000 µm, l = 2.5 m, vol. = 2 mL) for the extraction to occur. Further the aqueous and $CHCl_3$ continuous flow droplet was separated through our lab previously reported micro-separator and organic layer was re-circulated with additional pump. The stock solution of *N*-methyl piperazine **7a** (0.021 *M* in $CHCl_{3,}$) was directly connected with out-flowed product mixture **6a** at T_4-junction and infusing with the flow rate 1 ml/min into rectangular PTFE plate reactor (width = 1 mm, height = 1 mm; length = 5-meter, volume = 10) reactor. Under the stabilized reaction conditions, the integrated continuous flow reaction sequence (integrated continuous flow process system for the cascade condensation, cyclization, sulphonation and amination reaction) was continued for a period of 24 h for the gram scale synthesis of sildenafil **8a.** The reaction mixture was evaporated under reduced pressure to remove excess chloroform. The resulting mixture was diluted with chloroform, washed with water and brine solution. The organic phase was dried over anhydrous sodium sulfate, filtered and concentrated. Using the fully integrated continuous platform (condensation and cyclization reaction (16.0 min), *insitu* sulphonation (10 min.), quenching and

extraction (1.0 min) and separation (0.35 min), and finally amination (5 min) resulting in ca. 0.5 mmol h^{-1} productivity. Thus, we were able to produce 5.7 g of sildenafil after running the reaction for 24 h.

Table S6. Comparison table for the synthesis of sildenafil under batch and continuous flow process.

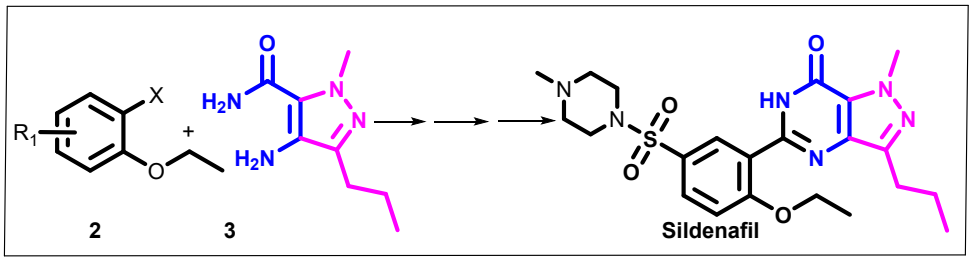

S.No.	X	Process	Time (h)	Yield (%)	Ref.
1	-COCl	Batch	10	51	[33]
2	-COCl	Batch (MW)	2	55	[34]
3	-COCOK	Batch	16	65	[35]
4	-COCl	Batch	24	60	[36]
5	-COOH	Batch	23	62	[37]
6	-CHO	Batch	26	60	[38]
7	-COOH	Batch	104	44	[39]
8	**-CHO**	**Flow process**	**0.54**	**65**	**This study**

7. Spectra

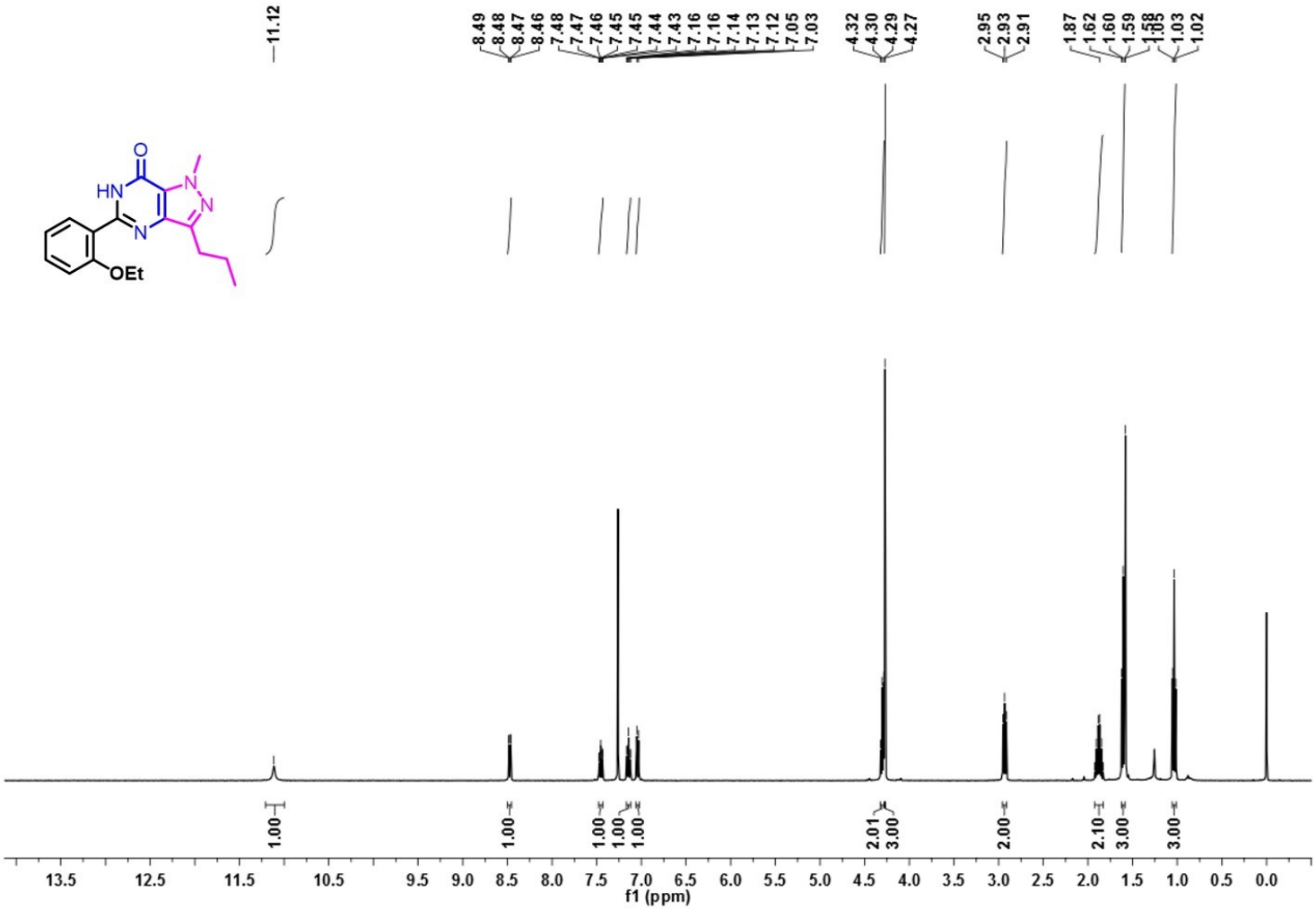

Figure S10. ^{1}H NMR spectra of 5-(2-ethoxyphenyl)-1-methyl-3-propyl-1,6-dihydro-7H-pyrazolo[4,3-d] pyrimidin-7-one **(4a**) in $CDCl_3$.

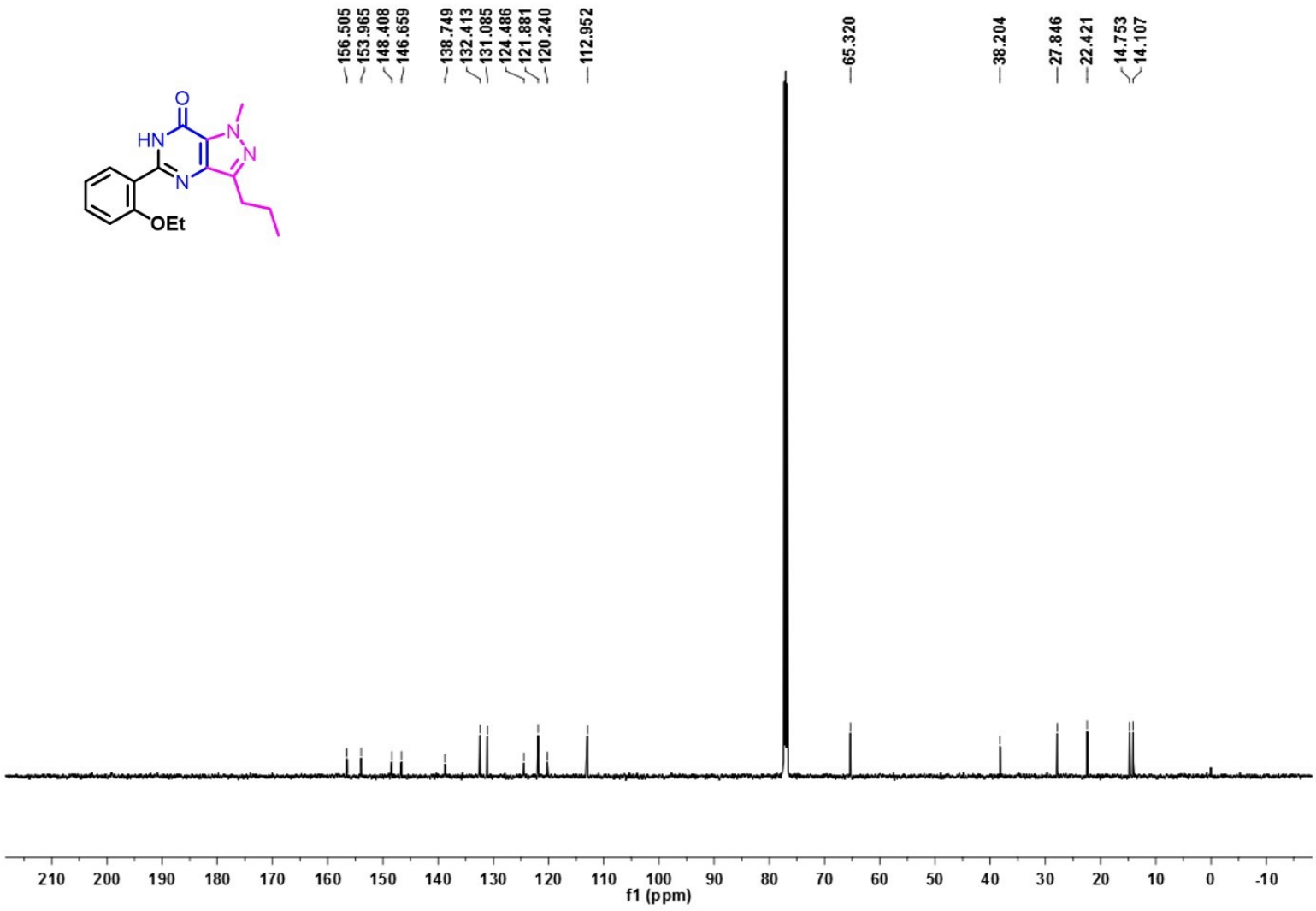

Figure S11. ^{13}C NMR spectra of 5-(2-ethoxyphenyl)-1-methyl-3-propyl-1,6-dihydro-7H-pyrazolo[4,3-d] pyrimidin-7-one **(4a)** in $CDCl_3$.

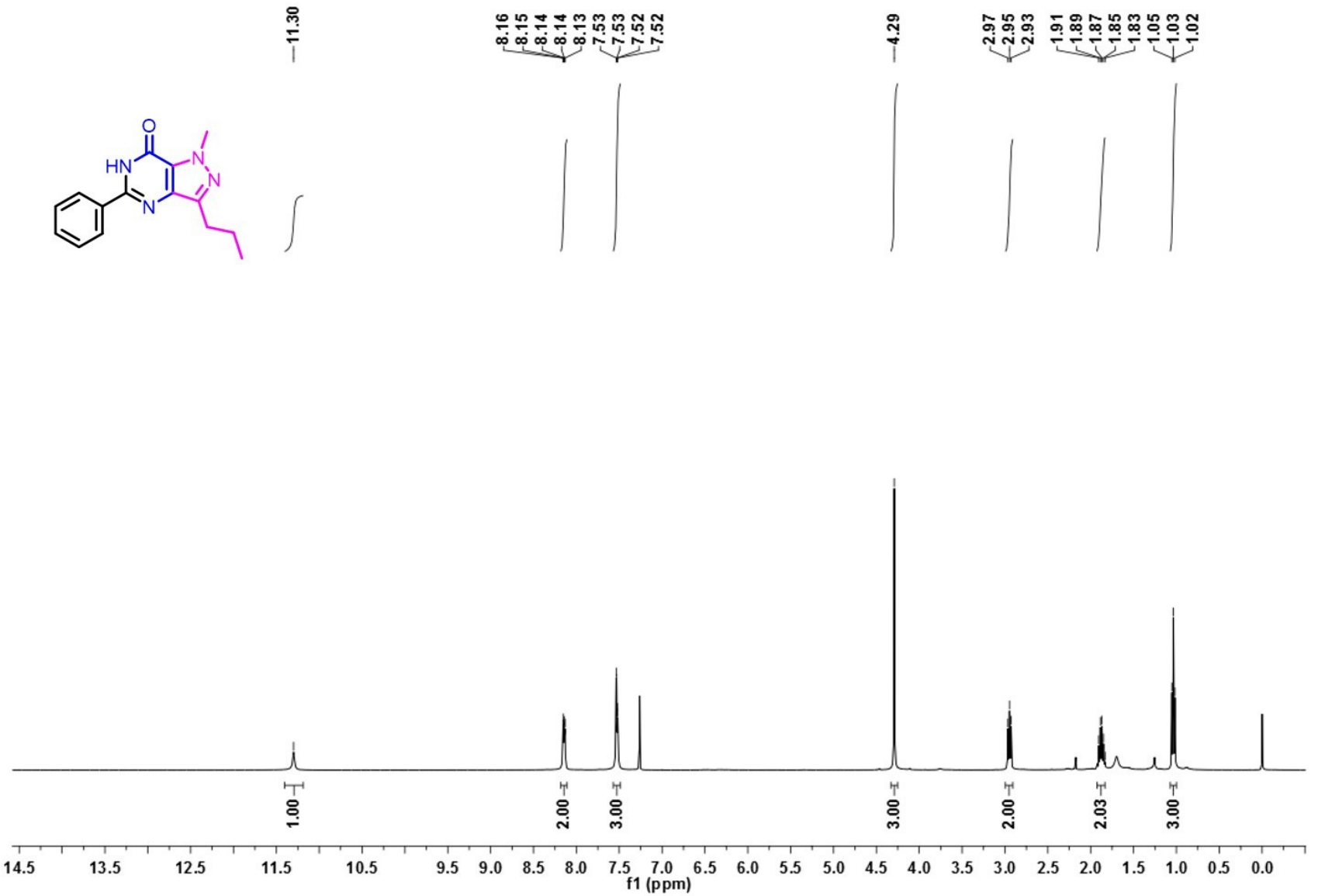

Figure S12. ^{1}H NMR spectra of 1-methyl-5-phenyl-3-propyl-1,6-dihydro-7H-pyrazolo[4,3-d] pyrimidin-7-one **(4b)** in $CDCl_3$.

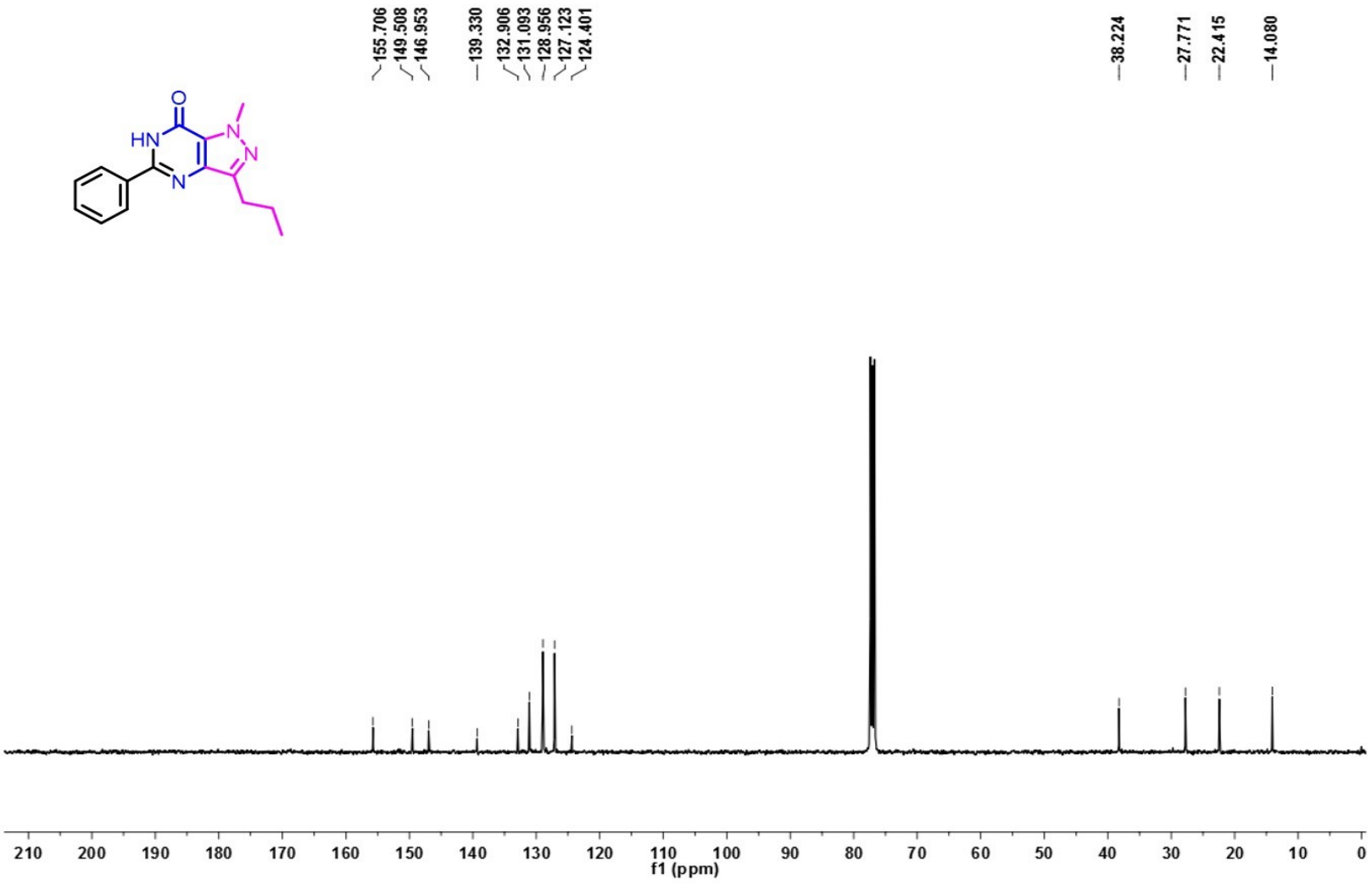

Figure S13. ^{13}C NMR spectra of 1-methyl-5-phenyl-3-propyl-1,6-dihydro-7H-pyrazolo[4,3-d] pyrimidin-7-one**(4b)** in $CDCl_3$.

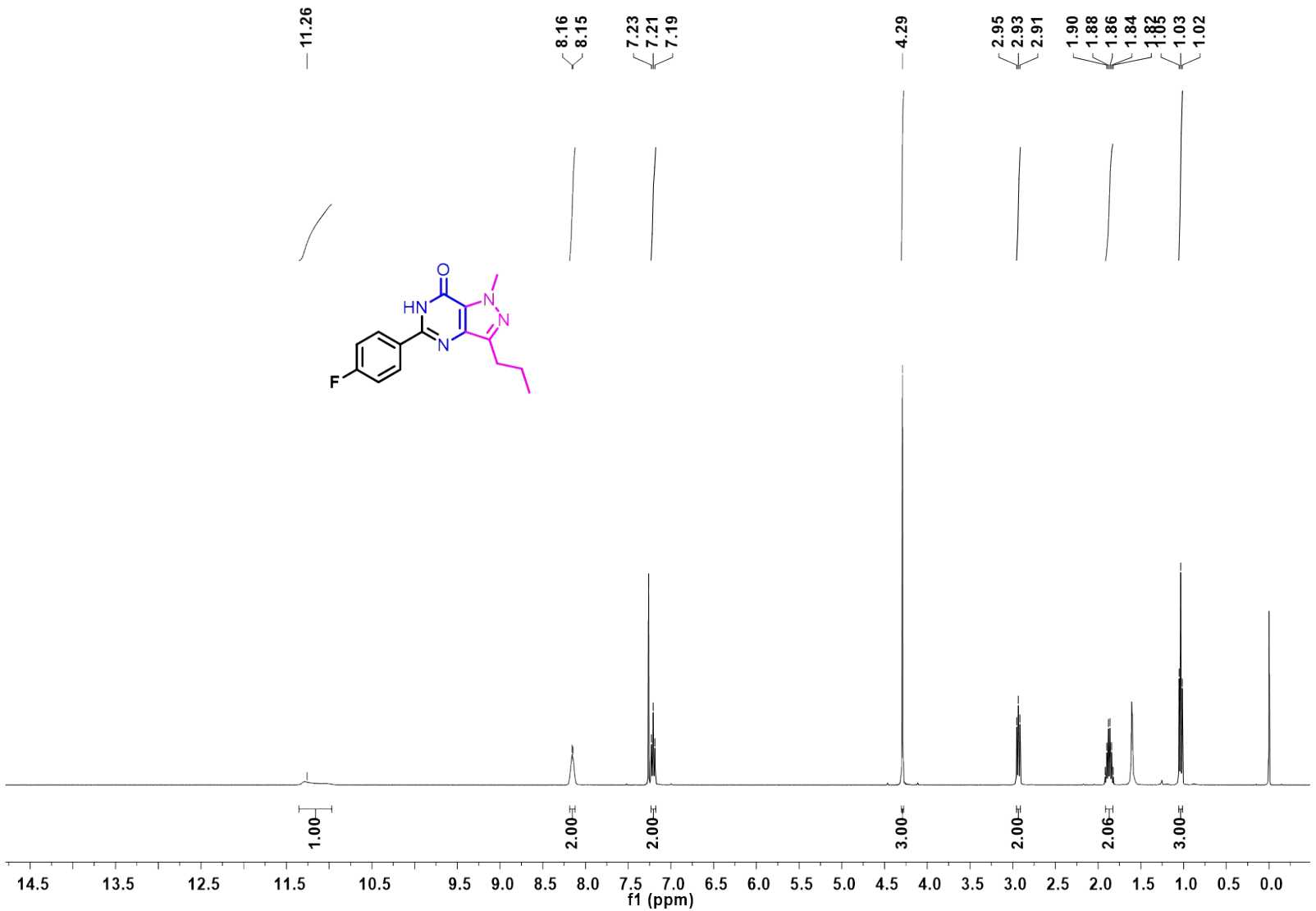

Figure S14. ^{1}H NMR spectra of 5-(4-fluorophenyl)-1-methyl-3-propyl-1,6-dihydro-7H-pyrazolo[4,3-d] pyrimidin-7-one **(4c)** in $CDCl_3$.

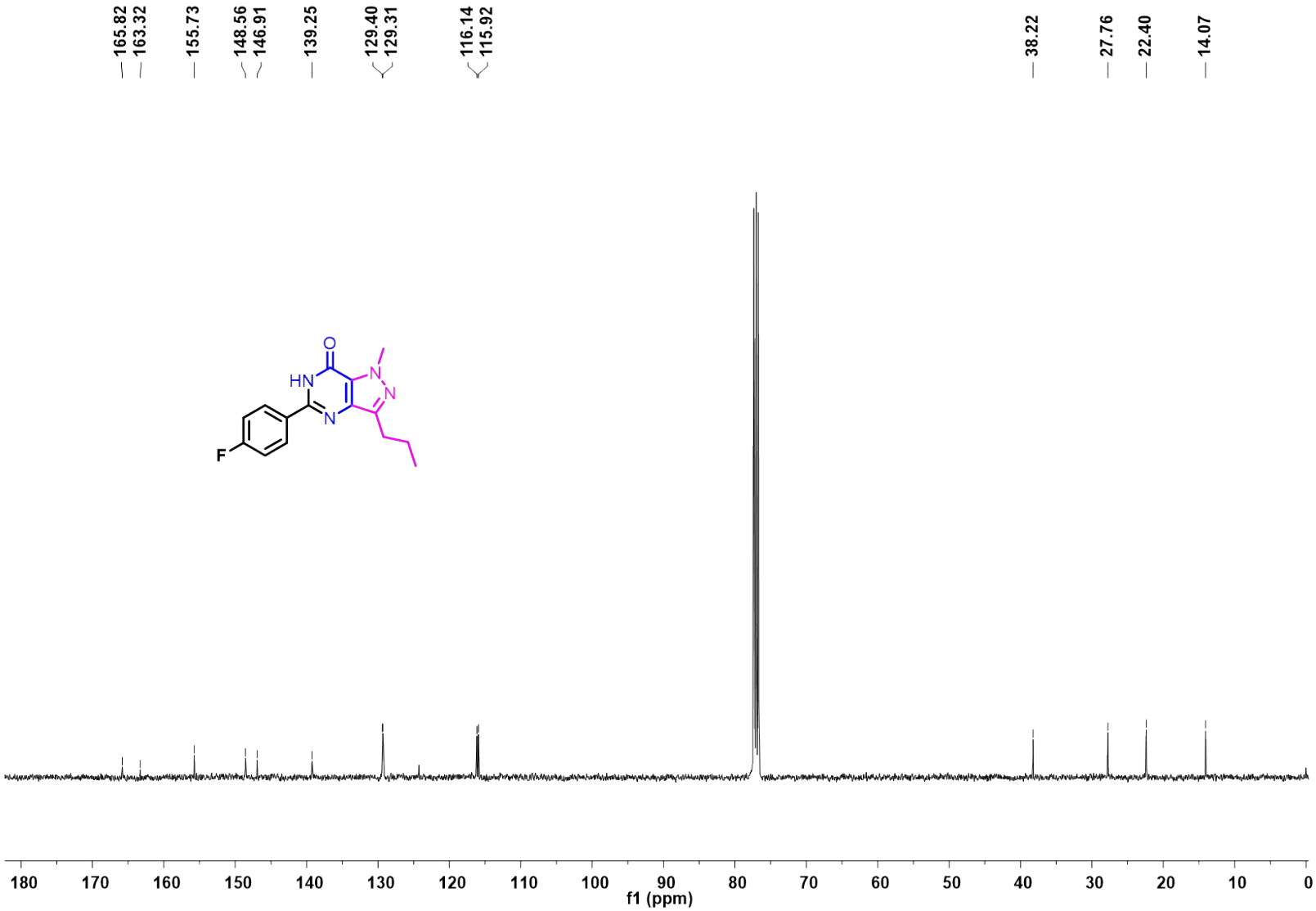

Figure S15. ^{13}C NMR spectra of 5-(4-fluorophenyl)-1-methyl-3-propyl-1,6-dihydro-7H-pyrazolo[4,3-d] pyrimidin-7-one**(4c)** in $CDCl_3$.

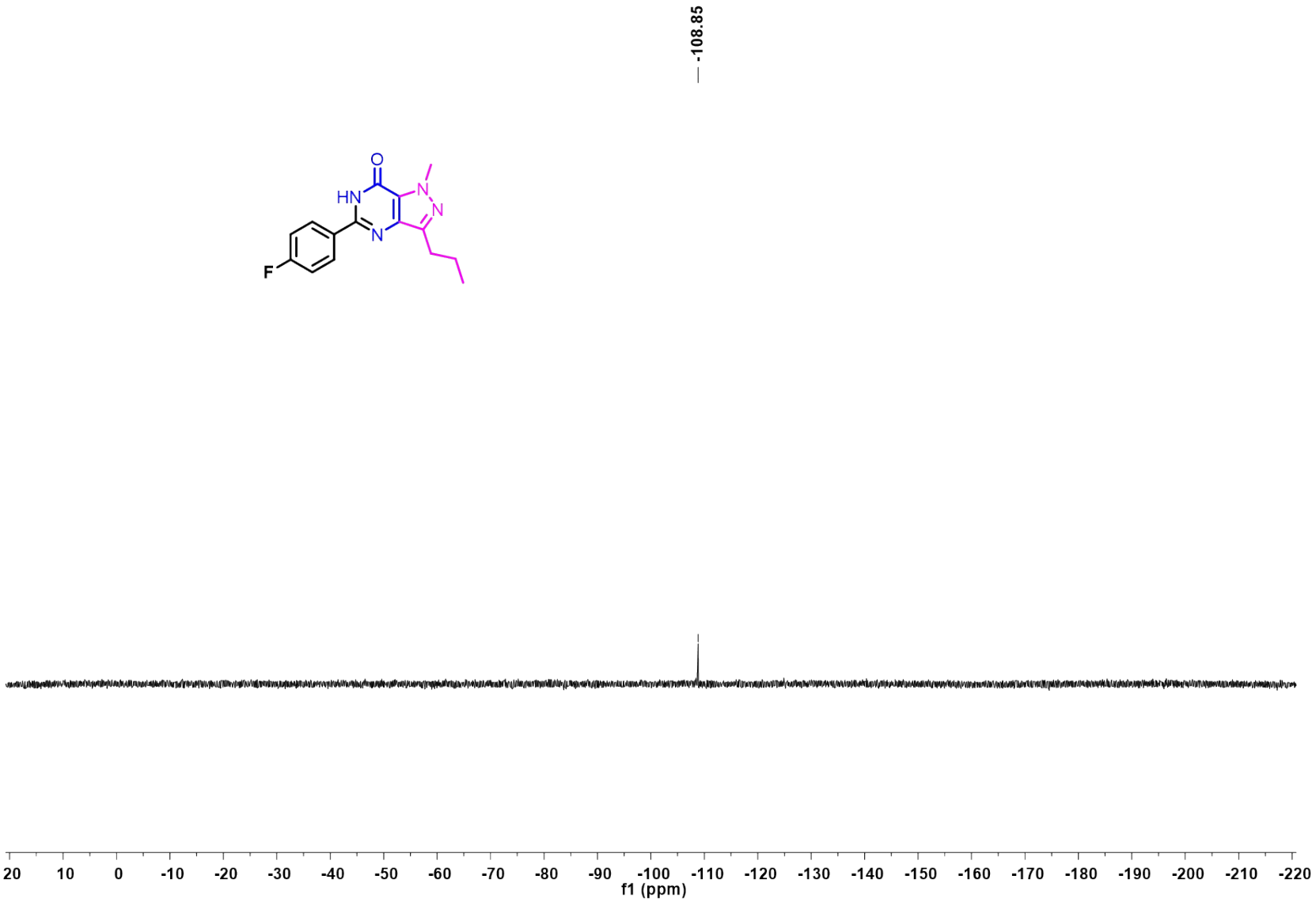

Figure S16. ^{19}F NMR spectra of 5-(4-fluorophenyl)-1-methyl-3-propyl-1,6-dihydro-7H-pyrazolo[4,3-d] pyrimidin-7-one**(4c)** in $CDCl_3$

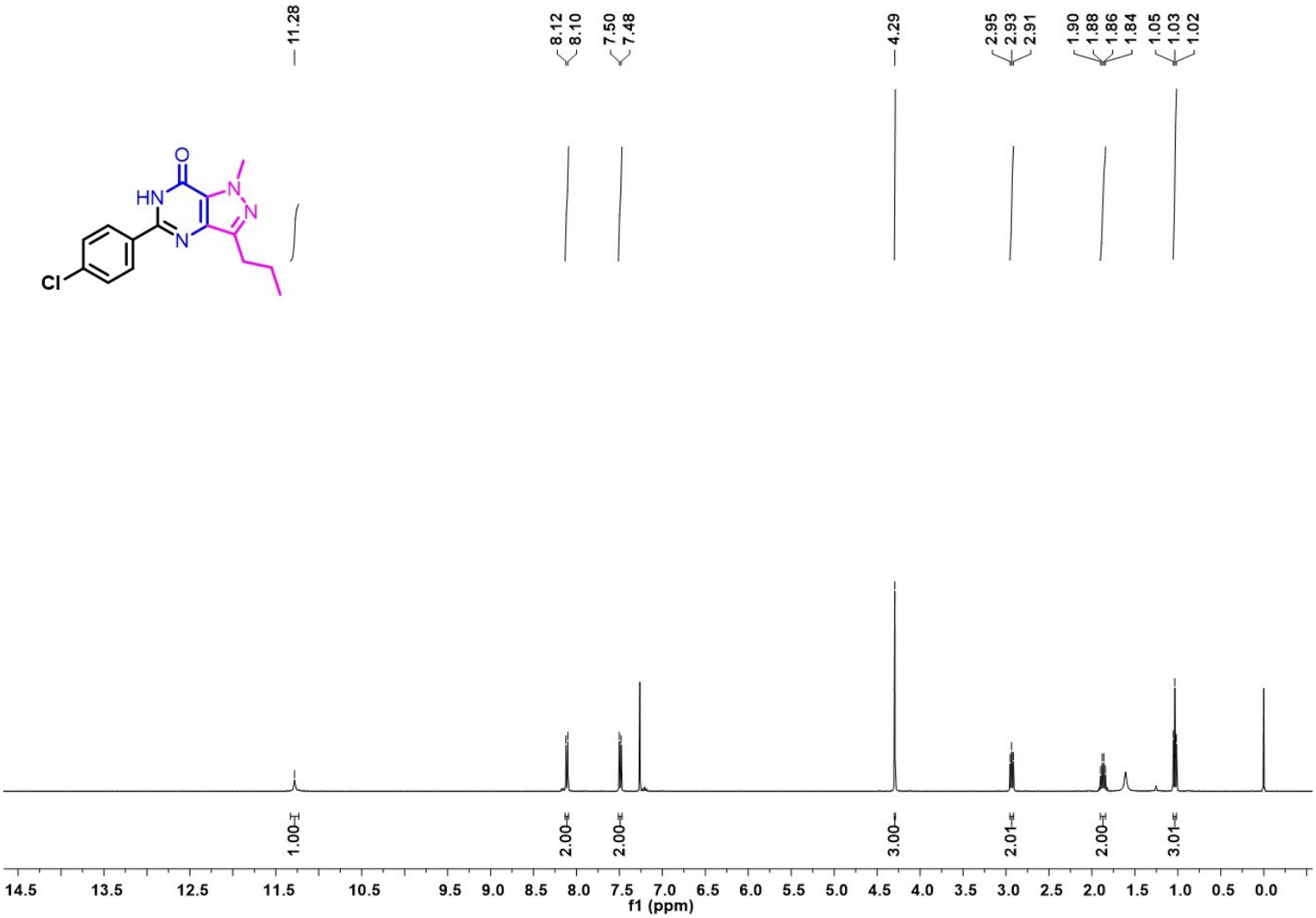

Figure S17. ^{1}H NMR spectra of 5-(4-chlorophenyl)-1-methyl-3-propyl-1,6-dihydro-7H-pyrazolo[4,3-d] pyrimidin-7-one **(4d)** in $CDCl_3$.

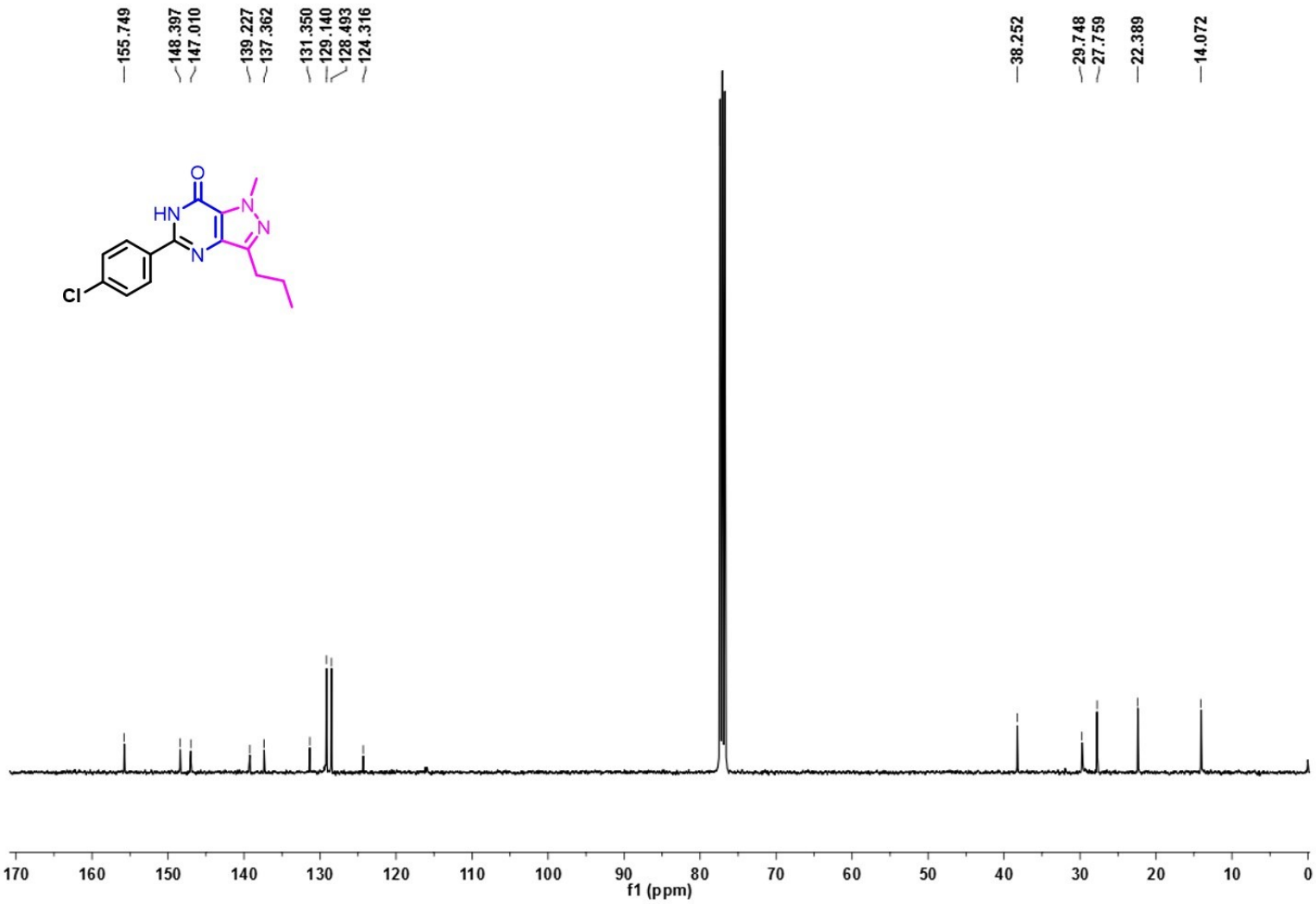

Figure S18. ^{13}C NMR spectra of 5-(4-chlorophenyl)-1-methyl-3-propyl-1,6-dihydro-7H-pyrazolo[4,3-d] pyrimidin-7-one **(4d)** in $CDCl_3$.

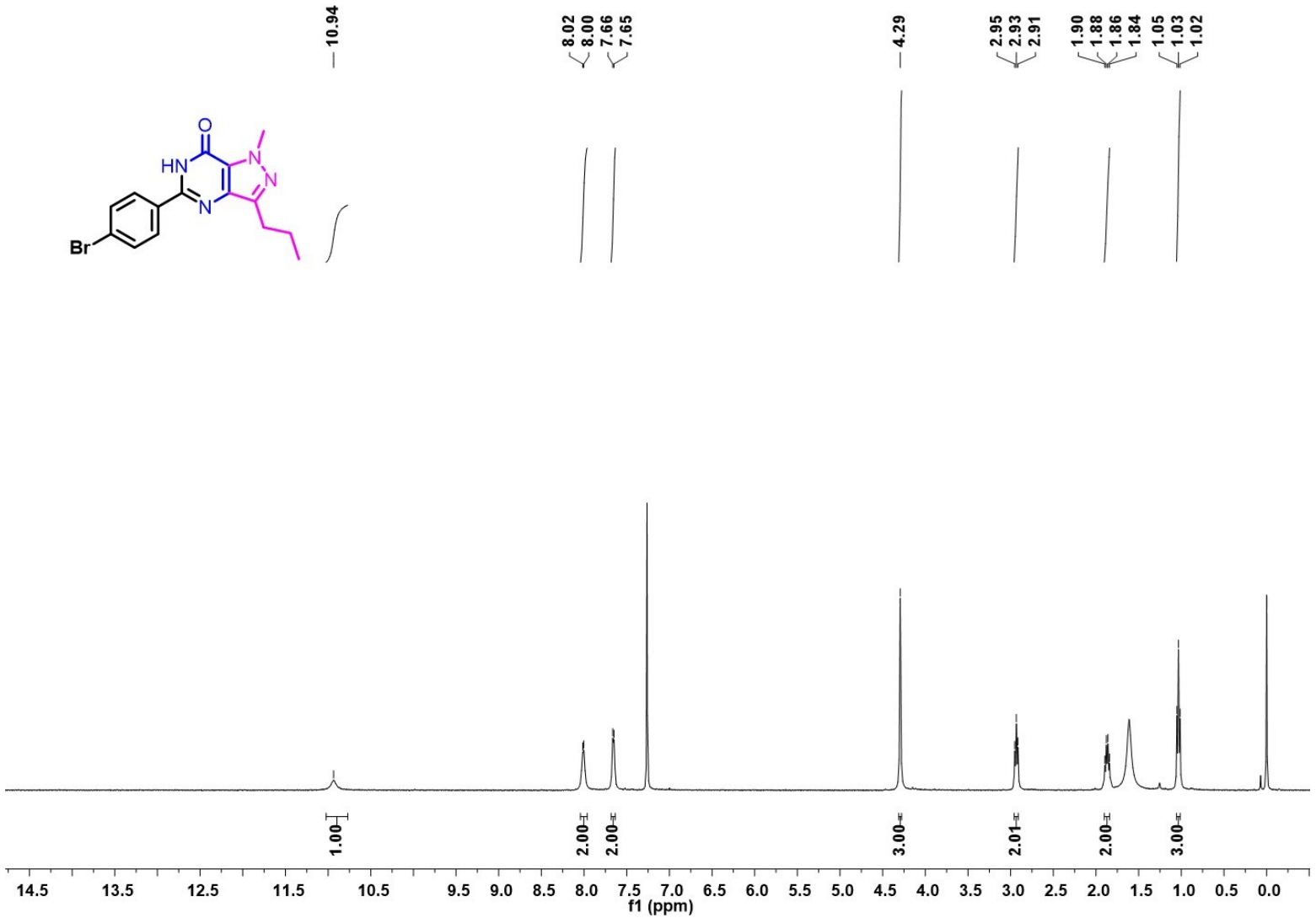

Figure S19. ^{1}H NMR spectra of 5-(4-bromophenyl)-1-methyl-3-propyl-1,6-dihydro-7H-pyrazolo[4,3-d] pyrimidin-7-one **(4e)** in $CDCl_3$.

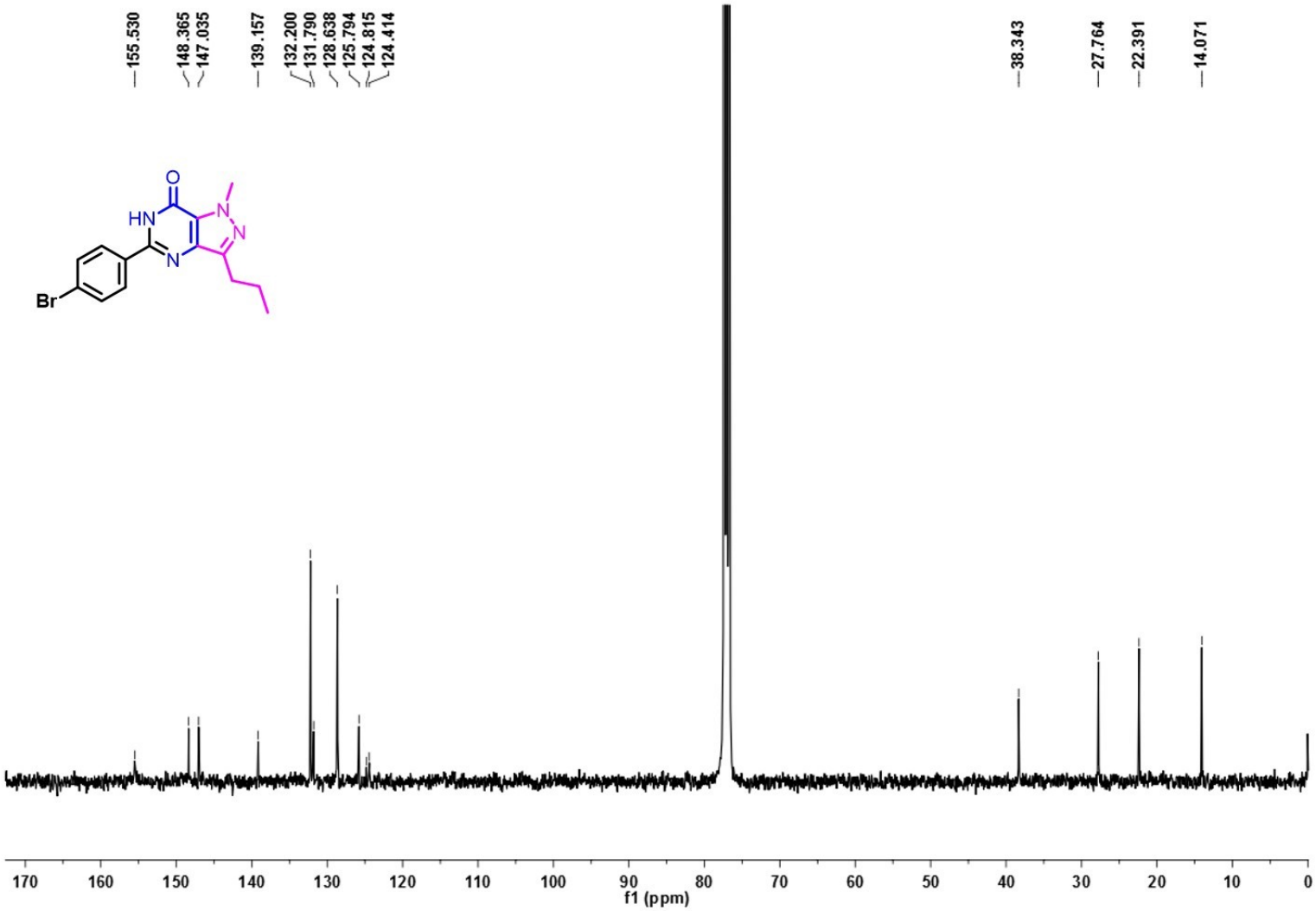

Figure S20. ^{1}H NMR spectra of 5-(4-bromophenyl)-1-methyl-3-propyl-1,6-dihydro-7H-pyrazolo[4,3-d] pyrimidin-7-one**(4e)** in $CDCl_3$.

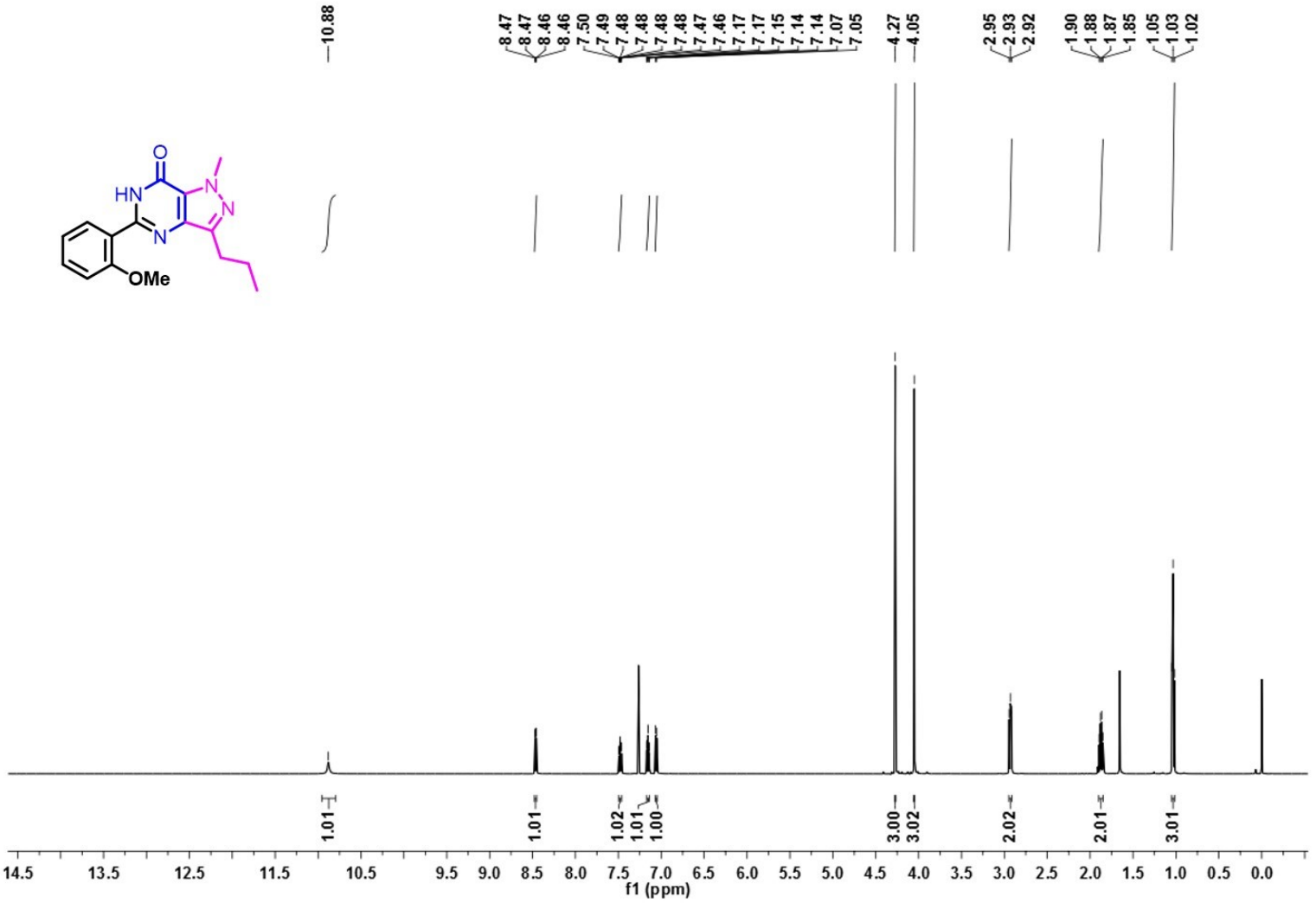

Figure S21. ^{1}H NMR spectra of 5-(2-methoxyphenyl)-1-methyl-3-propyl-1,6-dihydro-7H-pyrazolo[4,3-d] pyrimidin-7-one **(4f)** in $CDCl_3$.

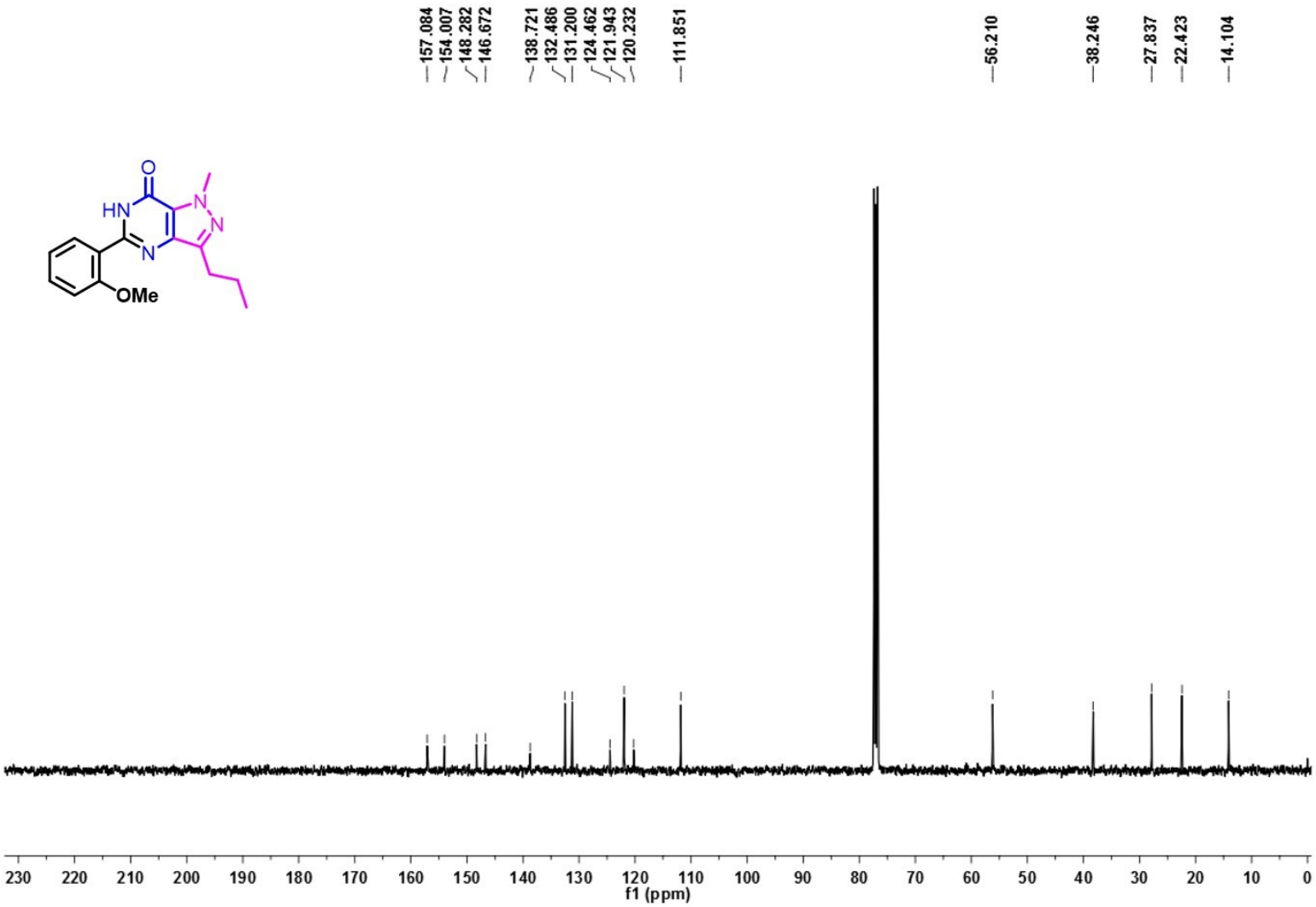

Figure S22. ^{13}CNMR spectra of 5-(2-methoxyphenyl)-1-methyl-3-propyl-1,6-dihydro-7H-pyrazolo[4,3-d] pyrimidin-7-one **(4f)** in $CDCl_3$.

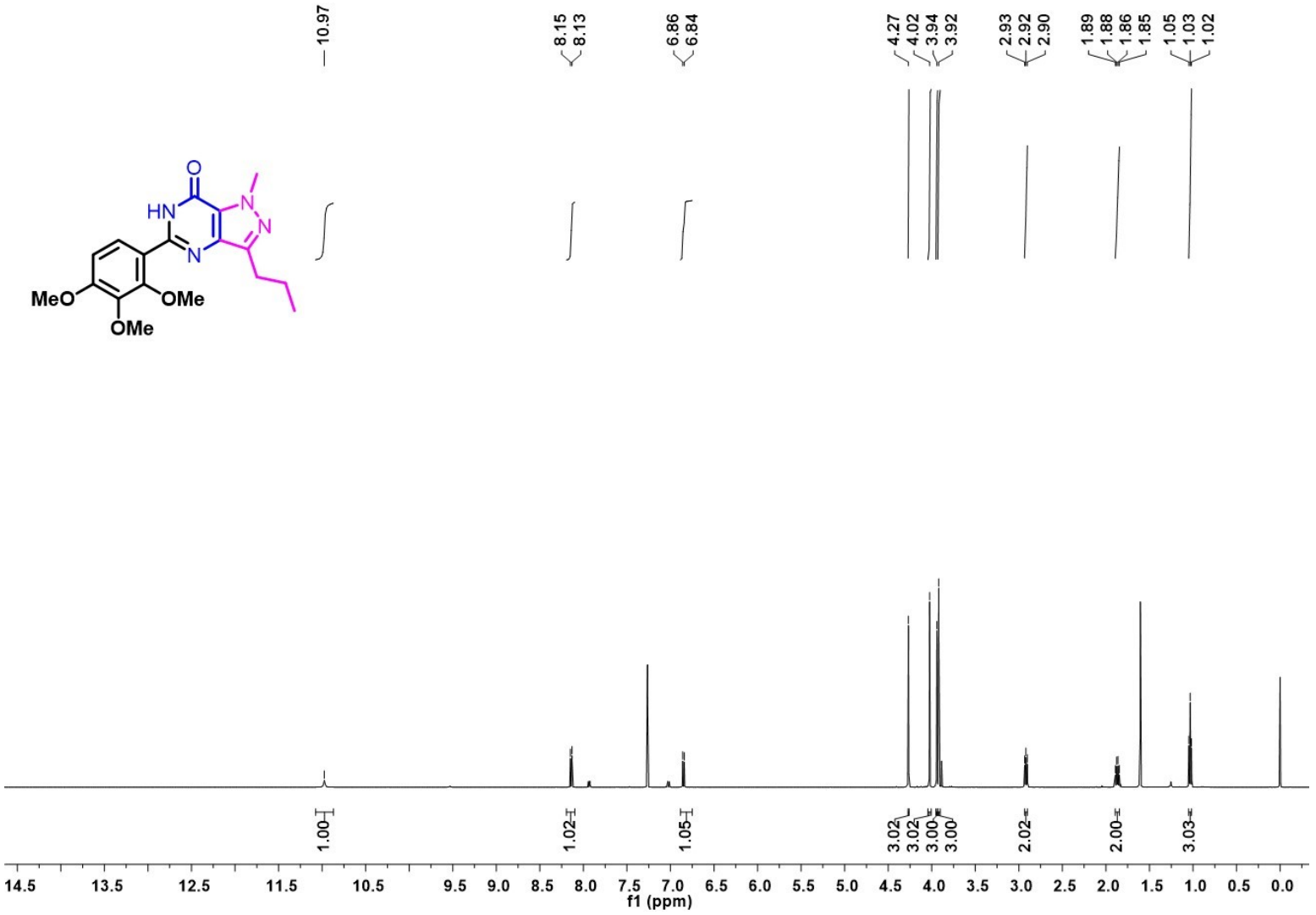

Figure S23. ^{1}H NMR spectra of 1-methyl-3-propyl-5-(2,3,4-trimethoxyphenyl)-1,6-dihydro-7H-pyrazolo[4,3-d] pyrimidin-7-one **(4g)** in $CDCl_3$.

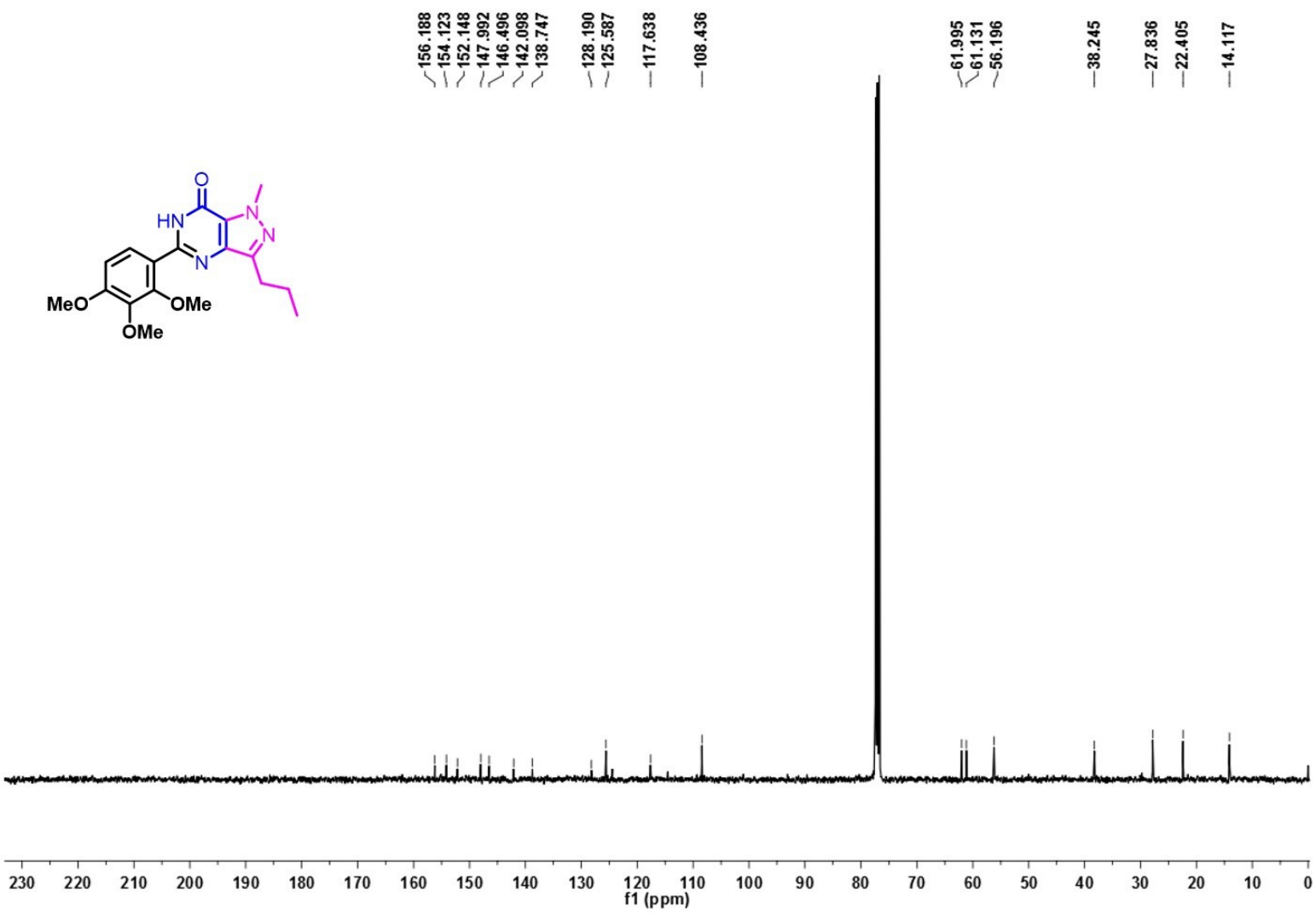

Figure S24. ^{13}C NMR spectra of 1-methyl-3-propyl-5-(2,3,4-trimethoxyphenyl)-1,6-dihydro-7H-pyrazolo[4,3-d] pyrimidin-7-one **(4g)** in $CDCl_3$.

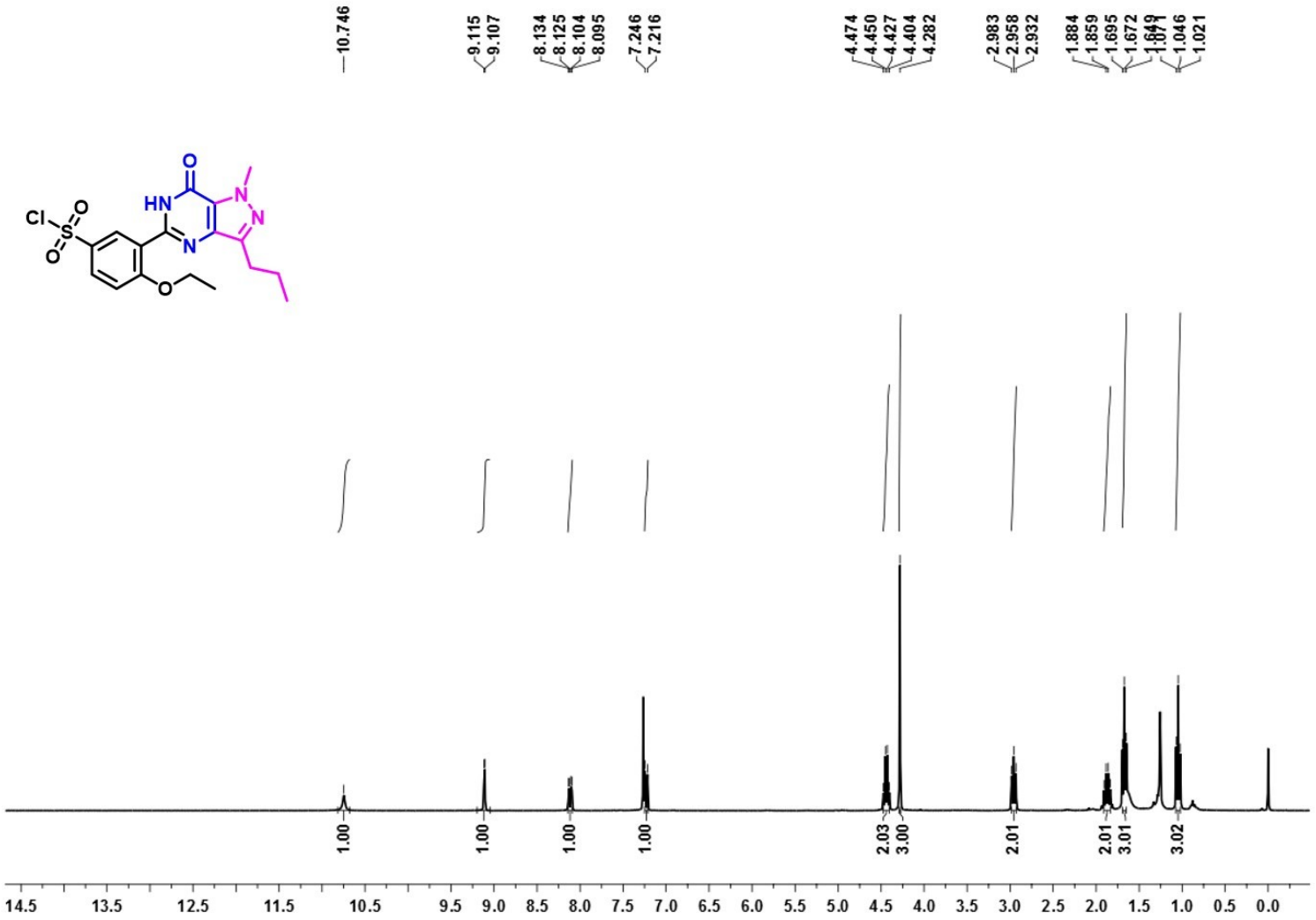

Figure S25. ^{1}H NMR spectra of 4-ethoxy-3-(1-methyl-7-oxo-3-propyl-6,7-dihydro-1H-pyrazolo[4,3-d] pyrimidin-5-yl) benzene sulfonyl chloride **(6)** in $CDCl_3$.

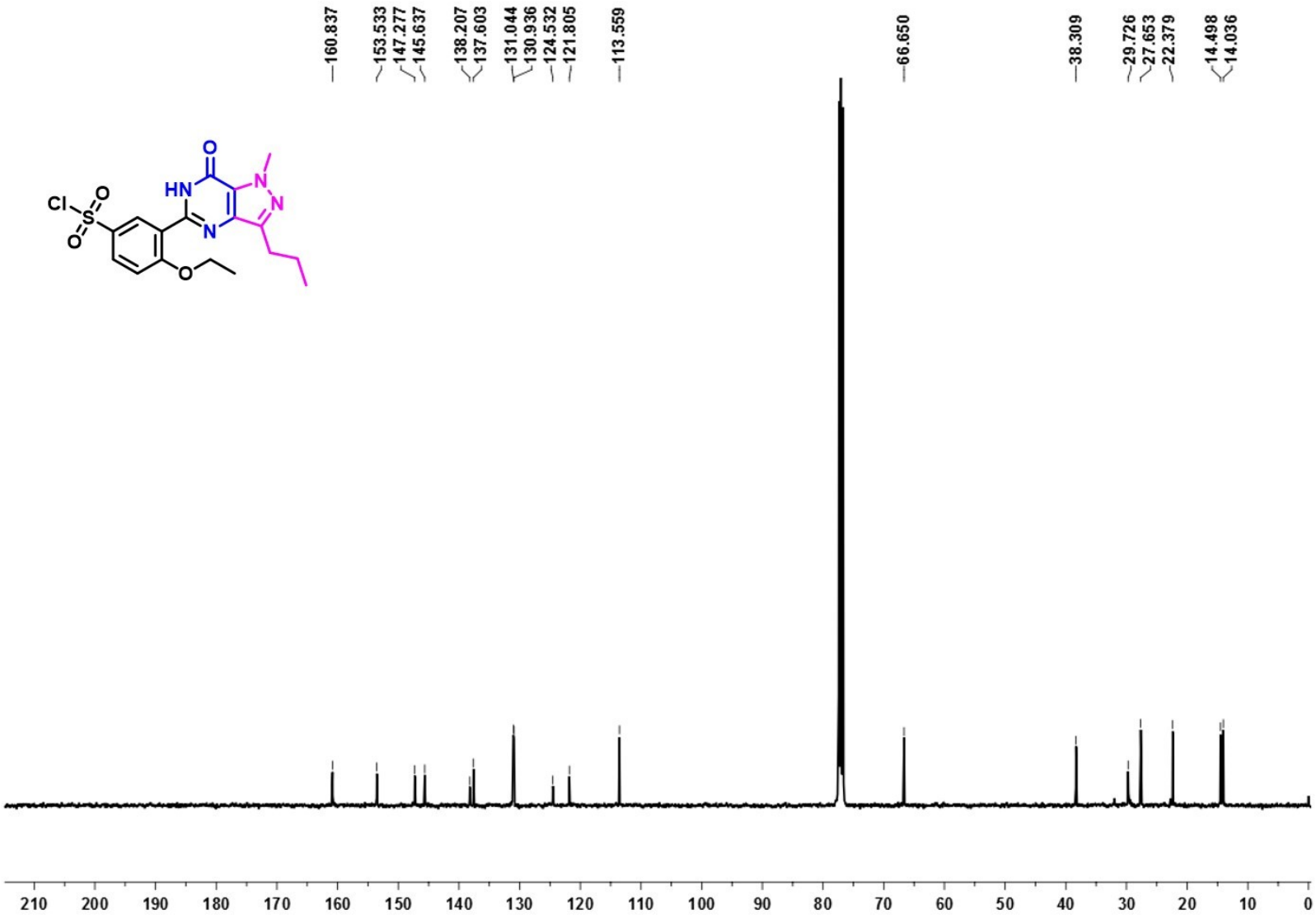

Figure S26. ^{13}C NMR spectra of 4-ethoxy-3-(1-methyl-7-oxo-3-propyl-6,7-dihydro-1H-pyrazolo[4,3-d] pyrimidin-5-yl) benzene sulfonyl chloride (**6)** in $CDCl_3$.

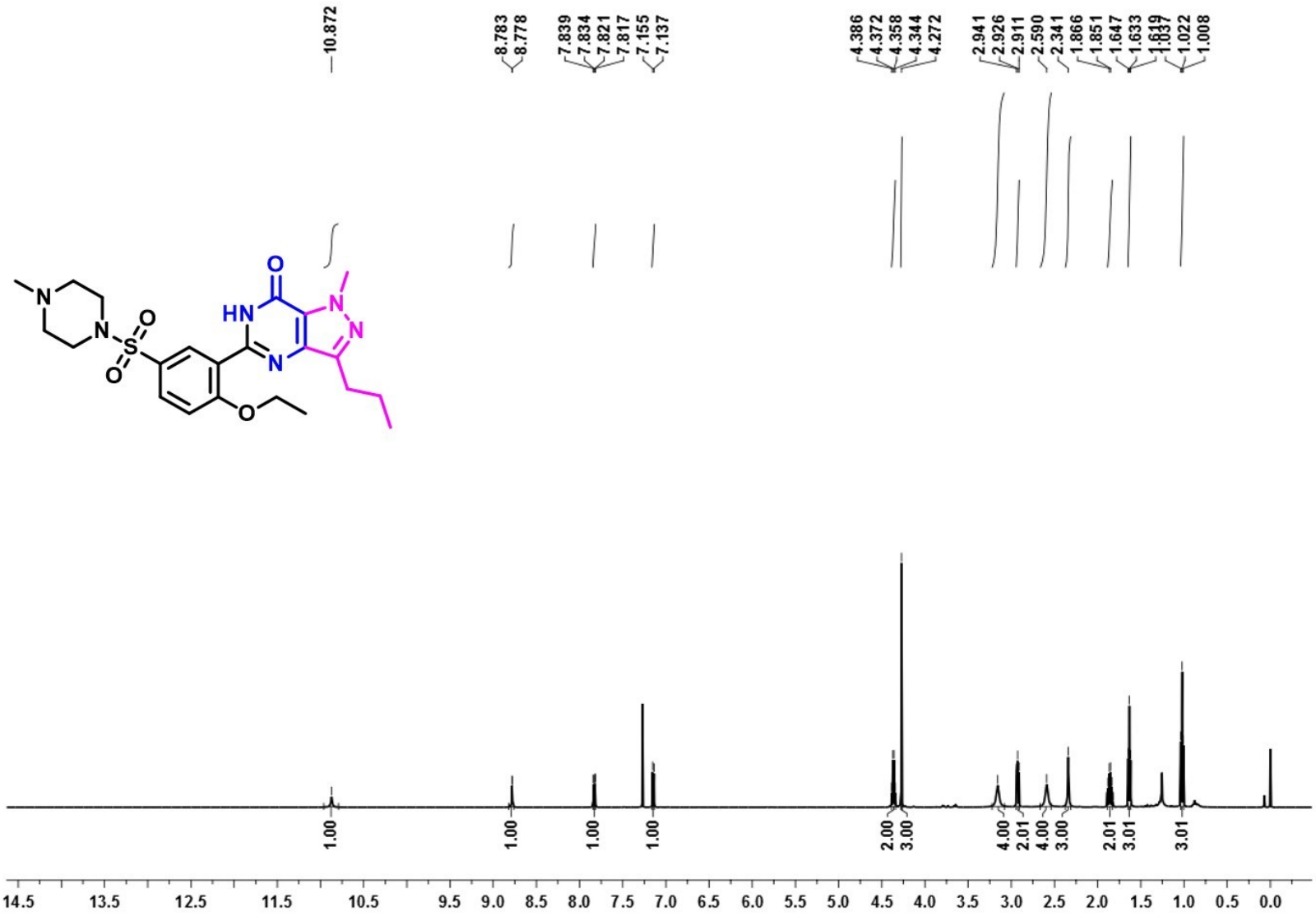

Figure S27. ^{1}H NMR spectra of 5-(2-ethoxy-5-((4-methylpiperazin-1-yl) sulfonyl) phenyl)-1-methyl-3-propyl-1,6-dihydro-7H-pyrazolo[4,3-d] pyrimidin-7-one **(8a)** in $CDCl_3$.

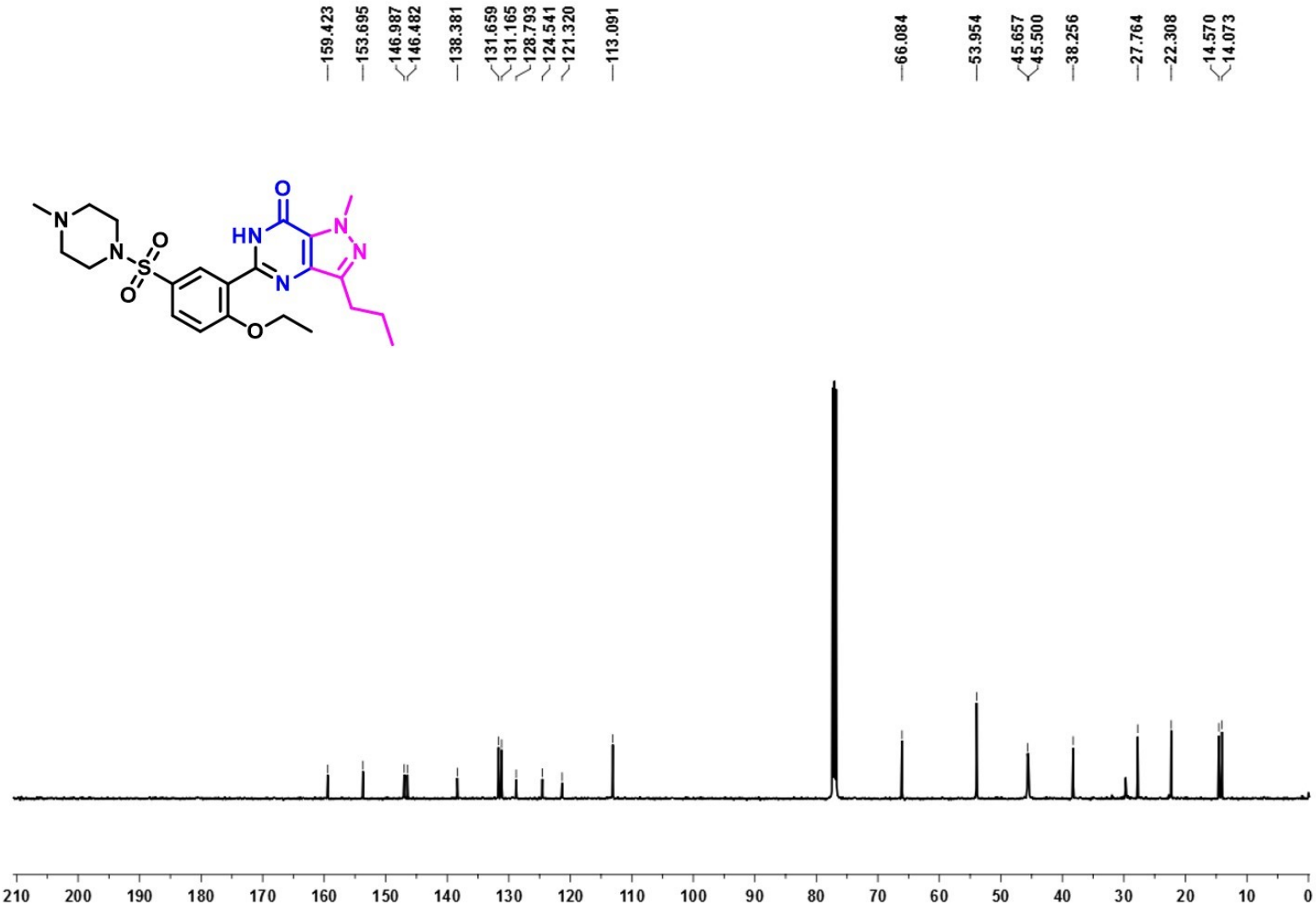

Figure S28. ^{13}C NMR spectra of 5-(2-ethoxy-5-((4-methylpiperazin-1-yl) sulfonyl) phenyl)-1-methyl-3-propyl-1,6-dihydro-7H-pyrazolo[4,3-d] pyrimidin-7-one **(8a)** in $CDCl_3$.

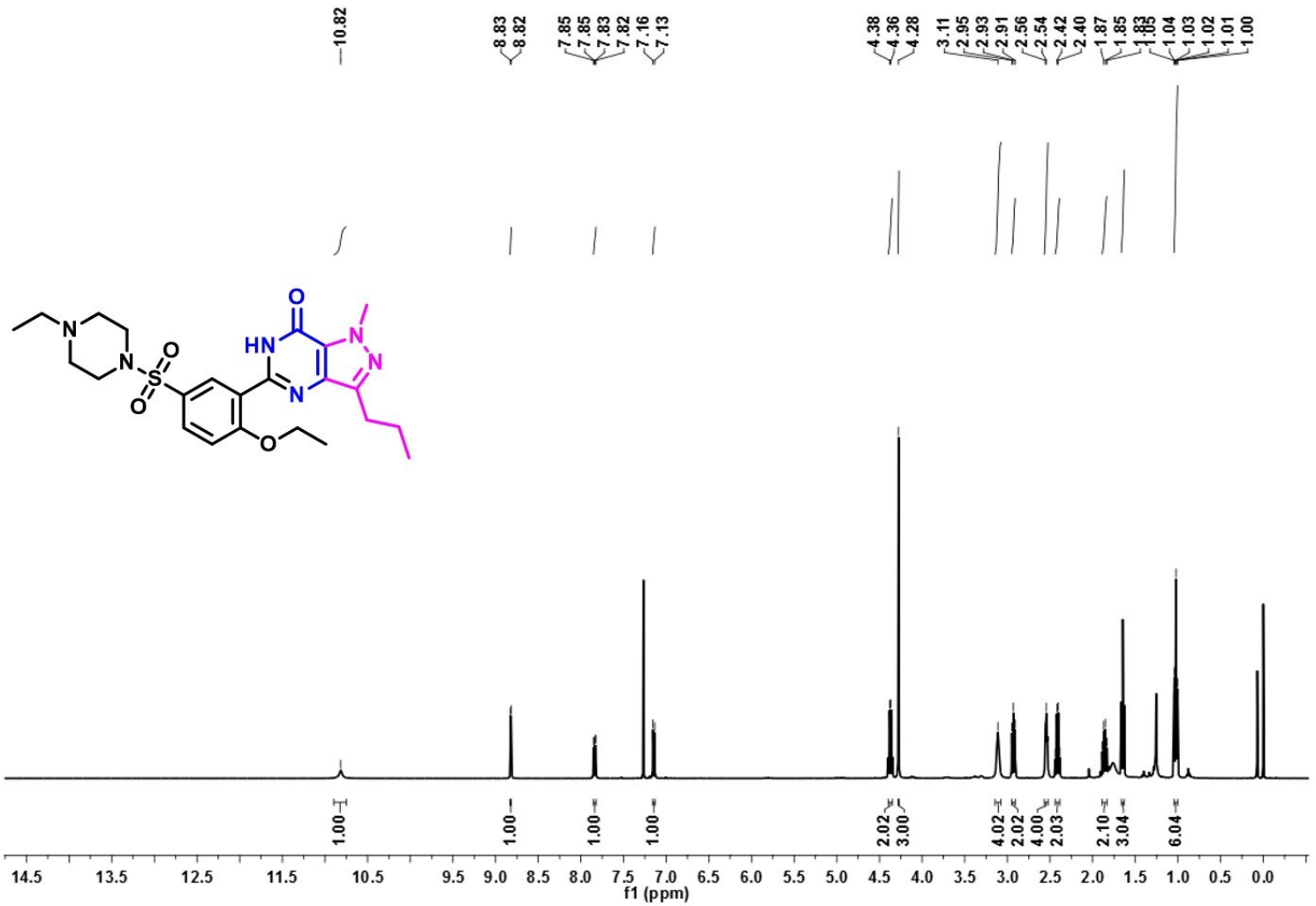

Figure S29. ^{1}H NMR spectra of 5-(2-ethoxy-5-((4-ethylpiperazin-1-yl) sulfonyl) phenyl)-1-methyl-3-propyl-1,6-dihydro-7H-pyrazolo[4,3-d] pyrimidin-7-one **(8b)** in $CDCl_3$.

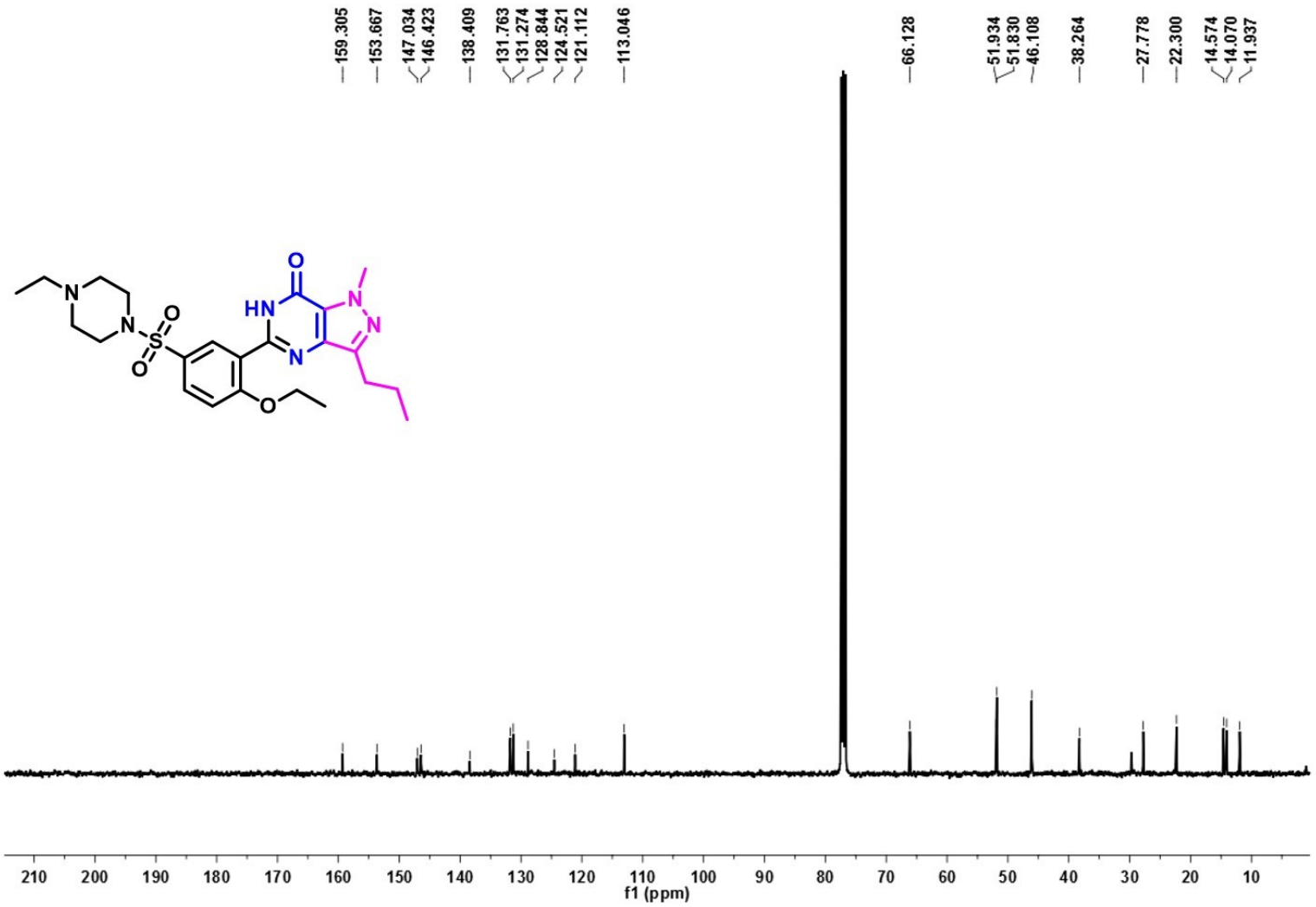

Figure S30. ^{13}C NMR spectra of 5-(2-ethoxy-5-((4-ethylpiperazin-1-yl) sulfonyl) phenyl)-1-methyl-3-propyl-1,6-dihydro-7H-pyrazolo[4,3-d] pyrimidin-7-one **(8b)** in $CDCl_3$.

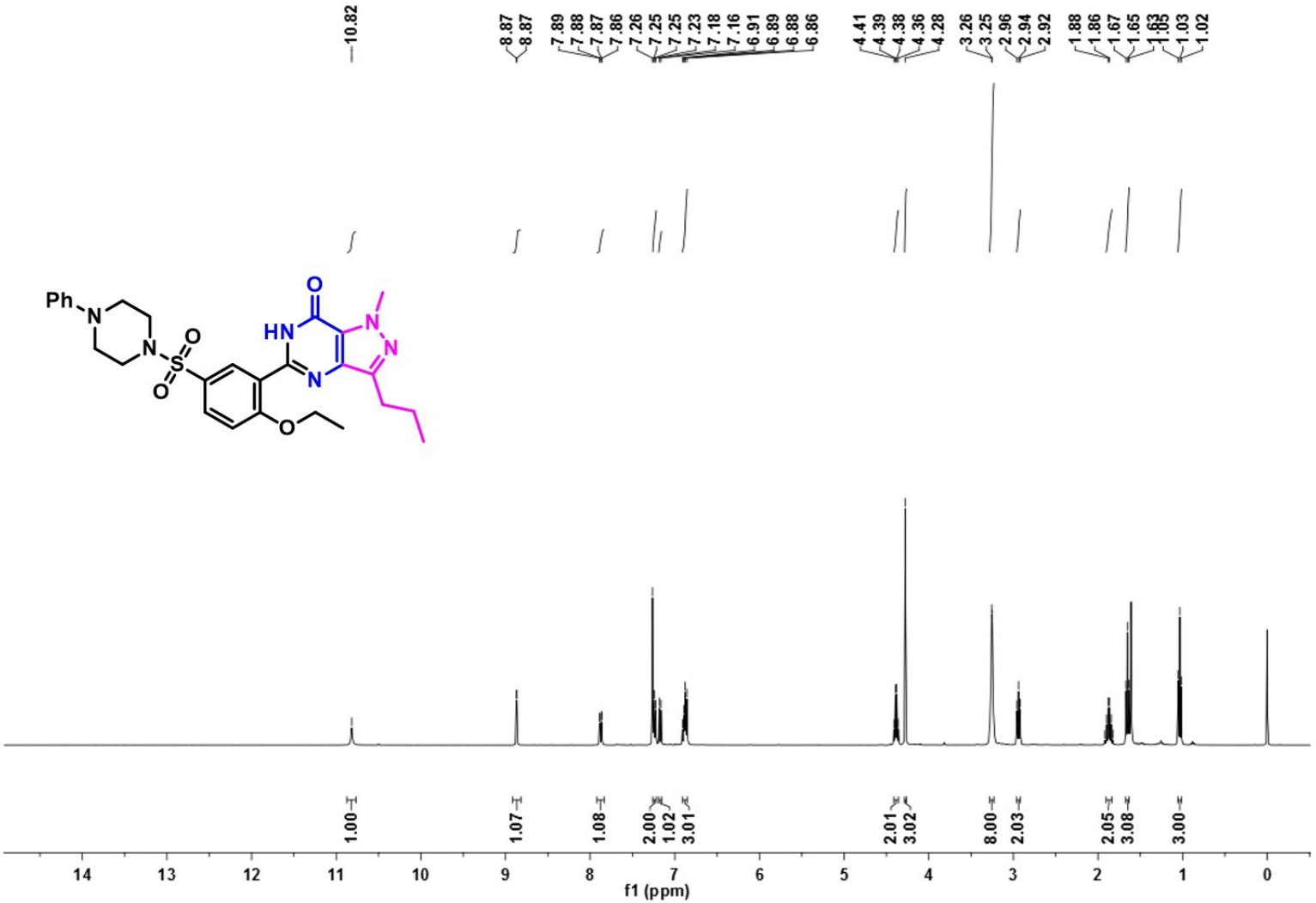

Figure S31. ^{1}H NMR spectra of 5-(2-ethoxy-5-((4-phenylpiperazin-1-yl) sulfonyl) phenyl)-1-methyl-3-propyl-1,6-dihydro-7H-pyrazolo[4,3-d] pyrimidin-7-one **(8c)** in $CDCl_3$.

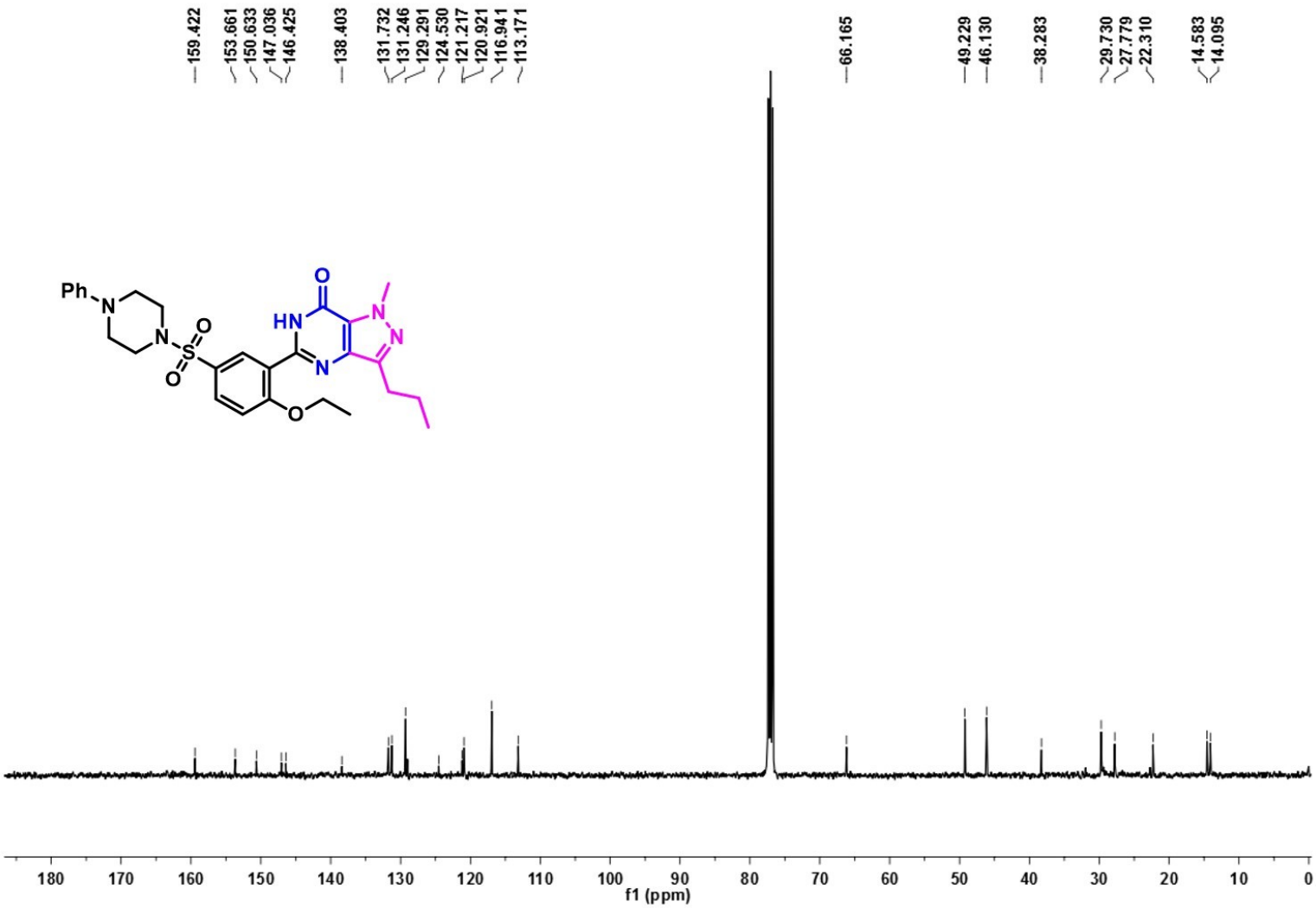

Figure S32. ^{13}C NMR spectra of 5-(2-ethoxy-5-((4-phenylpiperazin-1-yl) sulfonyl) phenyl)-1-methyl-3-propyl-1,6-dihydro-7H-pyrazolo[4,3-d] pyrimidin-7-one **(8c)** in $CDCl_3$.

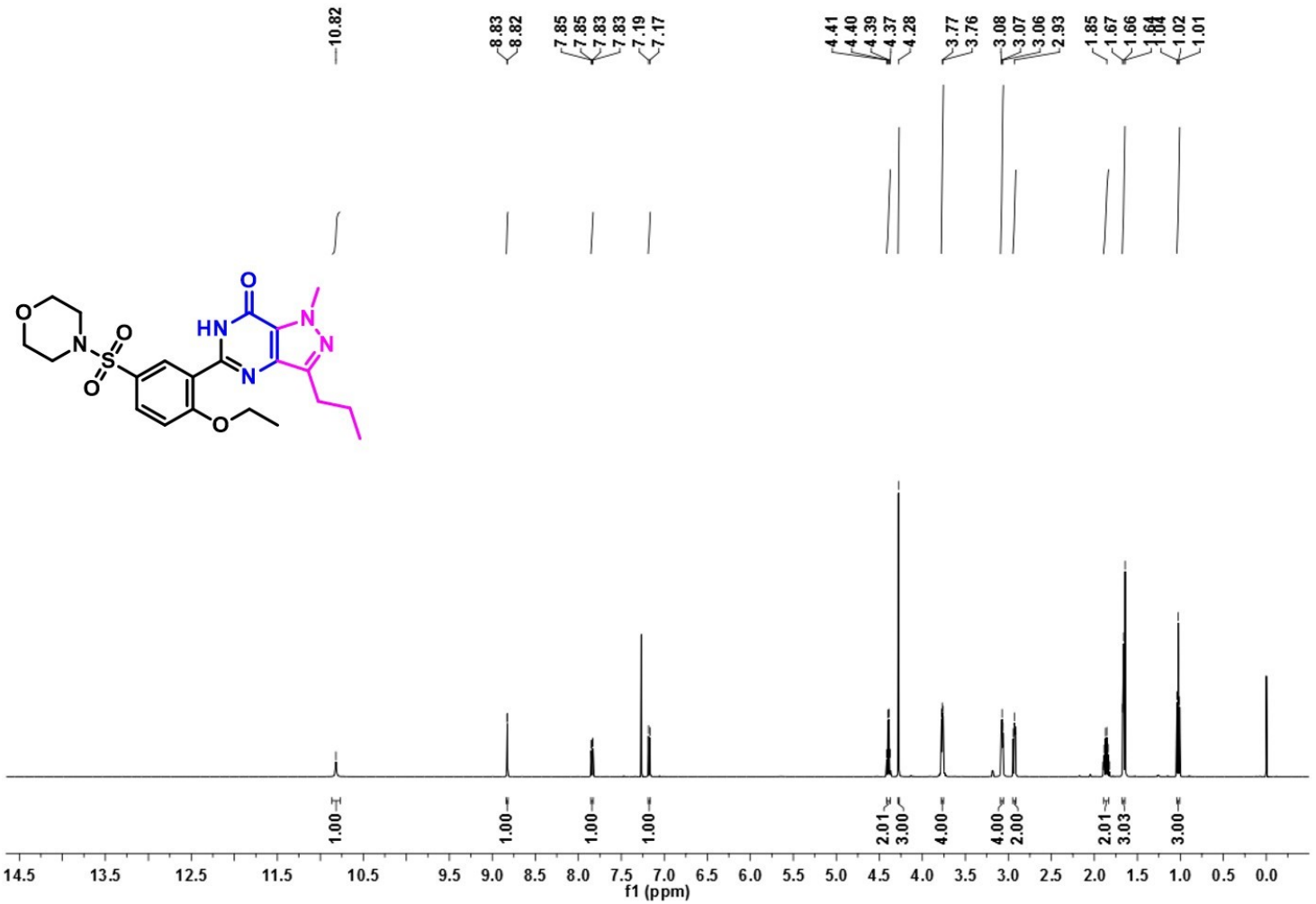

Figure S33. ^{1}H NMR spectra of 5-(2-ethoxy-5-(morpholino sulfonyl) phenyl)-1-methyl-3-propyl-1,6-dihydro-7H-pyrazolo[4,3-d] pyrimidin-7-one **(8d)** in $CDCl_3$.

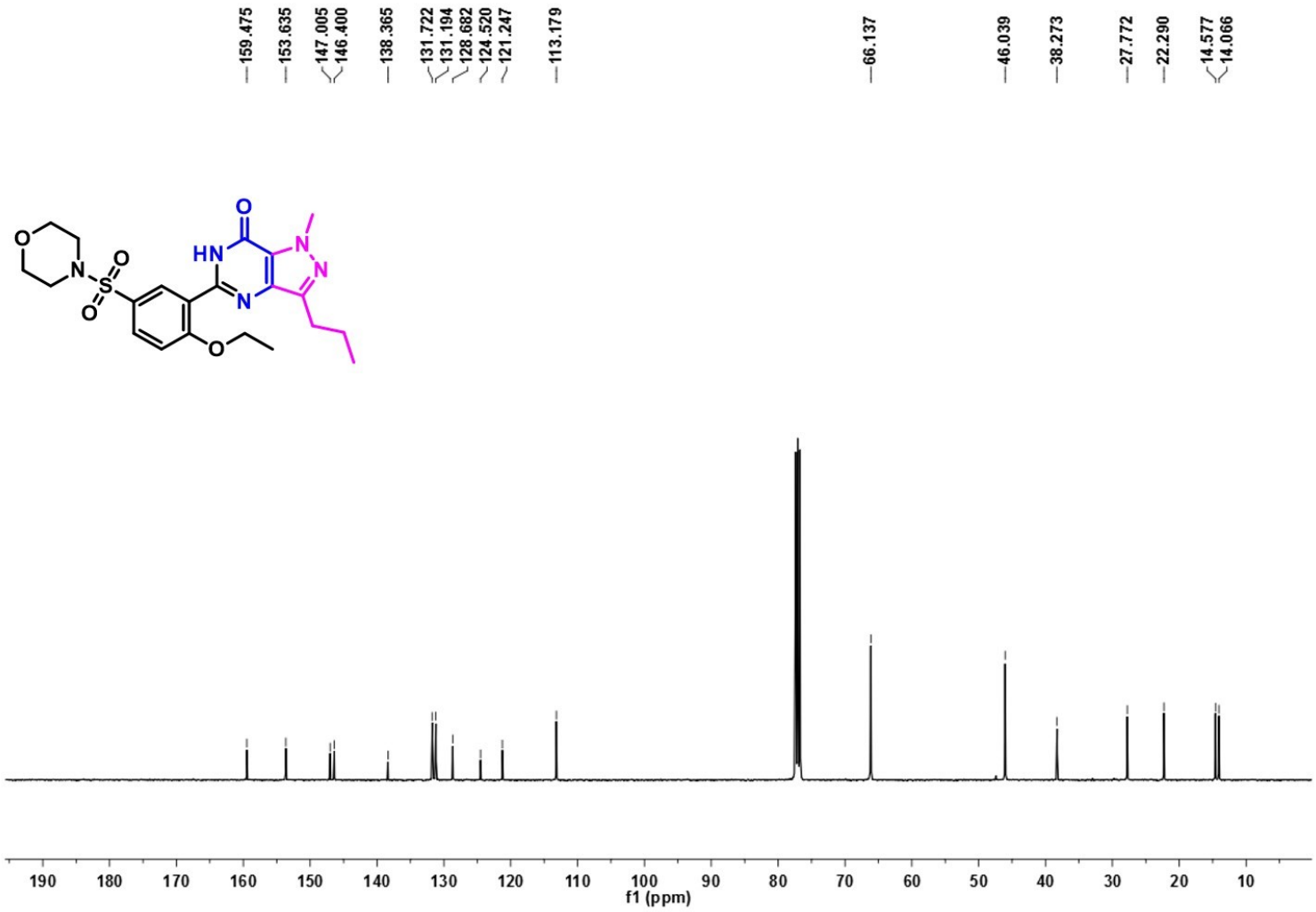

Figure S34. ^{13}C NMR spectra of 5-(2-ethoxy-5-(morpholino sulfonyl) phenyl)-1-methyl-3-propyl-1,6-dihydro-7H-pyrazolo[4,3-d] pyrimidin-7-one **(8d)** in $CDCl_3$.

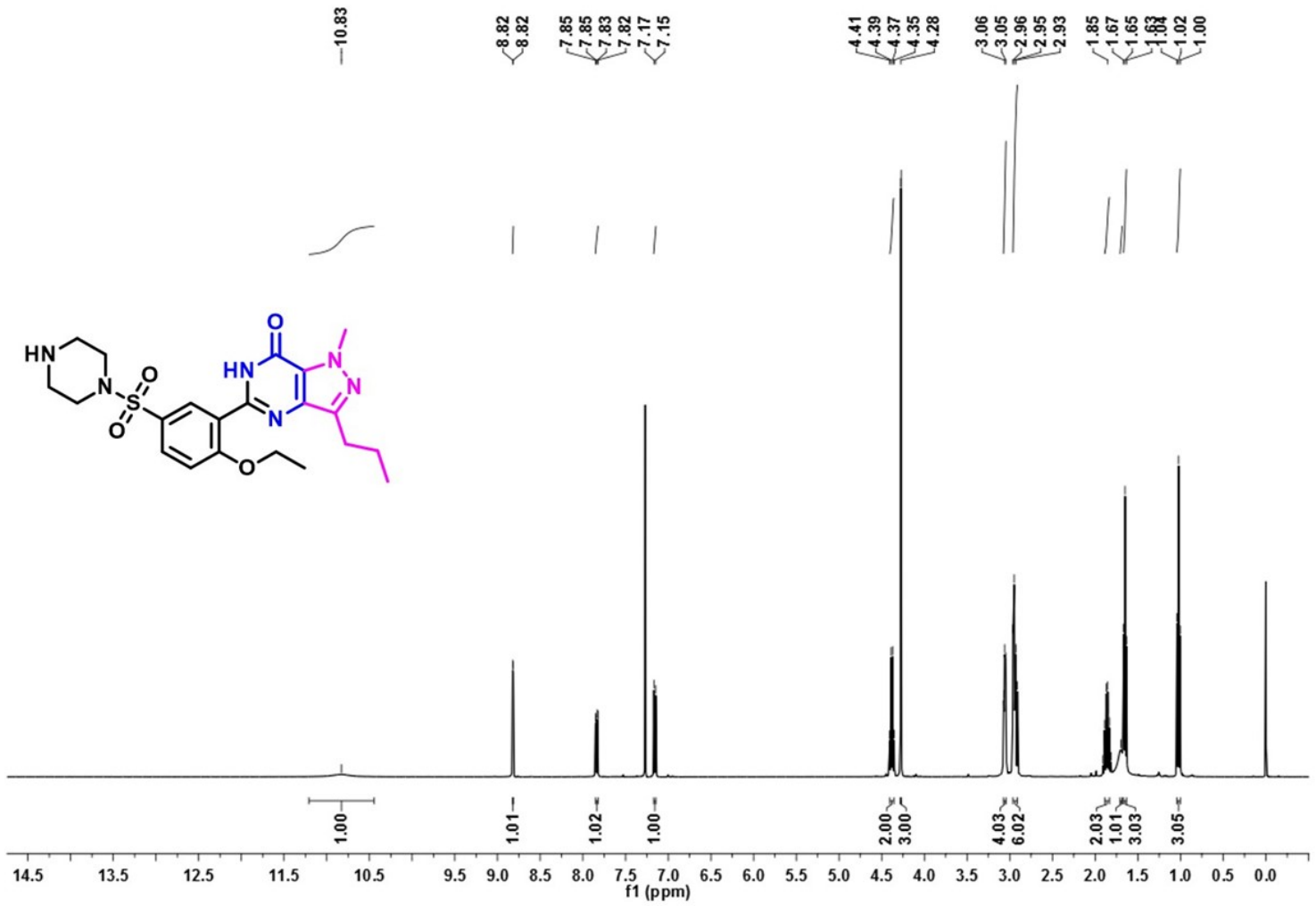

Figure S35.[1]H NMR spectra of5-(2-ethoxy-5-(piperazin-1-yl sulfonyl) phenyl)-1-methyl-3-propyl-1,6-dihydro-7H-pyrazolo[4,3-d] pyrimidin-7-one **(8e)** in $CDCl_3$.

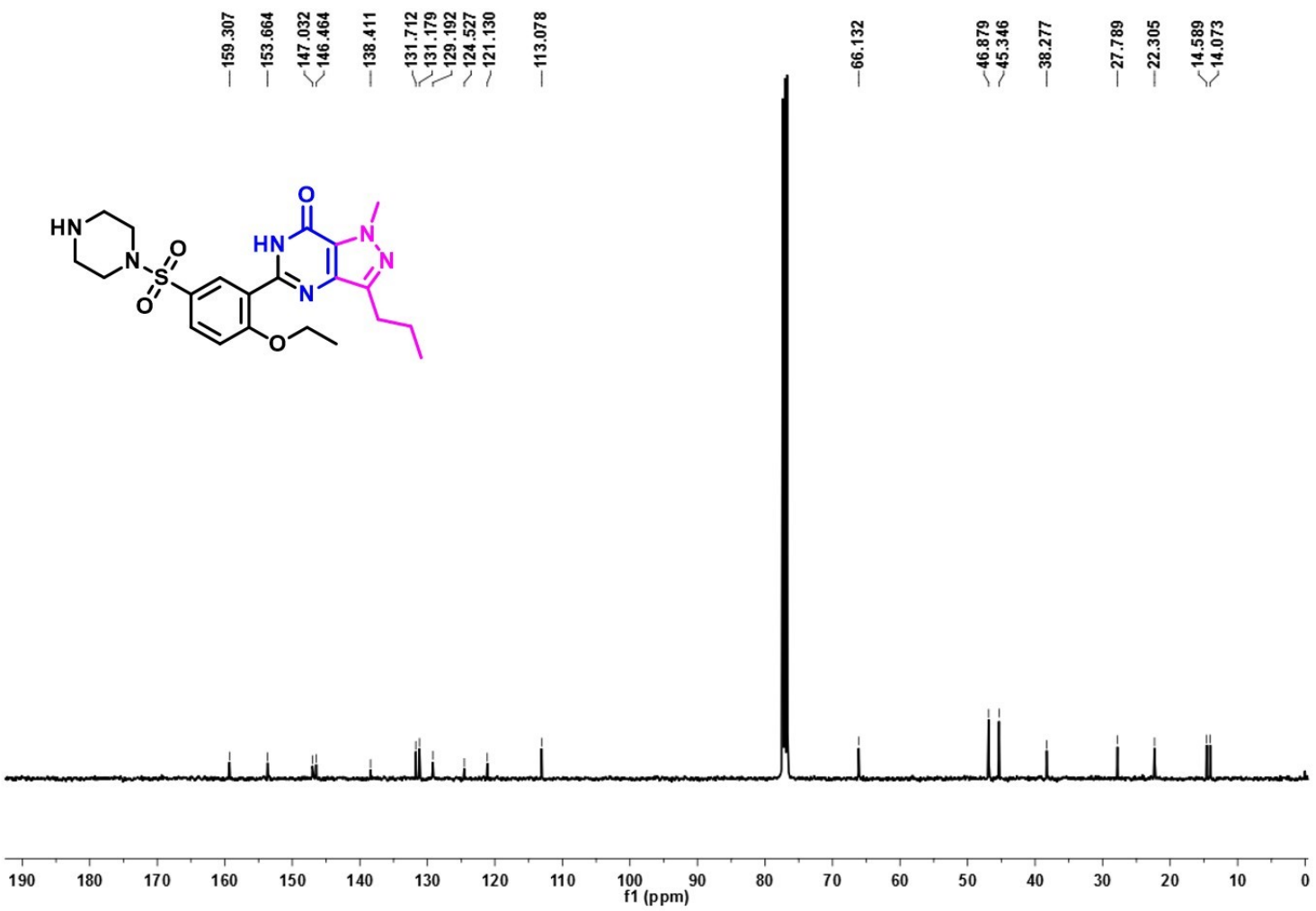

Figure S36.^{13}C NMR spectra of5-(2-ethoxy-5-(piperazin-1-ylsulfonyl) phenyl)-1-methyl-3-propyl-1,6-dihydro-7H-pyrazolo[4,3-d] pyrimidin-7-one **(8e)** in $CDCl_3$.

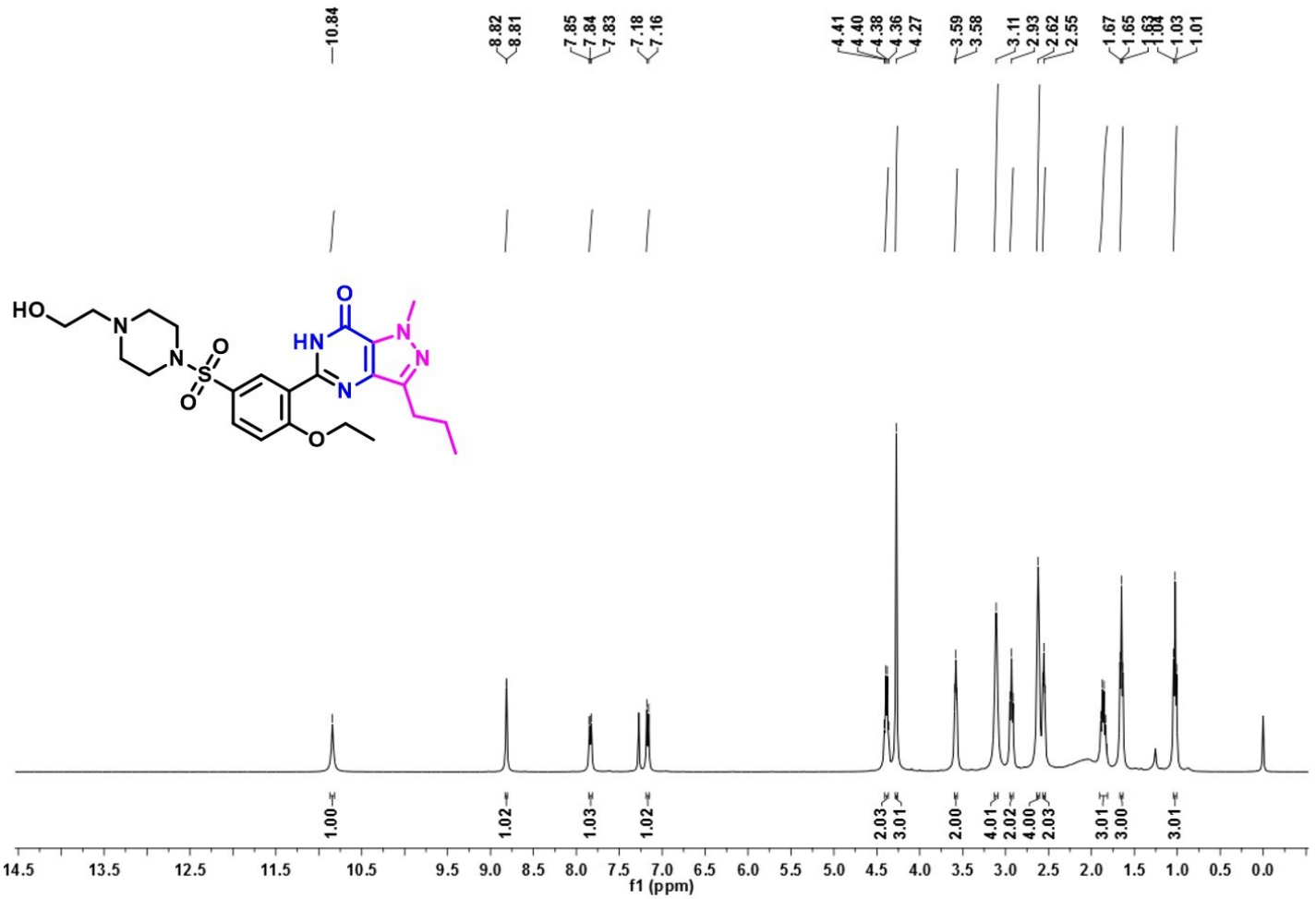

Figure S37.[1]H NMR spectra of 5-(2-ethoxy-5-((4-(2-hydroxyethyl) piperazin-1-yl) sulfonyl) phenyl)-1-methyl-3-propyl-1,6-dihydro-7H-pyrazolo[4,3-d] pyrimidin-7-one **(8f)** in $CDCl_3$.

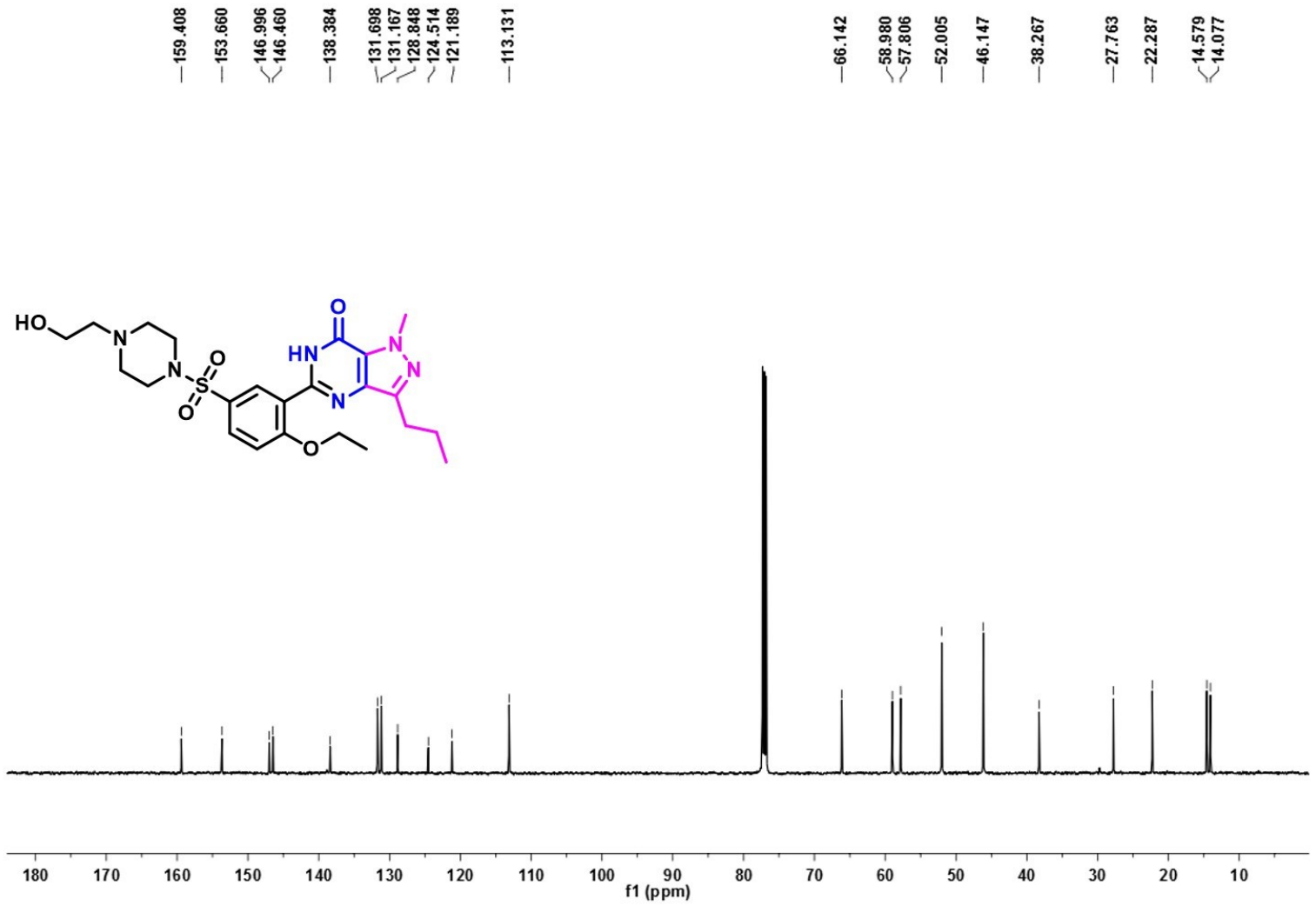

Figure S38. ^{13}C NMR spectra of 5-(2-ethoxy-5-((4-(2-hydroxyethyl) piperazin-1-yl) sulfonyl) phenyl)-1-methyl-3-propyl-1,6-dihydro-7H-pyrazolo[4,3-d] pyrimidin-7-one **(8f)** in $CDCl_3$.

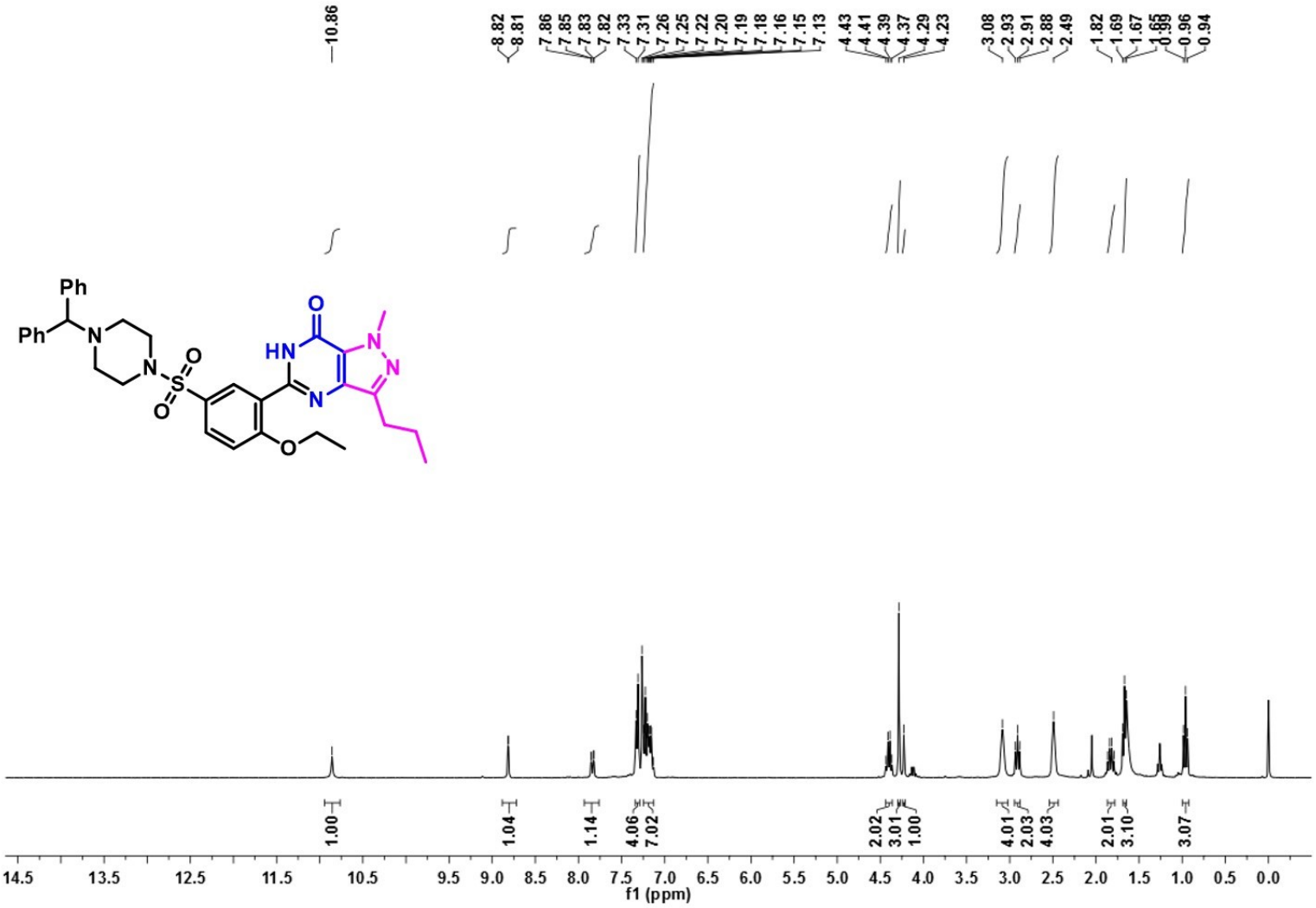

Figure S39. ^{1}H NMR spectra of5-(5-((4-benzhydrylpiperazin-1-yl) sulfonyl)-2-ethoxyphenyl)-1-methyl-3-propyl-1,6-dihydro-7H-pyrazolo[4,3-d] pyrimidin-7-one **(8g)** in $CDCl_3$.

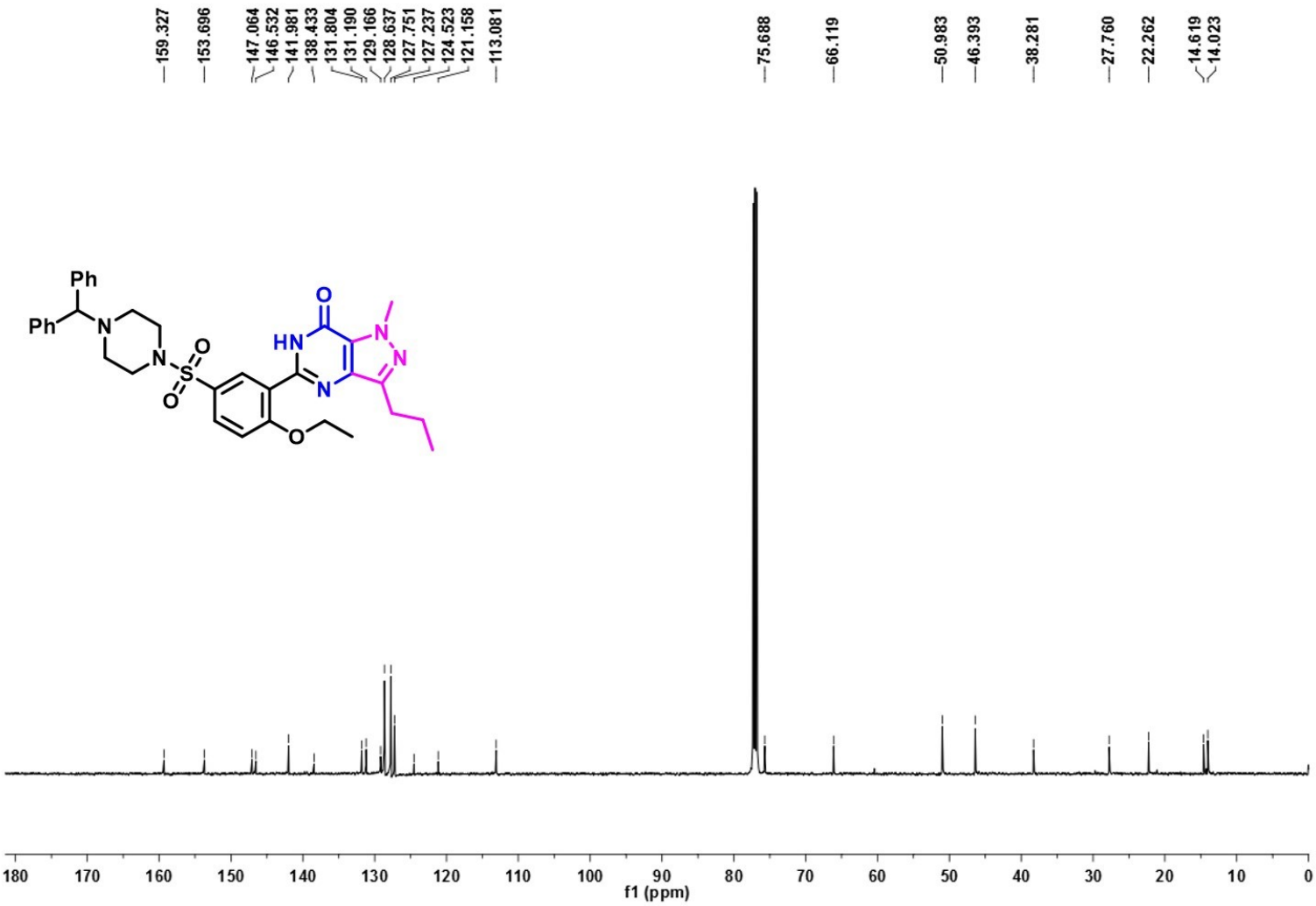

Figure S40. ^{13}C NMR spectra of5-(5-((4-benzhydrylpiperazin-1-yl) sulfonyl)-2-ethoxyphenyl)-1-methyl-3-propyl-1,6-dihydro-7H-pyrazolo[4,3-d] pyrimidin-7-one **(8g)** in $CDCl_3$.

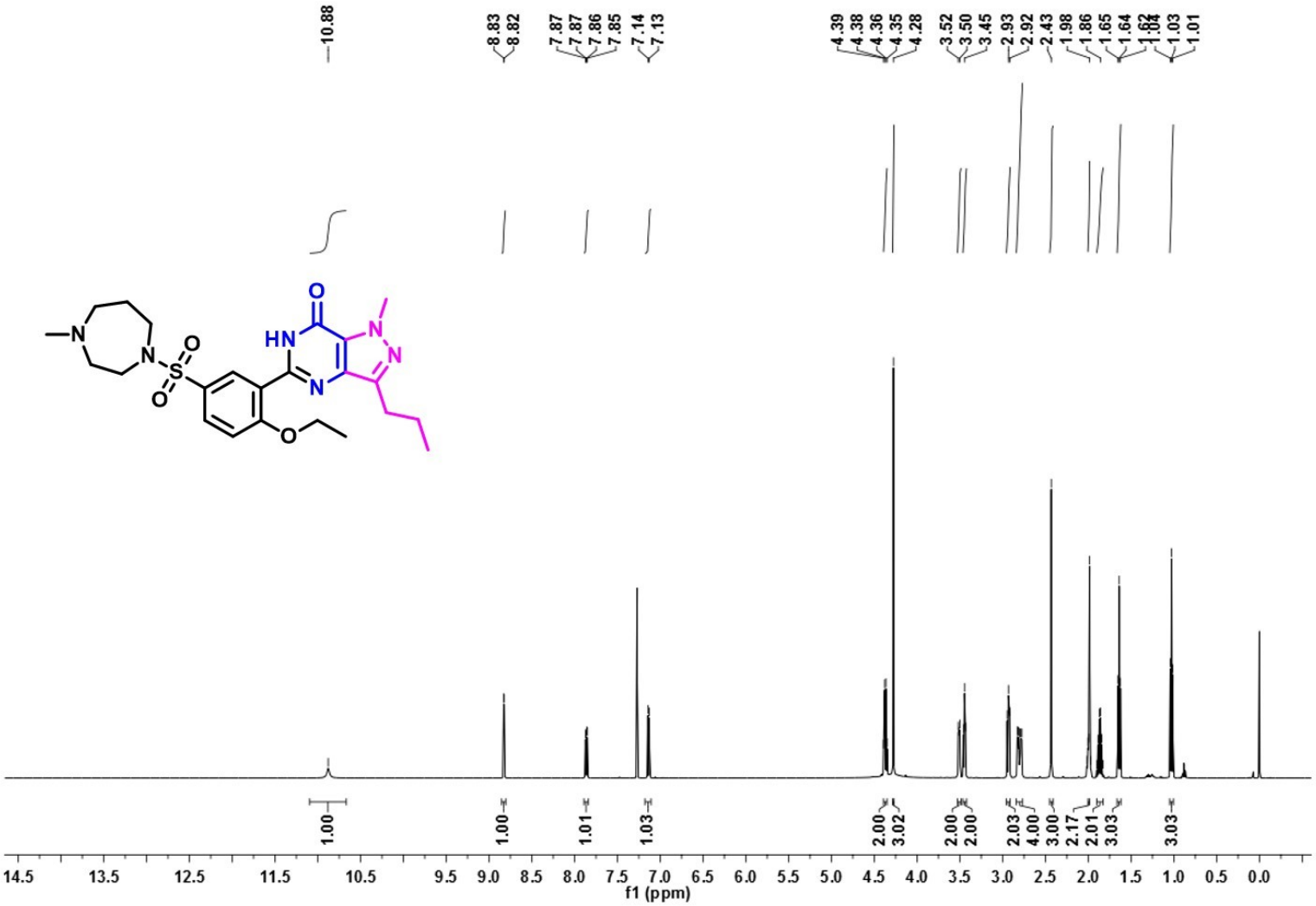

Figure S41. ^{1}H NMR spectra of5-(2-ethoxy-5-((4-methyl-1,4-diazepan-1-yl)sulfonyl)phenyl)-1-methyl-3-propyl-1,6-dihydro-7H-pyrazolo[4,3-d]pyrimidin-7-one **(8h)** in $CDCl_3$.

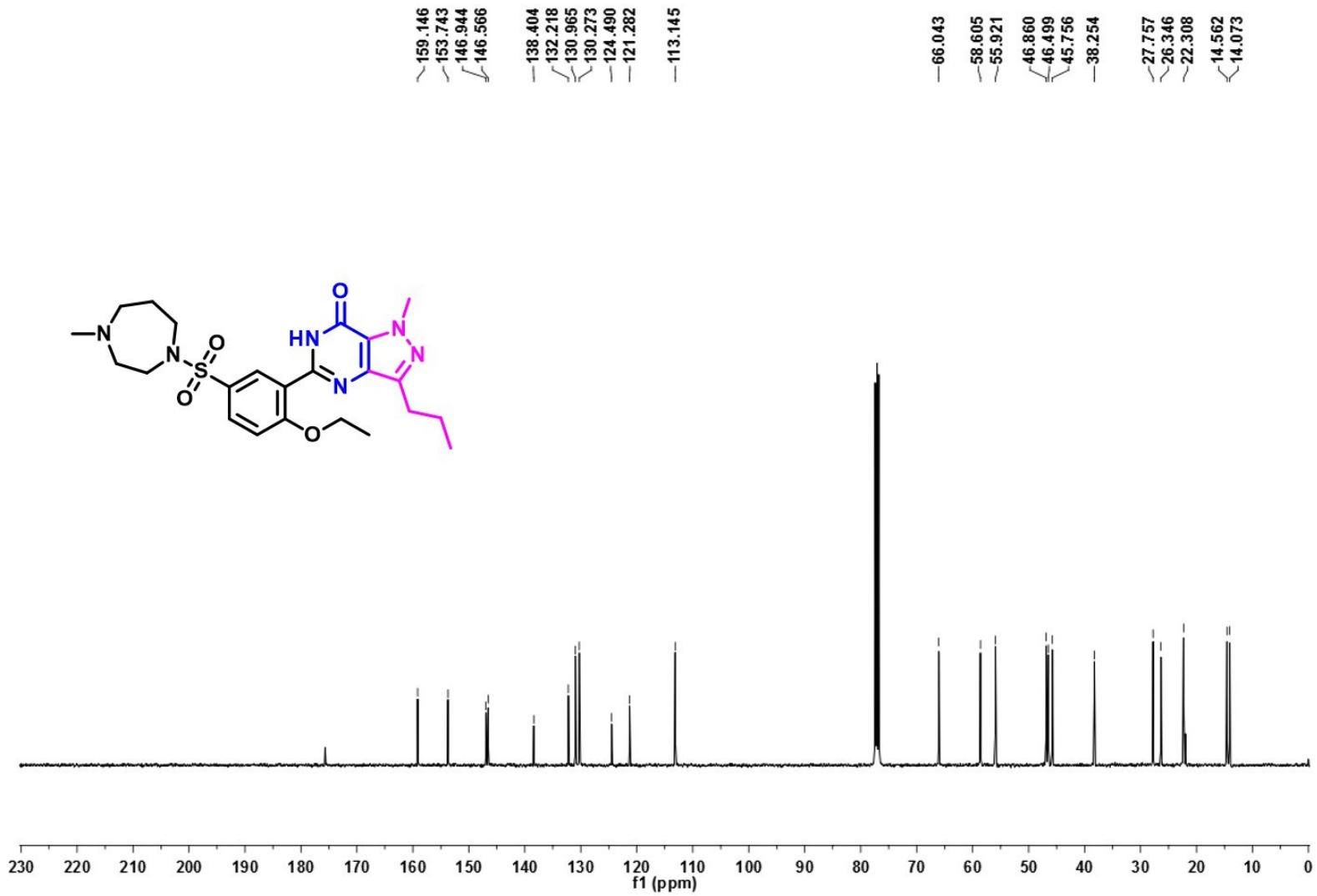

Figure S42.[13]C NMR spectra of 5-(2-ethoxy-5-((4-methyl-1,4-diazepan-1-yl) sulfonyl) phenyl)-1-methyl-3-propyl-1,6-dihydro-7H-pyrazolo[4,3-d] pyrimidin-7-one **(8h)** in $CDCl_3$.

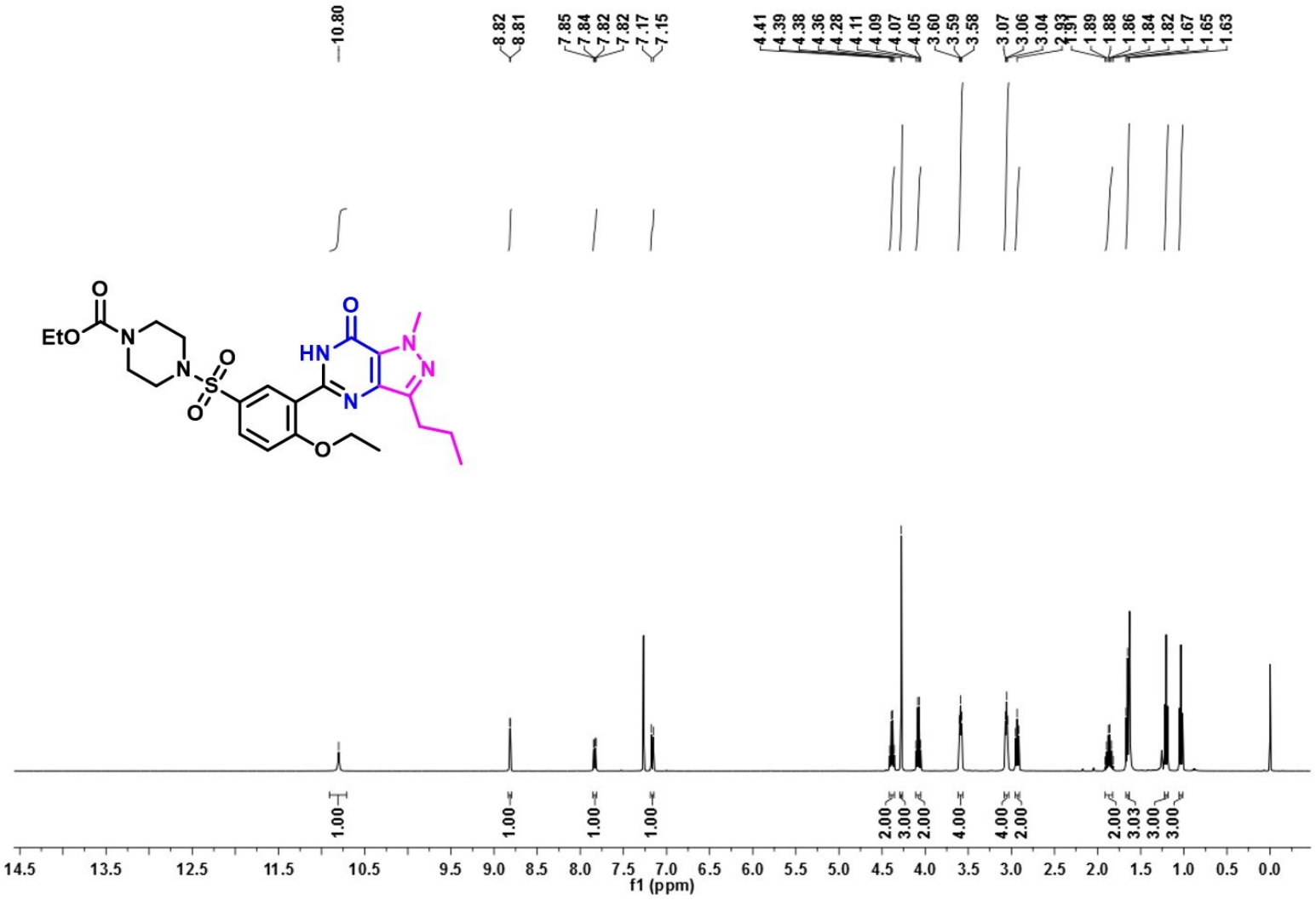

Figure S43. ^{1}H NMR spectra of ethyl 4-((4-ethoxy-3-(1-methyl-7-oxo-3-propyl-6,7-dihydro-1H-pyrazolo[4,3-d] pyrimidin-5-yl) phenyl) sulfonyl) piperazine-1-carboxylate **(8i)** in $CDCl_3$.

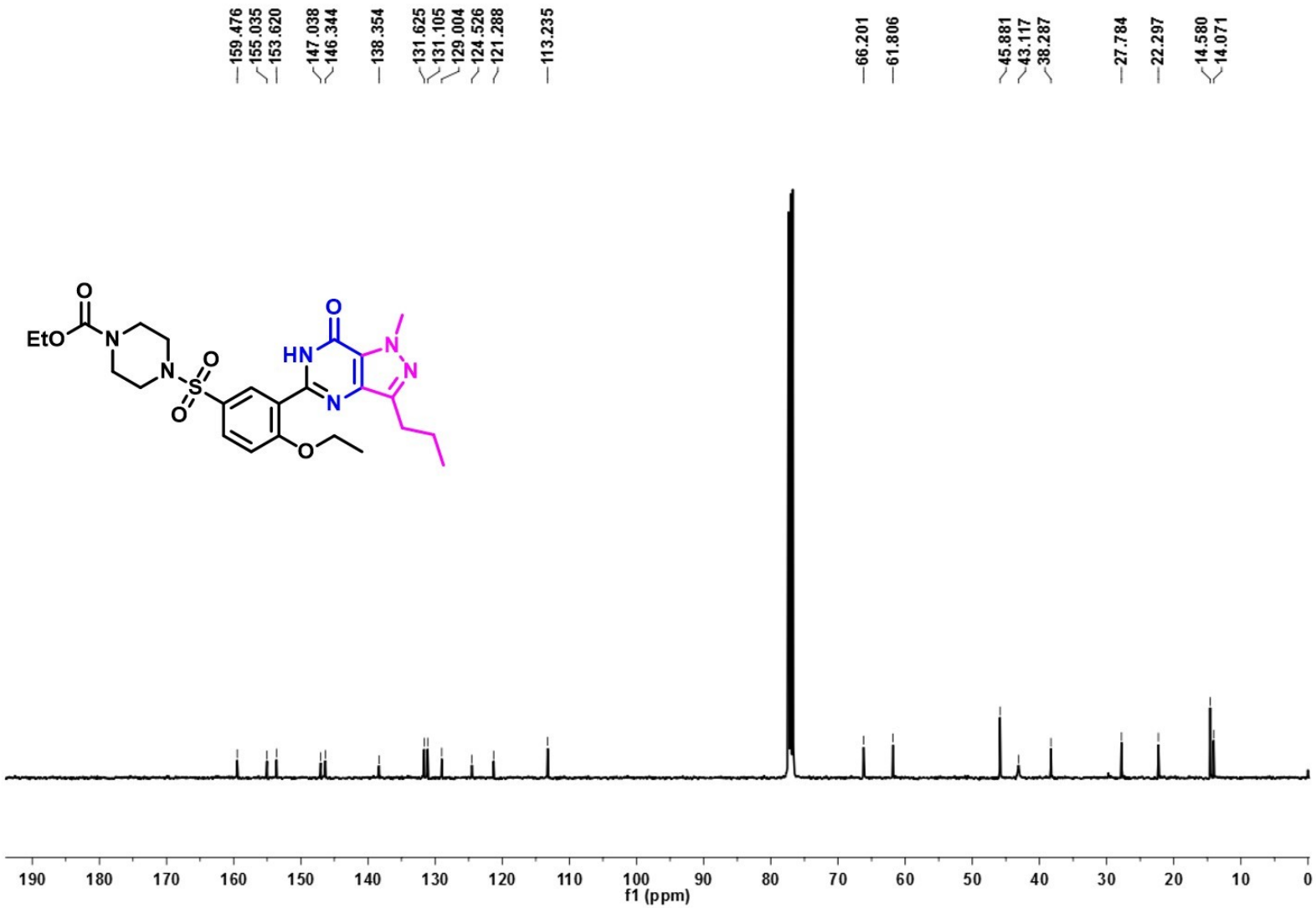

Figure S44. ^{13}C NMR spectra of ethyl 4-((4-ethoxy-3-(1-methyl-7-oxo-3-propyl-6,7-dihydro-1H-pyrazolo[4,3-d] pyrimidin-5-yl) phenyl) sulfonyl) piperazine-1-carboxylate **(8i)** in $CDCl_3$.

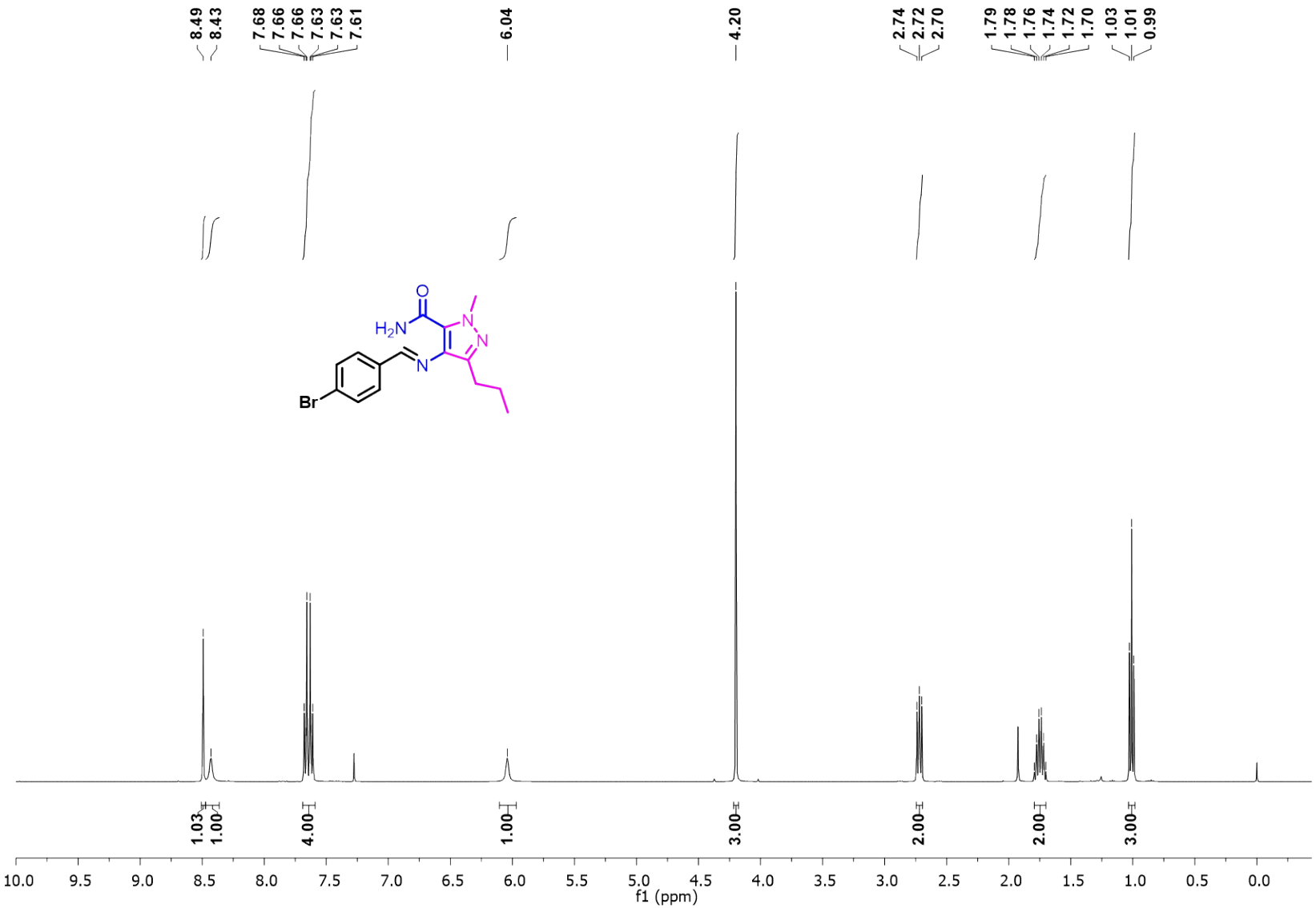

Figure S45. ^{1}H NMR spectra of (E)-4-((4-bromobenzylidene) amino)-1-methyl-3-propyl-1H-pyrazole-5-carboxamide **(**Imine-intermediate**)** in $CDCl_3$.

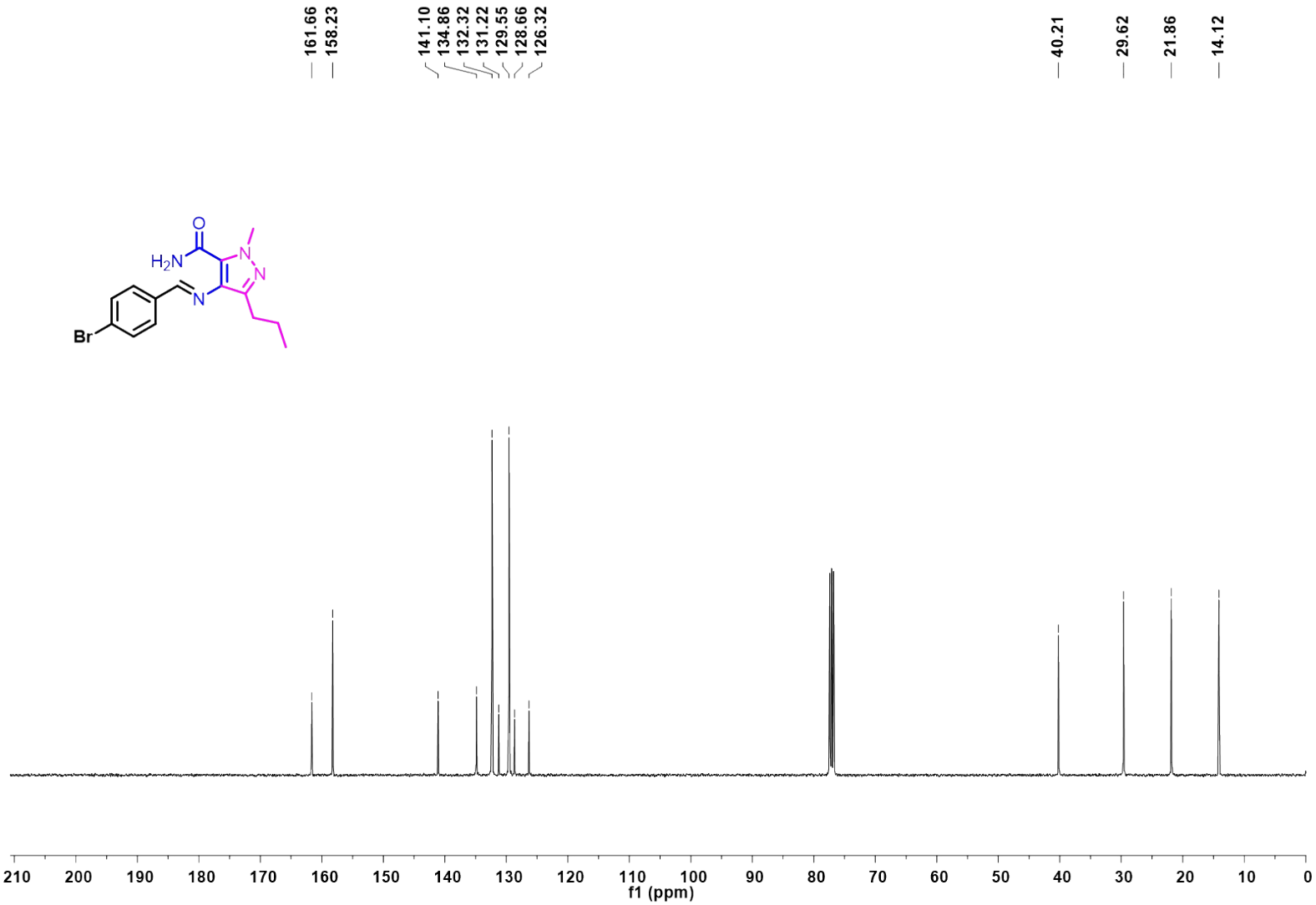

Figure S46. ^{13}C NMR spectra of (E)-4-((4-bromobenzylidene) amino)-1-methyl-3-propyl-1H-pyrazole-5-carboxamide **(**Imine-intermediate**)** in $CDCl_3$.

OSPC-Dr RATHOD

SHIMADZU LabSolutions

LC-MS DATA REPORT

Sample Code : PSH-BROMO-347-250 ML
Data File : 16102019.3.lcd
Method : CD HPLC-ISO.lcm
Injection Volume : 5
Date Acquired : 10/16/2019 11:33:50 AM
Report File : LC-MS Data Report.lsr
Chromatographic Conditions :

Chromatographic Conditions :
Colum: KINETEX-F5 (150 X 4.6mm, 5.0u)
Method: ISOCRATIC
Mobile phase: 77% ACN AND 0.1% FA IN WATER

Chromatogram

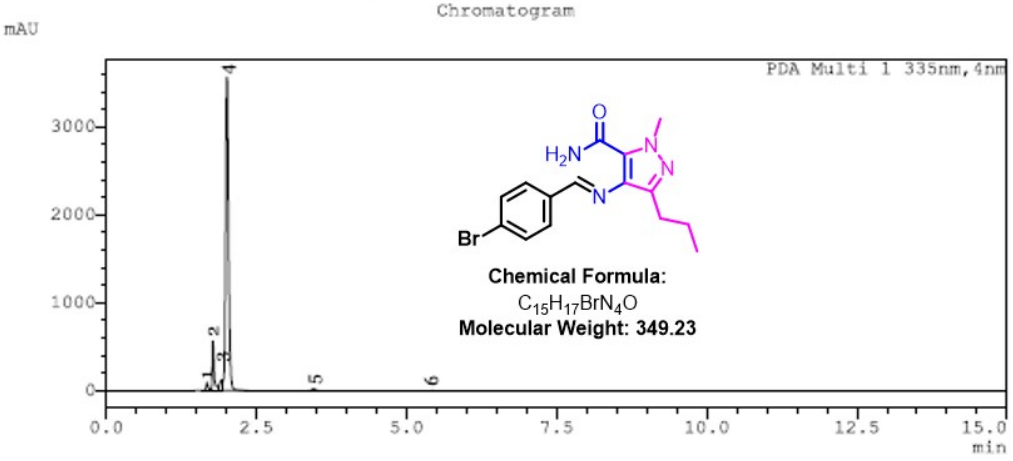

Peak Table

PDA Ch1 335nm

Peak#	Ret. Time	Peak Start	Peak End	Area	Area%
1	1.675	1.579	1.717	201274	1.403
2	1.775	1.717	1.856	1162935	8.105
3	1.921	1.856	1.941	476968	3.324
4	2.010	1.941	2.389	#########	86.378
5	3.450	3.339	3.659	103609	0.722
6	5.431	5.291	5.621	9804	0.068
Total				#########	100.000

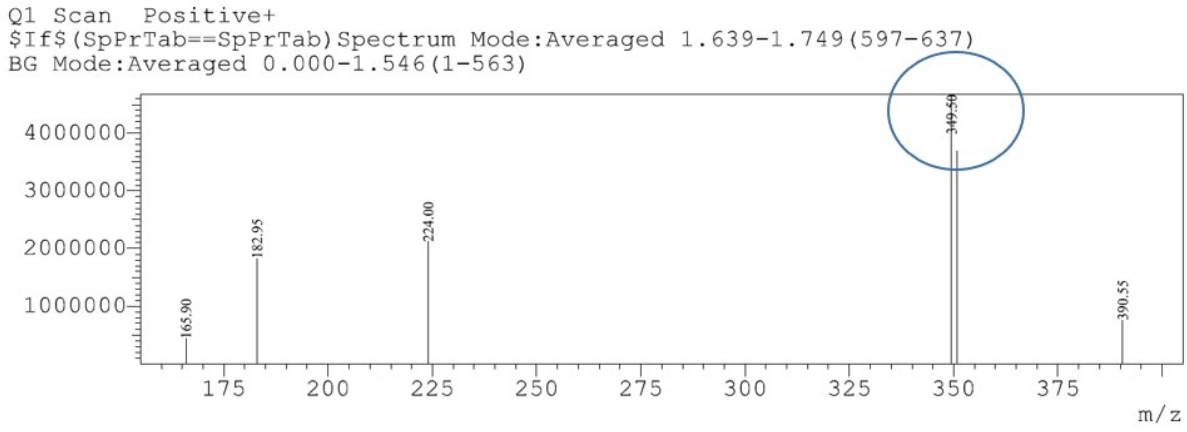

Figure S47. LC-MS data of (E)-4-((4-bromobenzylidene) amino)-1-methyl-3-propyl-1H-pyrazole-5-carboxamide **(**Imine-intermediate**)**

References

1. A. K. Singh; K. C. Basavaraju; S. Sharma; S. Jang; C. P. Park; D.-P. Kim, *Green Chem.,* 2014, **16**, 3024-3030.
2. J.-Y. Kim; W. H. Lee; J. W. Suk; J. R. Potts; H. Chou; I. N. Kholmanov; R. D. Piner; J. Lee; D. Akinwande; R. S. Ruoff, *Adv. Mater.,* 2013, **25**, 2308-2313.
3. S. Park; J. An; J. R. Potts; A. Velamakanni; S. Murali; R. S. Ruoff, *Carbon,* 2011, **49**, 3019-3023.
4. K. Singh; A. K. Singh; D. Singh; R. Singh; S. Sharma, *Catal. Sci. Technol.,* 2016, **6**, 3723-3726.
5. P. P. Upare; J.-W. Yoon; M. Y. Kim; H.-Y. Kang; D. W. Hwang; Y. K. Hwang; Kung, H. H.; Chang, J.-S., *Green Chem.,* 2013, **15**, 2935-2943.
6. F. Liu; J. Sun; L. Zhu; X. Meng; C. Qi; F.-S. Xiao, *J. Mater. Chem.,* 2012, **22**, 5495-5502.
7. J. Du; X. Hu; Q. Zhou, *RSC Adv.,* 2015, **5**, 27009-27017.
8. G. Das, H.H. Yoon, *Int. J. Nanomed*., 2015, ***10***, 55–66.
9. P. P. Upare , J.-W. Yoon , M. Y. Kim , H.-Y. Kang , D. W. Hwang , Y. K. Hwang , H. H. Kung and J.-S. Chang , Green Chem., 2013, 15 , 2935-2943.
10. P. Cui; J. Lee; E. Hwang; H. Lee, *ChemComm.,* 2011, **47**, 12370-12372.
11. W. M. Hussein; D. Feder; G. Schenk; L. W. Guddat; R. P. McGeary, *Eur. J. Med. Chem.,* 2018, **157**, 462-479.
12. R. Paramashivappa; P. Phani Kumar; P. V. Subba Rao; A. Srinivasa Rao, *J. Agric. Food Chem.,* 2002, **50**, 7709-7713.
13. H. A. Flores Toque; F. B. M. Priviero; C. E. Teixeira; E. Perissutti; F. Fiorino; B. Severino; F. Frecentese; R. Lorenzetti; J. S. Baracat; V. Santagada; G. Caliendo; E. Antunes; G. De Nucci, *J. Med. Chem.,*2008, **51**, 2807-2815.
14. C. Wang; L. Salmon; R. Ciganda; L. Yate; S. Moya; J. Ruiz; D. Astruc, *ChemComm.,* 2017, **53**, 644-646.

15. J. K. Laha; K. V. Patel; K. S. S. Tummalapalli; N. Dayal, *ChemComm.,* 2016, **52**, 10245-10248.

16. D. J. Dale; P. J. Dunn; C. Golightly; M. L. Hughes; P. C. Levett; A. K. Pearce; P. M. Searle; G. Ward; A. S. Wood, *Org. Process Res. Dev.,* 2000, **4**, 17-22.

17. G.-H. Tian; G.-X. Xia; W.-X. Jin; X.-J. Chen; S.-A. Lai; Y.-B. Wei; R.-Y. Ji; J.-S. Shen, *Chin. J. Chem.,* 2007, **25**, 241-245.

18. A. D. Hudwekar; G. L. Reddy; P. K. Verma; S. Gupta; R. A. Vishwakarma; S. D. Sawant, *Green Chem.,* 2017, **2**, 4963-4968.

19. R. J. Abdel-Jalil; M. Khanfar; S. Al-Gharabli; M. M. El-Abadelah; K. Eichele; M. U. Anwar,; Voelter, W., *ChemInform,* 2005, **36**.

20. N. Mulakayala; B. Kandagatla; Ismail; R. K. Rapolu; Rao, P.; C. Mulakayala; C. S. Kumar; J. Iqbal; S. Oruganti, *Bioorganic Med. Chem. Lett.,* 2012, **22**, 5063-5066.

21. G. L. Reddy; S. K. Guru; M. Srinivas; A. S. Pathania; P. Mahajan; A. Nargotra; S. Bhushan; R. A. Vishwakarma; S. D. Sawant, *Eur. J. Med. Chem.,* 2014, **80**, 201-208.

22. N. R. Reddy; G. M. Reddy; B. S. Reddy; P. P. Reddy, *J. Heterocycl. Chem.,* 2005, **42**, 751-754.

23. H. W. Hamilton; D. F. Ortwine; D. F. Worth; J. A. Bristol, *J. Med. Chem,.* 1987, **30**, 91-96.

24. K. C. Basavaraju; S. Sharma; R. A. Maurya; D. P. Kim, *Angew. Chem., Int. Ed. Engl.,* 2013, **52**, 6735-8.

25. Sharma, S.; Maurya, R. A.; Min, K. I.; Jeong, G. Y.; Kim, D. P., *Angew. Chem., Int. Ed. Engl.,* 2013,**52**, 7564-8.

26. R. A. Maurya; K.-I. Min; D.-P. Kim, *Green Chem.,* 2014,**16**, 116-120.

27. V. K. Sthalam; A. K. Singh; S. Pabbaraja, *Org. Process Res. Dev.,* 2019, **23**, 1892-1899.

28. C. Mustazza; A. Borioni; A. L. Rodomonte; M. Bartolomei; E. Antoniella; P. Di Martino; L. Valvo; I. Sestili; E. Costantini; M. C. Gaudiano, *J. Pharm. Biomed.,* 2014, **96**, 170-186.

29. D. Lv; Y. Cao; L. Chen; Z. Zhu; X. Chen; D. Li; D. Wang; S. Li; Y. Chai; F. Lu, *Anal. Chem.,* 2018, **90**, 10765-10770.

30. V. S. K. Indukuri; S. R. Gorantla; H. B. Vurimindi, *Lett. Org. Chem.,* 2011, **8**, 668-673.

31. R. De Souza; Elisa, Mannochio, R.Torres; Valter, Freire, *WO 02/12241 Al* 2002.

32. Lu, Yee-Fung, C. A. J. O., Yong Tao, *US 6,204,383 B1* 2001.

33. R. Paramashivappa, P. Phani Kumar, P. V. Subba Rao and A. Srinivasa Rao, *J. Agric. Food Chem*., 2002, **50**, 7709-7713.

34. H. A. Flores Toque, F. B. M. Priviero, C. E. Teixeira, E. Perissutti, F. Fiorino, B. Severino, F. Frecentese, R. Lorenzetti, J. S. Baracat, V. Santagada, G. Caliendo, E. Antunes and G. De Nucci, *J. Med. Chem*., 2008, **51**, 2807-2815.

35. J. K. Laha, K. V. Patel, K. S. S. Tummalapalli and N. Dayal, *Chem. Commun*., 2016, **52**, 10245-10248.

36. G. -H. Tian, G. -X. Xia, W. -X. Jin, X. -J. Chen, S. -A. Lai, Y. -B. Wei, R. -Y. Ji and J. -S. Shen, *Chin. J. Chem*., 2007, **25***,* 241-245.

37. D. J. Dale, P. J. Dunn, C. Golightly, M. L. Hughes, P. C. Levett, A. K. Pearce, P. M. Searle, G. Ward and A. S. Wood, *Org. Process Res. Dev*., 2000, **4**, 17-22.

38. A. D. Hudwekar, G. L. Reddy, P. K. Verma, S. Gupta, R. A. Vishwakarma and S. D. Sawant, *ChemistrySelect,* 2017, **2**, 4963-4968.

39. S. Steiner, J. Wolf, S. Glatzel, A. Andreou, J. M. Granda, G. Keenan, T. Hinkley, G. Aragon-Camarasa, P. J. Kitson, D. Angelone and L. Cronin, *Science,* 2019, **363**, eaav2211.